R-6811-1   16

INTERIM REPORT

INVESTIGATION OF POSITIVE-TYPE

SHAFT SEALS

R ROCKETDYNE

A DIVISION OF NORTH AMERICAN ROCKWELL CORPORATION
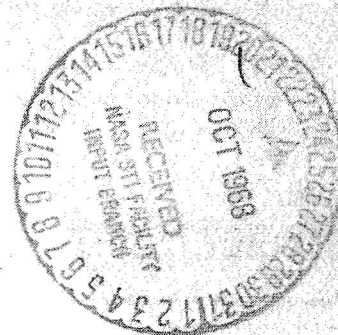
GPO PRICE $ _____

CSFTI PRICE(S) $ _____

Hard copy (HC) _____   -

Microfiche (MF) _____   -

ff 653 July 65

ROCKETDYNE

A DIVISION OF NORTH AMERICAN ROCKWELL CORPORATION
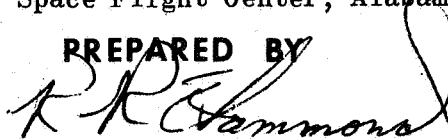6633 CANOGA AVENUE, CANOGA PARK, CALIFORNIA 91304

R-6811-1   16

INTERIM REPORT
INVESTIGATION OF POSITIVE-TYPE
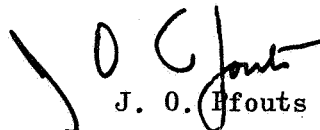### SHAFT SEALS

Contract NAS8-11325

Prepared For

National Aeronautics and Space Administration
George C. Marshall Space Flight Center
Propulsion and Vehicle Engineering Laboratory
Marshall Space Flight Center, Alabama

PREPARED BY

R. R. Hammond

APPROVED BY

J. O. Pfouts

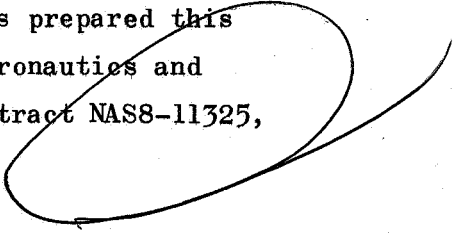| DATE	REV. BY	PAGES AFFECTED	REMARKS

FORM R18-G REV. 9-67

FOREWORD

Rocketdyne, a Division of North American
Rockwell Corporation, has prepared this
report under National Aeronautics and
Space Administration Contract NAS8-11325,
G.O. 8624.

ABSTRACT

A series of new type seal concepts were
generated, and three of the most promising
were detailed for fabrication and testing
to evaluate the designs for future turbo-
pump applications. Descriptions of the
various concepts, basis for the final
selections of the seals for evaluation,
and results of testing are included.

CONTENTS

ILLUSTRATIONS

PAGES IX(9) AND X(10) ARE MISSING FROM ORIGINAL DOCUMENT.

TABLES

INTRODUCTION

The continued advancement of rocket engine turbomachinery has required the development of new shaft seal technology to cope with the extremes of temperature and speed. Although seal engineering technology has progressed significantly, turbomachinery performance demands have also increased particularly in the areas of high speed, high pressure, throttle-ability (wide speed range), and extended life.

The static portion of the mechanical seal, referred to as the secondary seal, must maintain its integrity while accepting axial shaft displacements caused by elastic deformations, fluid pressure pulsations, and vibrations. This report summarizes efforts directed toward development of new concepts intended to solve some of the problems of secondary sealing.

This report is divided into two parts, the first covering secondary seals, design approaches, and static analysis. The second part covers an evaluation of secondary seals through testing at simulated turbopump operating conditions, and documents the results obtained with particle damping.

SUMMARY

A program to investigate the secondary seal area of positive-type shaft seals was initiated and resulted in the evaluation of 18 seal concepts; 3 of which were selected for fabrication and performance analysis.

The welded metal bellows was selected as the secondary seal for all three seals, each having a different method of controlling the oscillatory motion of the bellows caused by the mechanical vibration and pressure pulsating environment of the turbopump. Of the three concepts selected and tested, one design considered (known as the particle damped seal) was shown to have the desirable damping characteristics to reduce bellows failures.

Further refinement and testing of the particle damped seal indicates a useful concept to reduce vibration inputs within the frequency band investigated. A further study to determine the operating limitations of particle damping as applied to face seals and to analyze factors involved in efficiency would be beneficial.

SECONDARY SEAL PROGRAM

PROGRAM OBJECTIVES

The basic program was directed at generating new approaches to the problem
of secondary sealing with emphasis on advancing seal technology for future
turbopump generations.

To meet the program requirements the following tasks were established:

1. Generate a number of new approaches to the secondary seal based
    on advanced turbopump operating parameters

2. Evaluate these concepts to arrive at several of the most
    promising

3. Perform detailed analyses and designs resulting in procurement
    of test seals of the selected concepts

4. Conduct nonrotating tests to evaluate concepts and to provide
    information for future designs

DESIGN CONCEPT SELECTION

Seal design criteria were based on expected future turbopump performance
requirements. Future pump discharge pressures are expected to be higher
than current levels and the pressure at the seal cavity could readily be
100 percent above current practice. The seal temperature environment
is expected to be in a range of -323 to +1000 F.

Seventeen seal concepts were evolved. After a thorough analysis and investigation, the following three designs were selected for detailed investigation and possible fabrication.

1. Piston Damped Seal (Fig. 1)

2. Purged Double Lip Seal

3. Orifice Damped Seal (Fig. 2)

Upon further investigation, the purged double lip seal was dropped because of temperature limitations and susceptibility to contamination. Late in the program a new concept evolved, known as the particle damped seal and was the subject of effort under a program extension.

The result of the secondary seal selection evaluation was the conclusion that the concept having the greatest number of advantages is the welded metal bellows. The metal bellows design provides the most positive method of preventing secondary seal leakage, with a minimum number of potential leak paths.

The high performance of the metal bellows mechanical seal can be attained if a method is provided for controlling the potentially unstable seal face movements induced by vibratory inputs and fluid pressure pulsations. The ability of the bellows to function as a stable secondary portion of the mechanical seal has a major part in controlling leakage and life of the sealing faces. As a result of the potentially unstable behavior of bellows, considerable attention has been given throughout the seal industry to the problems of bellows damping.

A conventional method of retarding unstable motion of bellows is by frictional devices, usually spring loaded, contacting the bellows convolutions and/or the bellows carrier. Although effective, the amount of damping is not easily controlled and damper material and contacting surfaces are subject to wear. In addition, if the input vibration becomes large, a higher frictional load is then necessary for adequate control. Simultaneously, this higher load increases energy input and the potential for ignition of exposed propellants. The three damping concepts selected for evaluation under the investigation covered in this report do not depend upon exposed friction damping.

Based on the selection of the metal welded bellows, a test program was outlined to study the effects of incorporating bellows vibration damping devices to ensure that the damper does not impair the normal operation of the bellows with reference to primary seal separation and bellows life. A test program was planned to include axial cycling of the bellows both mechanically and through pressure pulsations to observe bellows integrity and seal performance. A test was planned to accelerate the mating ring away from the bellows carrier to determine bellows response or recovery rate. Vibration tests were planned to observe the reaction of the bellows to vibration input. Other tests were also planned for analysis of total seal face loading and normal quality control inspection tests.

CONCLUSIONS

Piston Damped Seal

The piston damped seal (Fig. 1) employs a viscous method of controlling induced vibratory motion of the bellows and consists of a piston ring contained in the housing maintaining a close clearance with the carbon retainer

High Pressure
Side

Mounting Bolt Circle

Housing
Inconel 600

Piston

Seal Face and
Bellows Carrier
Inconel 600

Rear Carrier
Inconel 600

Mate

Welded Bellows
Inconel 750
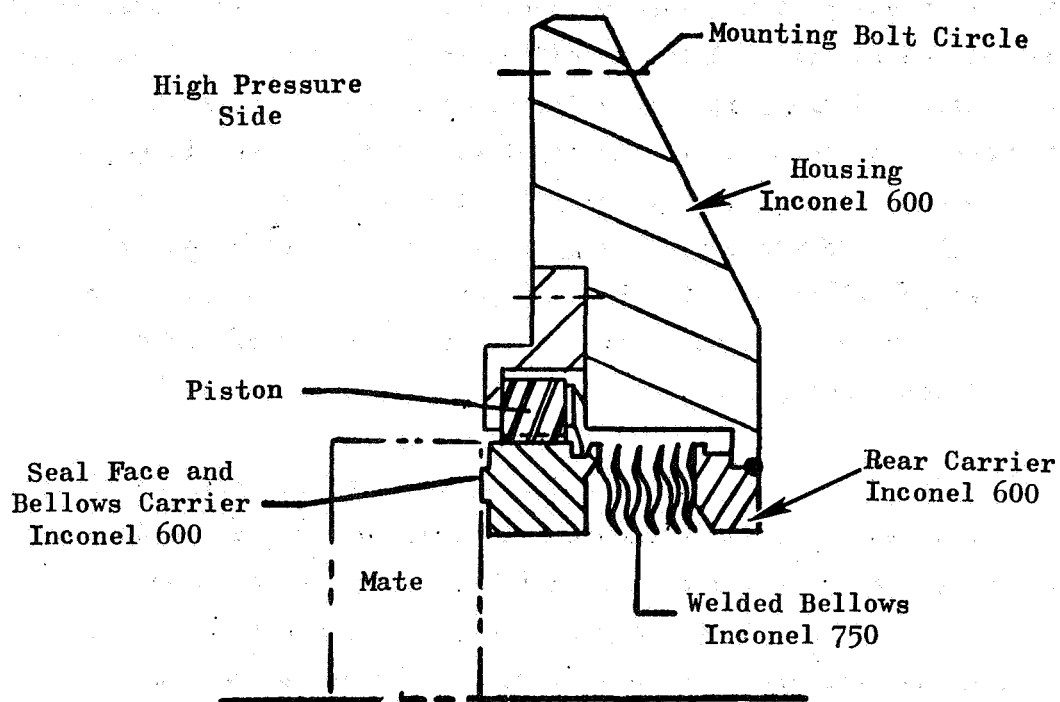
¢ SCALE 2X

Figure 1. Piston Damped Seal Design

outer diameter. The sealing fluid surrounding the bellows OD is forced
through the controlled clearance as axial movement of the bellows changes
the volume between the housing and bellows.

Based on initial computer studies describing damping characteristics in
terms of displacement vs time response, the seal shows a definite reduction
in amplitude when the piston clearance is reduced to 0.002 inches from
0.010 inches. A conclusion based on pressurized cryogenic tests conducted
on actual hardware is that a relatively high density and viscosity is re-
quired. The tests also show that the use of a piston does not impair
normal bellows operation, which indicates that excessive damping is not
obtained under the selected test conditions. No apparent damping exists
in a gas environment, which precludes the utility of this design in the
turbine area.

Although damping is apparently obtainable in a cryogenic fluid when a close
clearance is maintained, a further reduction in clearance is accompanied by
rubbing and will approach the method of frictional damping currently employed
in the seal industry. Because of a somewhat restricted use, the piston
damped seal was ruled out for further refinement. A more practical use
for this design would be in seals for oils or similar fluids of relatively
high viscosity and for application where rubbing contact may be permissible.

Orifice Damped Seal

The orifice damped seal (Fig. 2) also utilizes viscous friction to absorb
imposed axial vibration. The design consists of two cavities formed by
two pairs of radially stacked welded bellows and separated by an orifice
plate. The end fitting of one bellows cavity has a sealing surface to
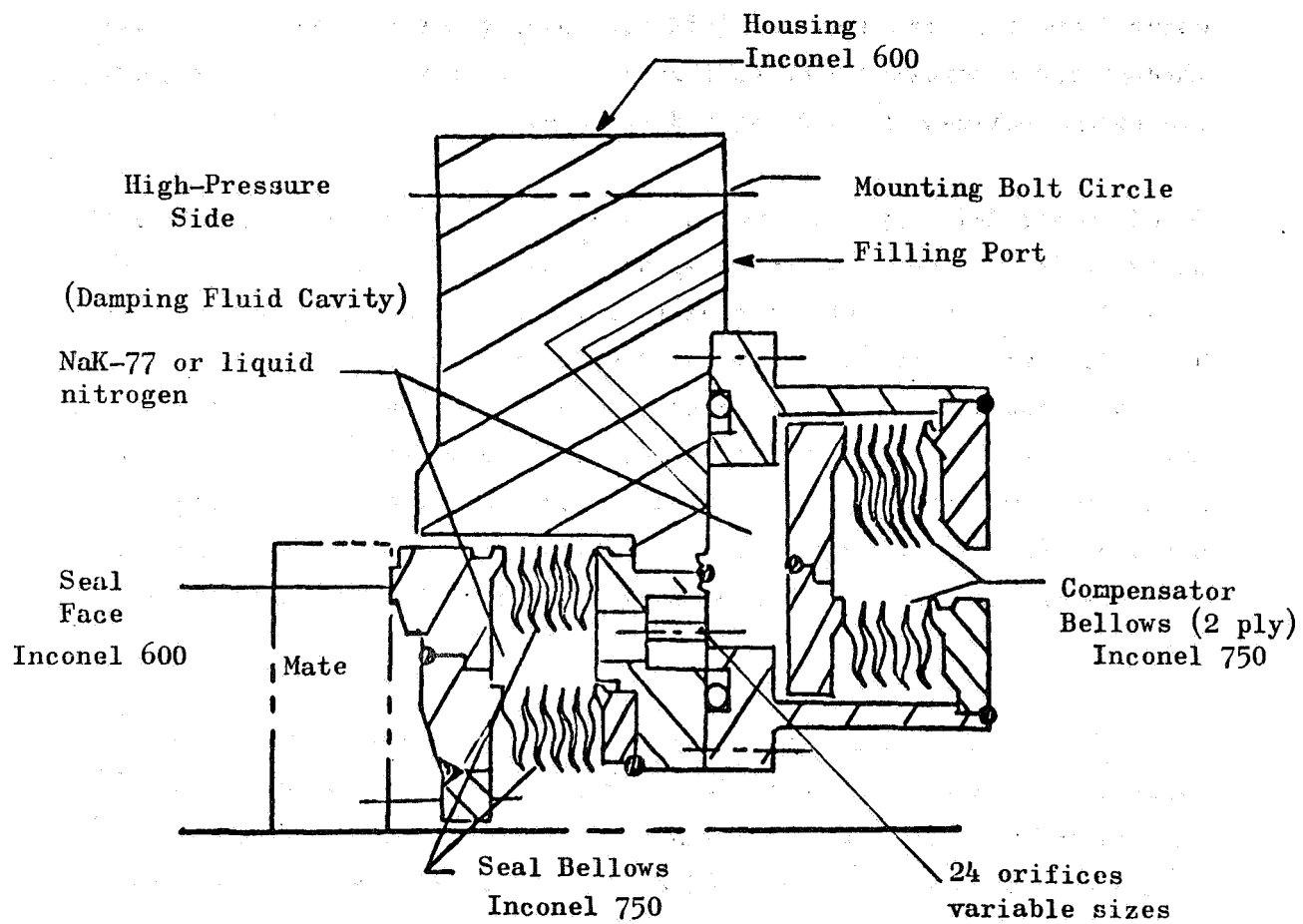
Figure 2. Orifice Damped Seal Design

mate with an adjacent rotating sealing surface. The end fitting on the other bellows cavity closes the system. Both cavities are filled with a liquid metal or a cryogenic fluid as the temperature environment dictates.

As the seal face is subjected to axial movements, the damping fluid contained in the bellows cavity is forced through the orifices creating viscous forces to absorb input energy. The rear bellows cavity or compensator assembly accumulates the volume of fluid forced through the orifices and also acts to increase or decrease the total volume due to a fluid temperature/density change.

For a cryogenic application, the fluid to be sealed also becomes the damping medium. To obtain significant damping, a fluid with the high density associated with liquids must be used. Analog computer calculations have indicated that little damping is obtained with a gaseous medium at the relatively small displacements of this seal. This seal design is more suited to high-temperature applications because the damping fluid (not the process fluid) can be contained and sealed in the bellows cavity. For the purpose of this study, liquid metal sodium-potassium (NaK) was used. The application of this concept is apparently feasible for temperature environments other than cryogenic; however, further research and design refinements to improve the detail design are necessary before the orifice damped seal can be considered a practical reality.

Particle Damped Seal

The particle damped seal (Fig. 3) consists of a conventional bellows seal design using a stationary bellows welded to a sealing face and loaded against an adjacent rotating sealing surface. In addition, a series of 24 cylinders

Housing 304 stainless

Fill Ports

24 cylinders 304
Stainless, containing
Molybdenum spherical
particles 40 microns

Bellows Carrier
and Seal Face
Inconel 600

Bellows, Inconel 750,
10 Convolutions
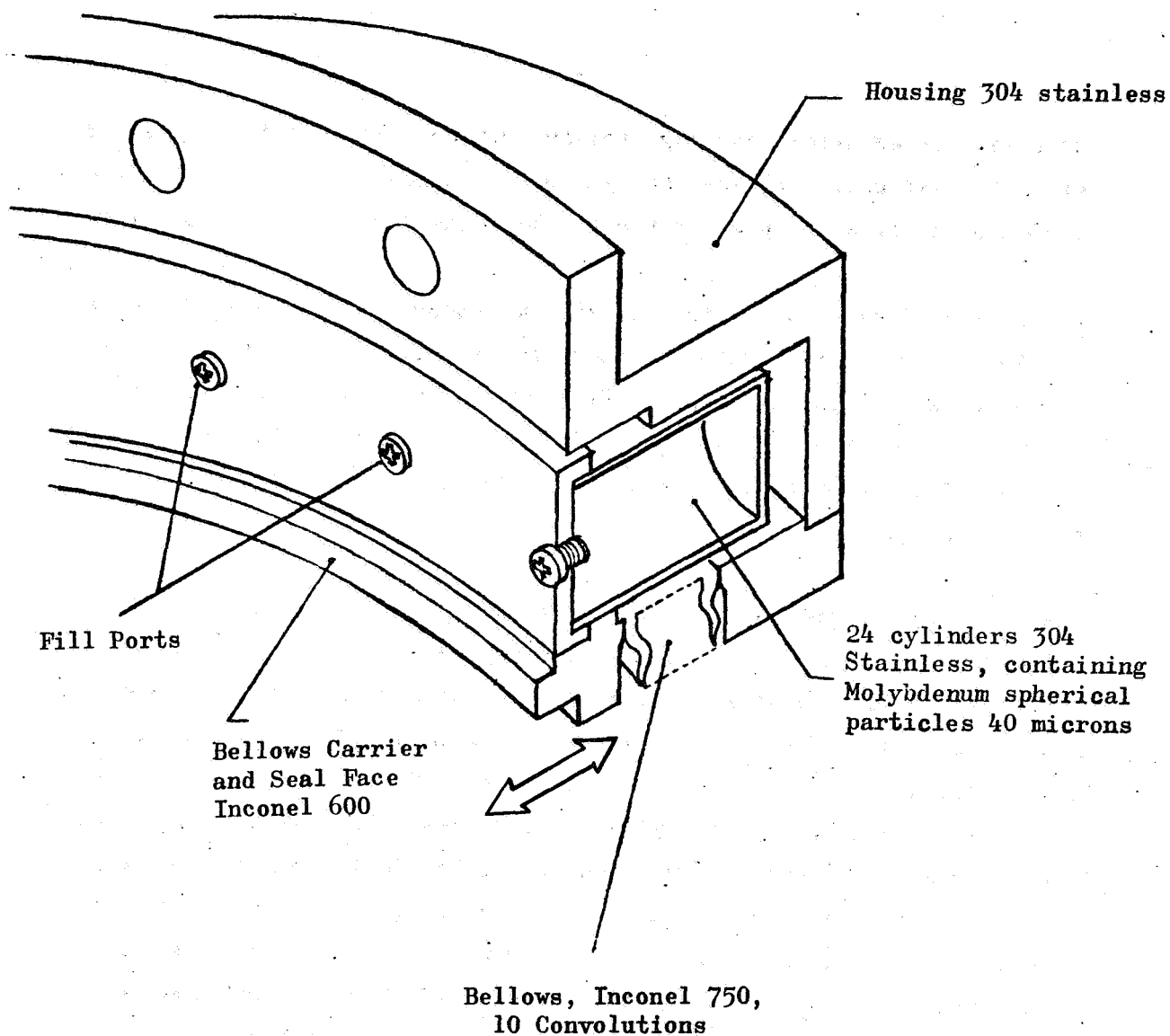
Housing OD 6.039
Carrier ID 3.340

Figure 3 . Particle Damped Seal Design

12

are welded to a radial extension of the sealing surface placing the cylinders at the OD of the bellows. The cylinders are filled to an effective level with molybolenum spherical particles. The spherical particles react to vibration inputs by absorbing displacement energy through inertia and friction of the particle masses acting on the inside surface of the cylinders.

The prime advantages over conventional vibration damping devices and other concepts considered in this program are simplicity of design and reliability potential with no contamination or fire risk when in the proximity of propellants. In addition, effective damping can be obtained over a wide range of temperatures, from cryogenic to turbine gas environments.

Vibration data taken during testing of the particle damped seal indicate effective damping of seal nonrotating parts with the potential advantages of increasing carbon seal face life and improving leakage characteristics.

CONCEPT DESIGN

PISTON DAMPED SEAL

Figure 4 depicts the final design of the piston damped seal. The parameters of this design are:

Mass (M) = 0.00065 lb sec^2/in.

Spring Rate (K) = 400 lb/in.

Bellows Effective Diameter = 3.60 inches

Piston Diameter = 3.80 inches

Radial Piston Clearances = 0.002, 0.004, 0.006, 0.008, 0.010 inch

The material of the welded bellows is Inconel 750 with 0.006-inch plate thickness. The piston is solid and has a radial clearance maintained constant by three small equally spaced pads on the piston, and contacting the bellows carrier OD.

During the parameter study involving a gas medium, no appreciable damping was obtained for this seal with the small axial motion involved. A damping coefficient of sufficient magnitude is obtained from a liquid nitrogen medium.

The generalized equation solved for use in the parameter study is

$$\frac{d^2x}{dt^2} + Kx + C \left(\frac{dx}{dt} \right)^2 = 0$$
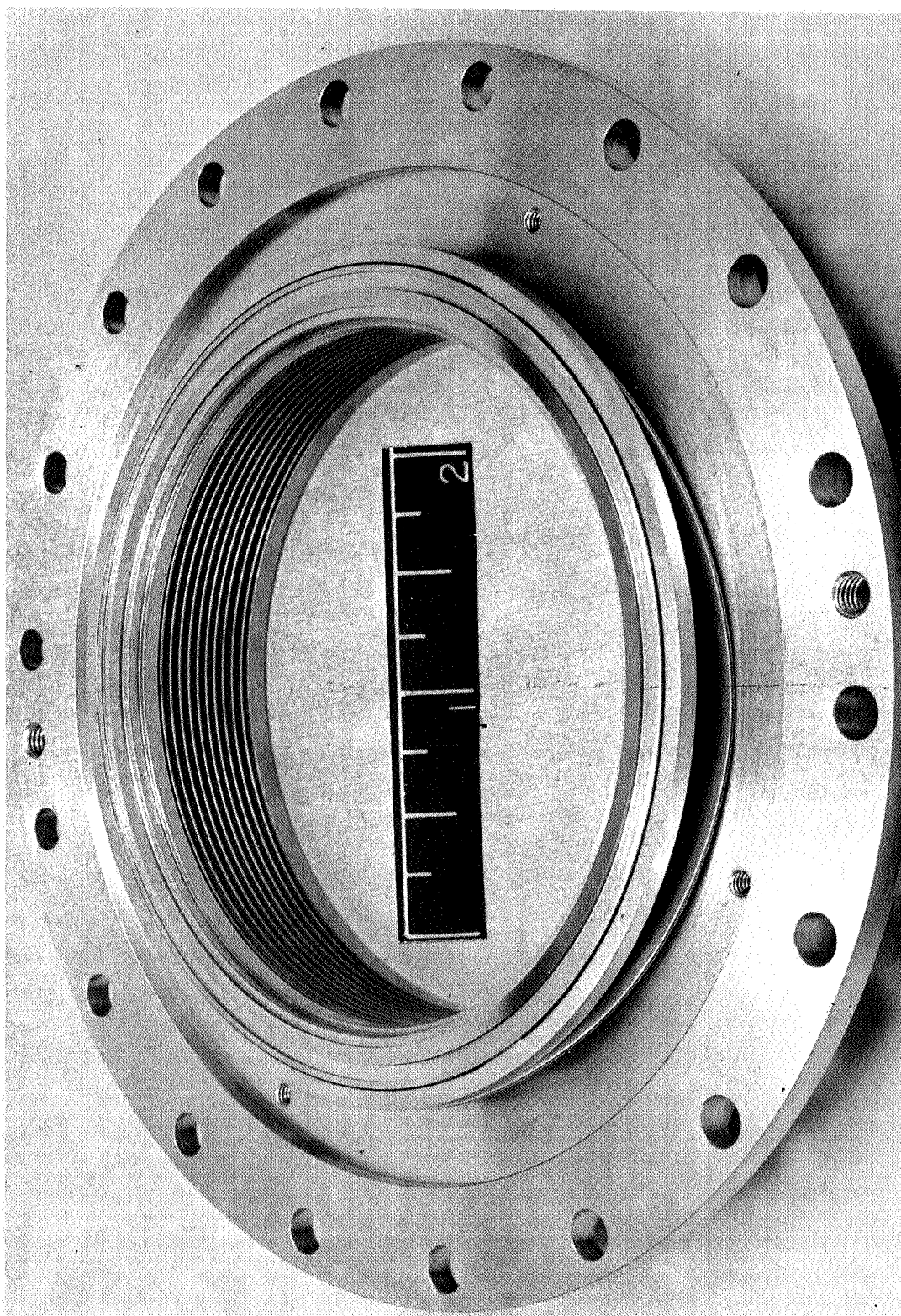
Figure 4. Piston Damped Seal

Turbulent flow was assumed to exist through the piston ring clearance. Figures 5, 6, and 7 show the displacement vs normalized time for several piston ring clearances. Radial clearances from 0.002 to 0.010 inches were evaluated. Table 1 compares some of the results of the parameter study. The additional nomenclature used is as follows:

T = time lapse in milliseconds to reach zero displacement from a unit compression for turbulent flow through the piston clearance.

WN = natural frequency in cps of the spring mass system

C/C_c = Damping ratio of the system for turbulent flow through the clearance

The ratio C/C_c is the ratio of the damping coefficient (c) to the critical damping coefficient (C_c) of the system.

Upon concluding the parameter study which resulted in defining the physical size of the seal and establishing the limits of control parameters with respect to computed damping characteristics, the hydraulic balance and unit face load of the seal was considered.

Seal face loading is one of the primary factors affecting sealing and dynamic seal life, and is dependent on two forces; the spring load exerted by the bellows and the hydraulic force imposed on the bellows plates by the environmental pressure.

Because the bellows plates will deform due to either a change in pressure or deflected length (Δl), the bellows characteristics are closely examined. The effect of bellows deformation changes the effective hydraulic area of the plates and directly affects the seal face loading. The hydraulic

17
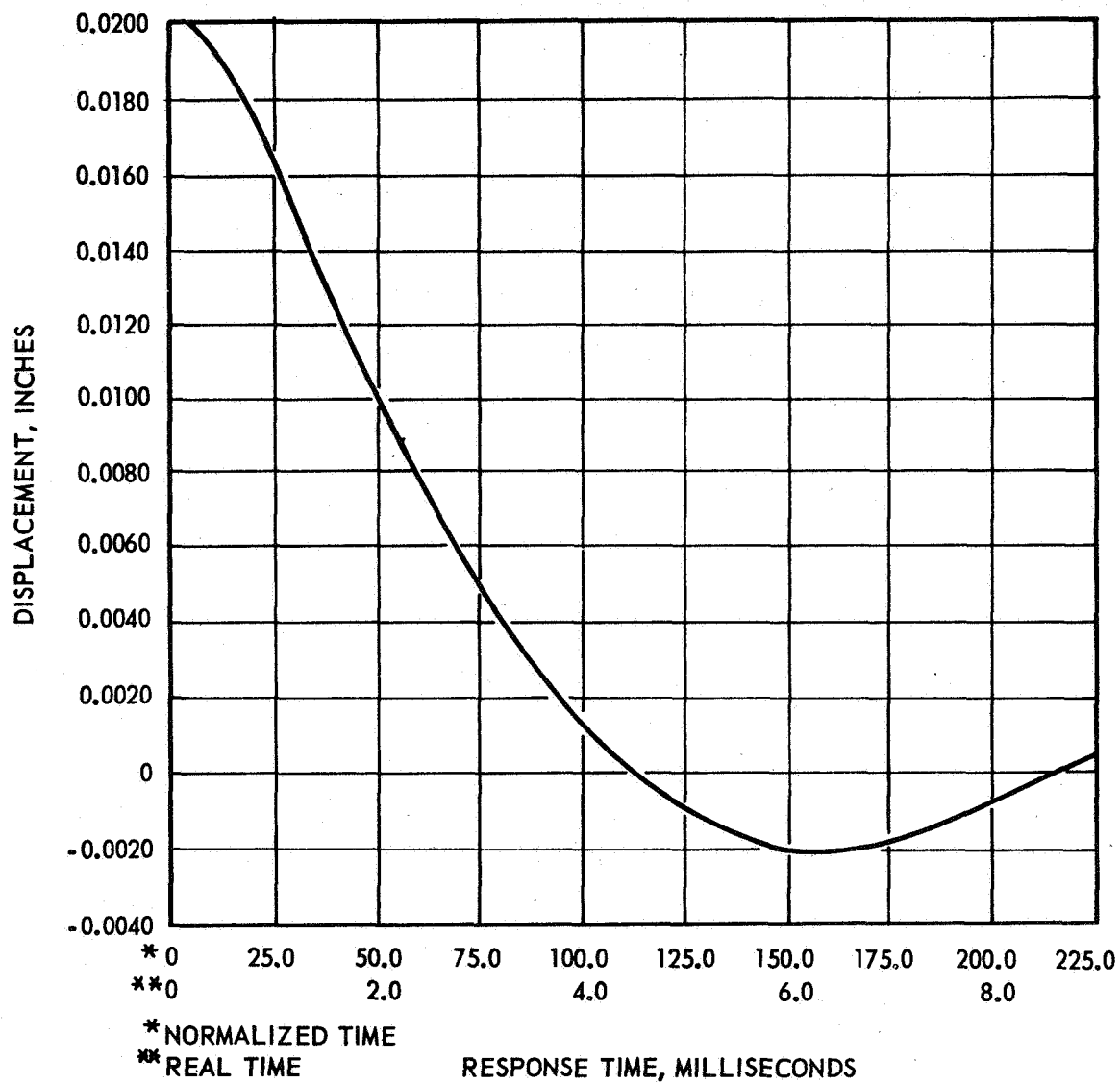
Figure 5. Computer Data on Piston Damped Seal, Radial Clearance = 0.002 inch

18
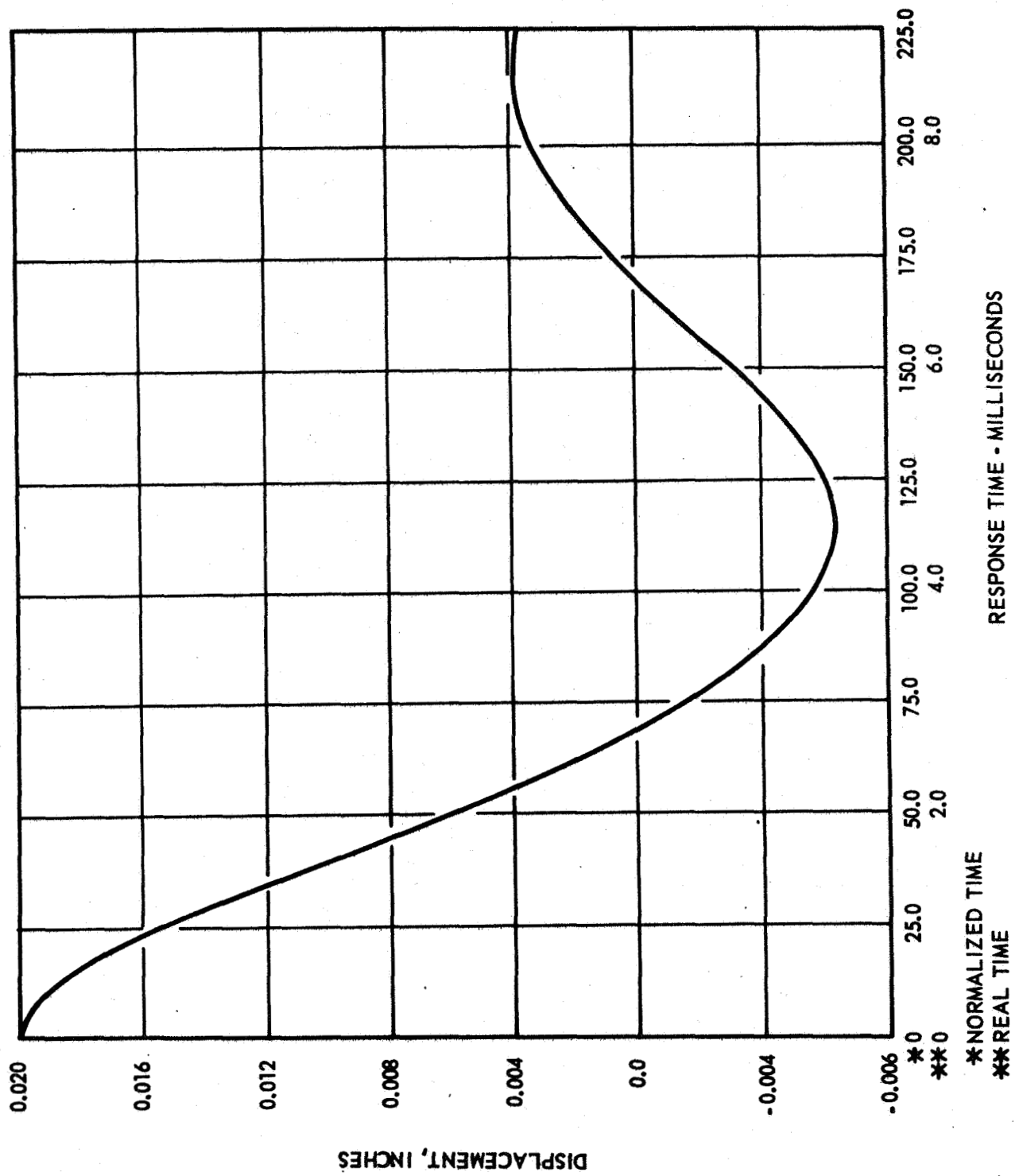
Figure 6. Computer Data on Piston Damped Seal, Radial Clearance = 0.003 inch

19
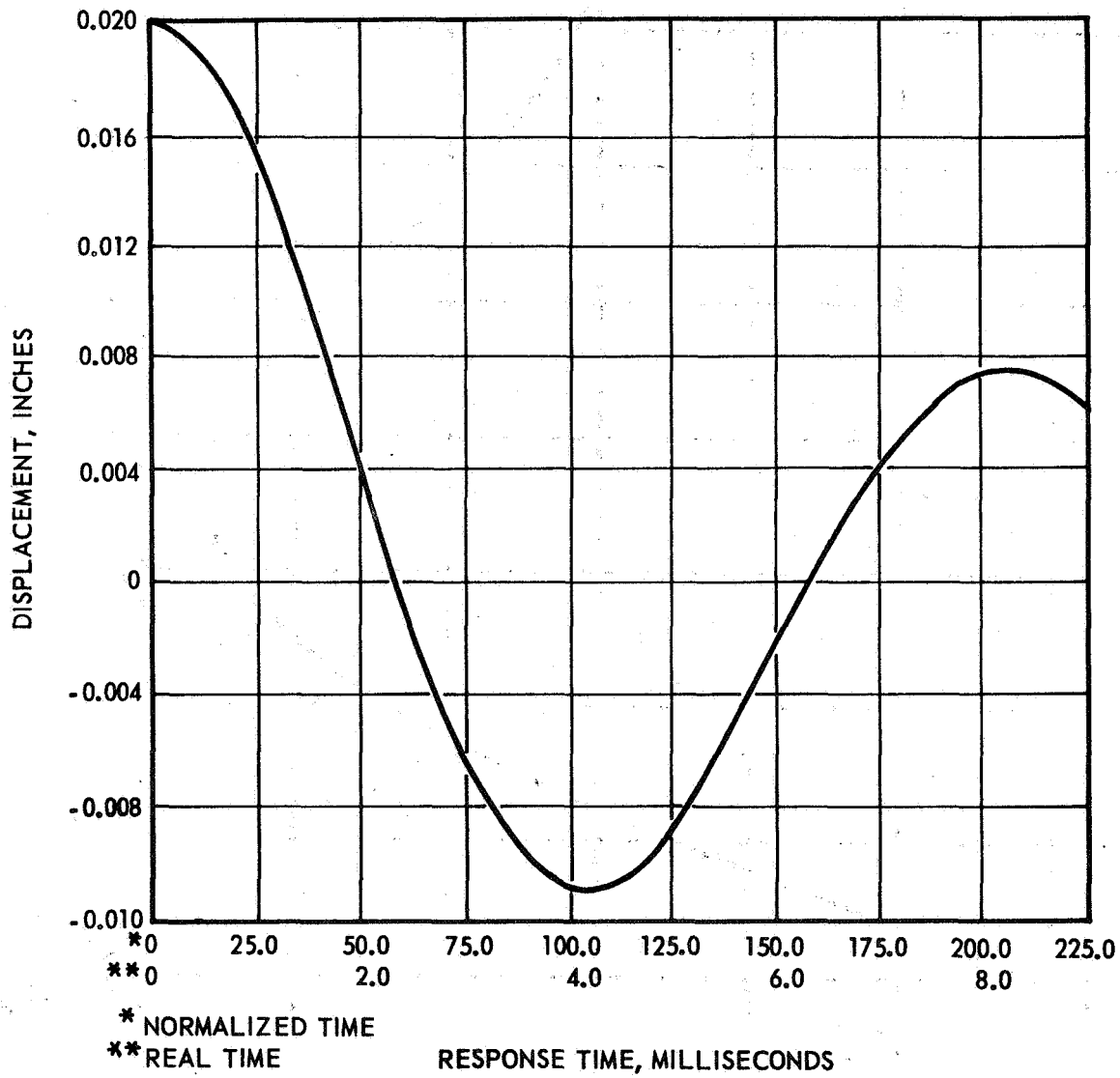
Figure 7.   Computer Data on Piston Damped Seal,
Radial Clearance = 0.04 inch

TABLE 1

COMPUTER RESULTS, PISTON SEAL

M, lb sec^2/in	K, lb/in	RC, inches	RB, inches	RN, inches	H, inches	Xo, inches	WN, cps	C/C$_c$ X10^4	T, Millesiconds
0.00065	400	1.900	1.800	1.840	0.002	0.020	125	1540	4.5
					0.003			450	2.7
					0.004			190	2.3
					0.005			99	2.18
					0.010			12	2.05
					0.020			1.5	2.04
					0.005	0.050		99	2.39
					0.010			12	2.08
					0.020			1.5	2.04
					0.005		139	88	2.14
	500				0.010			11	1.86
					0.020			1.4	1.83

analogy is normally used in considering seal operation; therefore, a change in deformation changes the hydraulic area. The effective hydraulic area is a computed value, normally in terms of the effective diameter (De) as shown below.
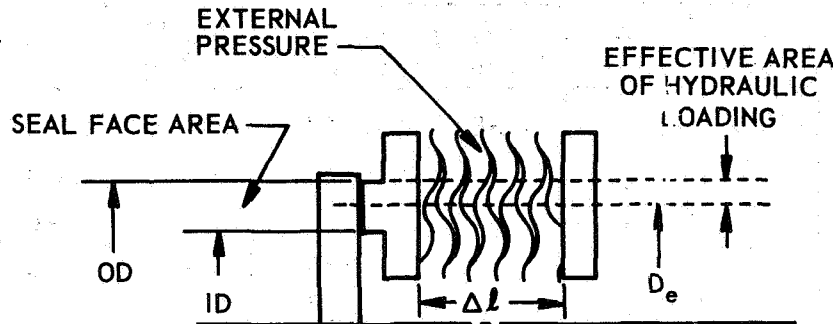
Computation of the effective diameter in this case does not include the pressure distribution across the seal face width because during tests to obtain seal face loading data, the face is coated with an adhesive to establish a known sealing point at the seal face OD.

Therefore, the effective hydraulic area is

$$\pi/4 \ (OD^2 - D_e{}^2) = \frac{Fh}{P}$$

where

$$Fh \ = \ \text{hydraulic force}$$

$$P \ = \ \text{imposed pressure}$$

$$D_e \ = \sqrt{OD^2 - \frac{4Fh}{\pi \, P}}$$

For computation of the seal face diameters a balance ratio is required which is expressed as

$$B = \frac{\text{effective hydraulic area}}{\text{seal face area (Af)}}$$

A balance ratio of 0.7 was chosen for these seal designs to provide a margin for dimensional tolerances and variation of pressure distribution across the seal face.

Based on hydraulic force data obtained from the seal vendor, the seal face diameters are computed relative to the established balance ratio of 0.7. For this case, the diameters chosen are:

$$OD \ 3.680 \ ^{+0.000}_{-0.002}$$

$$ID \ 3.516 \ ^{+0.002}_{-0.000}$$

ORIFICE DAMPED SEAL

Figure 8 depicts the final design of the orifice damped seal. Listed below are the control parameters governing operation of the seal.

$$M_1 \ = \ 0.0009 \ \frac{lb\text{-}sec^2}{in.}$$

$$A_3 \ = \ 0.20 \ sq \ in. \ to \ 0.05 \ sq \ in.$$

$$N \ = \ 15 \ to \ 25$$

$$M_2 \ = \ 0.0012 \ \frac{lb.\text{-}sec^2}{in.}$$

$$K_1 \ = \ 500 \ lb/in.$$

$$A_1 \ = \ 4.1 \ sq \ in.$$

$$K_2 \ = \ 2000 \ lb/in.$$

$$A_2 \ = \ 5.0 \ sq \ in.$$

where

M_1 = effective mass of seal and fitting

M_2 = effective mass of compensator end fitting

A_1 = area of seal cavity

Labels in figure:
- Housing
- Primary Bellows
- Compensator Bellows Assy.
- 2 Filling Ports for Damping Fluid
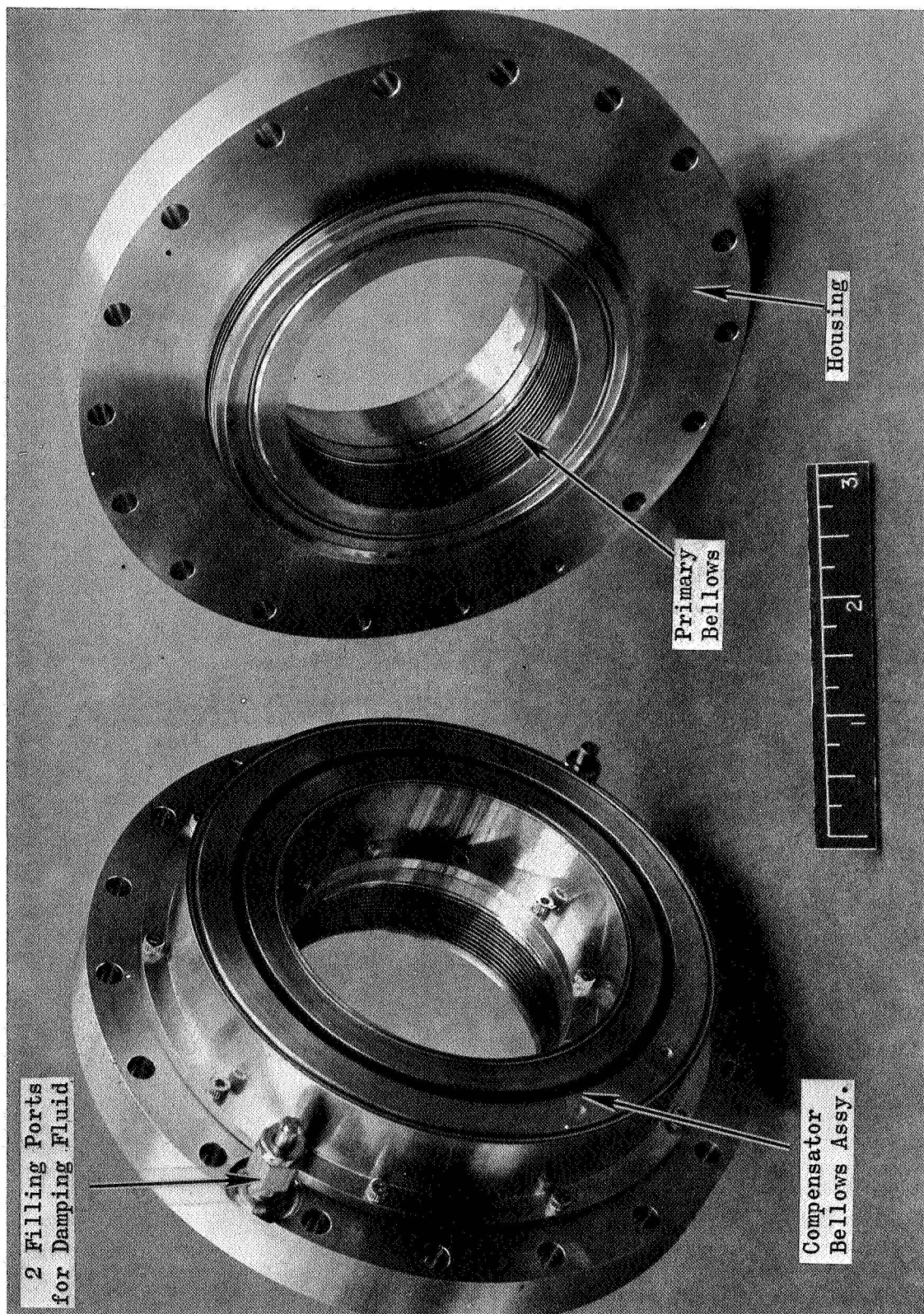
5AJ31-12/9/65-C1

Figure 8. Orifice Damped Seal

24

A_2 = area of compensator cavity

A_3 = total area of orifice

N = number of holes

K_1 = spring rate of seal bellows

K_2 = spring rate of compensator bellows

The generalized equations solved for the fluid conditions of laminar and turbulent flow are

$$\frac{d^2x}{dt^2} + Kx + \frac{C_{dx}}{dt} = 0 \text{ for laminar}$$

and

$$\frac{d^2x}{dt^2} + Kx + C\left(\frac{dx}{dt}\right)^2 = 0 \text{ for turbulent}$$

Some of the results of the computer study varying the control parameters are shown in Table 2.

Computer analysis indicates damping can be obtained with the described system using liquid nitrogen; however, a stable condition of liquid is required during all periods of operation. Sodium potassium, used as the damping medium, is a more predictable fluid especially in a temperature environment of 1000 F or greater.

Sodium potassium is a eutectic alloy called NaK - 77 (77-percent K and 23-percent Na) and is being used as the damping medium in the orifice damped seals for operation in a 1000 F gaseous environment. A review of the present day hydraulic fluids revealed that they would not be as satisfactory as NaK over the temperature range of interest, 70 to 1000 F.

TABLE 2

COMPUTER RESULTS, ORIFICE SEAL

M_1 lb sec²/ sq in	M_2 lb sec²/ sq in	A_1 sq in	A_2 sq in	K_1 lb/sq in	K_2 lb/sq in	A_3 sq in	N	D_o, inch	$T(l)$ milli-second	$T(t)$ milli-second	Wn, cps	C/Cc (t) X10⁴	C/Cc (l) X10⁴
0.0009	0.0012	4	5.0	500	2000	0.20	15 →	0.132	1.34	1.46	190	1.00	1.68
						0.10		0.092	1.55	2.19	164	3.47	8.22
		NaK DAMPING MEDIUM				0.05	20 →	0.066	1.91	5.25	134	11.30	37.87
						0.20		0.112	1.34	1.47	190	1.34	1.94
						0.10	25 →	0.080	1.55	2.29	164	4.62	9.49
						0.20		0.100	1.34	1.49	190	1.67	2.17
						0.10		0.070	1.55	2.39	164	5.78	10.61
						0.05		0.050	1.91	1.59	134	18.84	48.89
						0.20	15 →	0.132	1.36	1.49	187	0.28	1.82
		IN₂ DAMPING MEDIUM				0.10		0.092	1.59	2.27	160	0.97	8.82
						0.05	20 →	0.066	1.97	5.57	129	3.14	40.32
						0.20		0.112	1.36	1.51	187	0.38	2.10
						0.10	25 →	0.080	1.59	2.39	160	1.29	10.18
						0.20		0.100	1.36	1.53	187	0.47	2.35
						0.10		0.070	1.59	2.49	160	1.61	11.39
						0.05		0.050	1.97	1.57	129	5.24	52.06

NOMENCLATURE

(l) = LAMINAR
(t) = TURBULENT
N = NO. OF HOLES
Do = DIAMETER OF ORIFICE
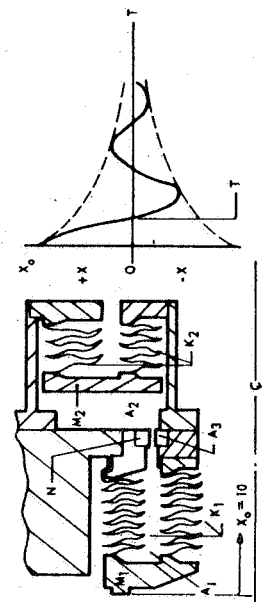
The properties of interest in this program are wide operating temperature range, low density, high thermal conductivity, and relatively good chemical stability. NaK-77 has a melting point of 12 F and boils at about 1443 F under atmospheric pressure. The density is comparable to that of conventional hydraulic fluids, while its viscosity is somewhat lower than that of water. Figures 9 through 13 show the vapor pressure, viscosity, density, thermal conductivity, and specific heat of NaK-77 as a function of temperature.

Because of the hazards imposed when using NaK, safety precautions are required. Listed below is an outline to show the response of NaK to certain environments.

1. Water reacts violently with NaK, to form hydrogen gas and the oxides and hydroxides of sodium and potassium. The heat of reaction is great enough to ignite mixtures of hydrogen and oxygen if air is present.

2. Alcohols react mildly with NaK at room temperature and may be used for cleaning under controlled conditions. Reaction is fastest with methyl and ethyl alcohol, slower with the heavier alcohols such as propyl and butyl. Air must be excluded from the cleaning system.

3. At room temperature, bulk NaK open to the air reacts slowly with oxygen to form a surface scum. If spilled, small particles of NaK may ignite spontaneously, particularly with dust and many combustible materials. The ignition temperature for bulk NaK in air is about 400 F.

4. Carbon tetrachloride reacts violently and explosively with NaK.
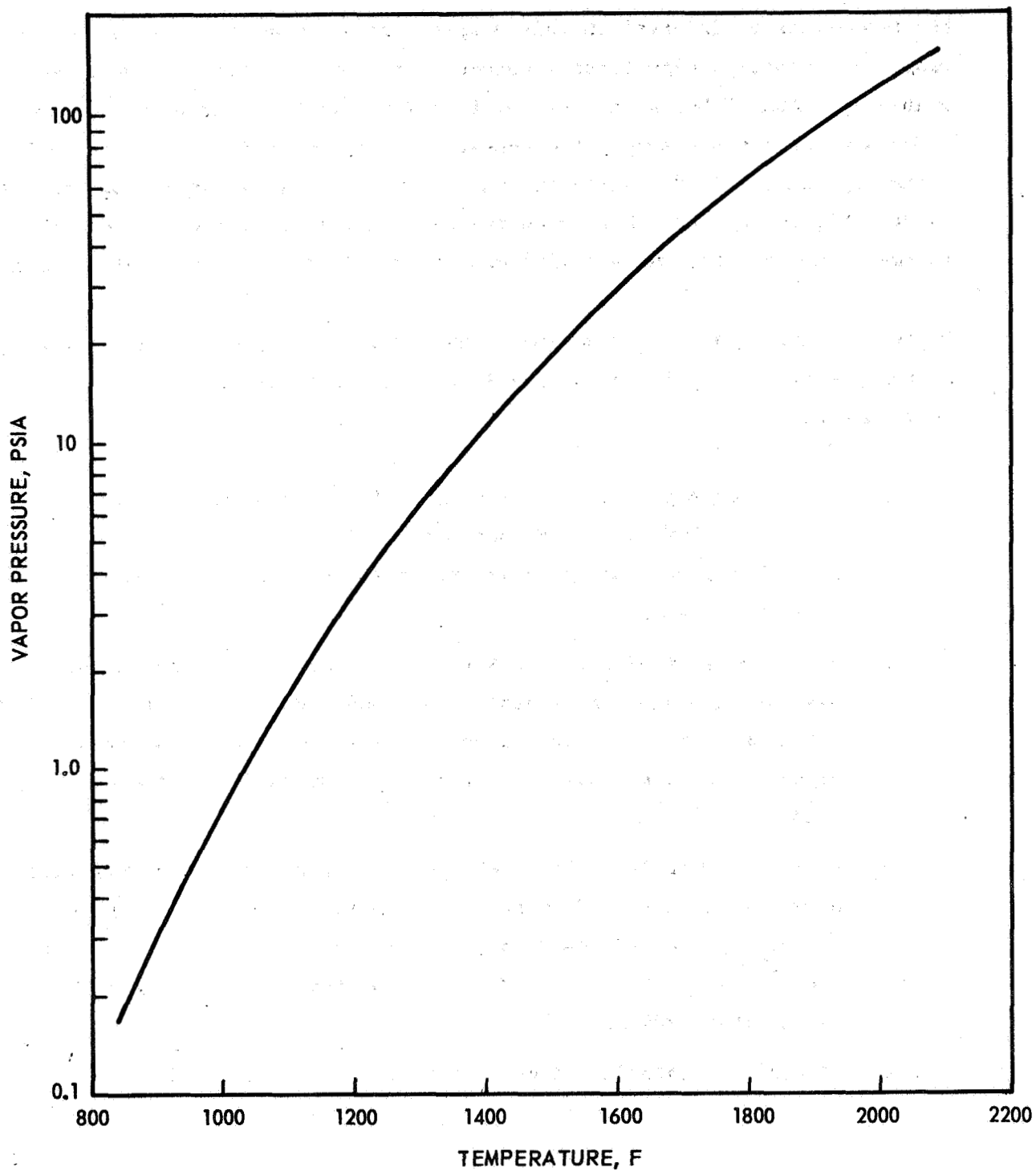
Figure 9.   Vapor Pressure vs Temperature, NaK-77
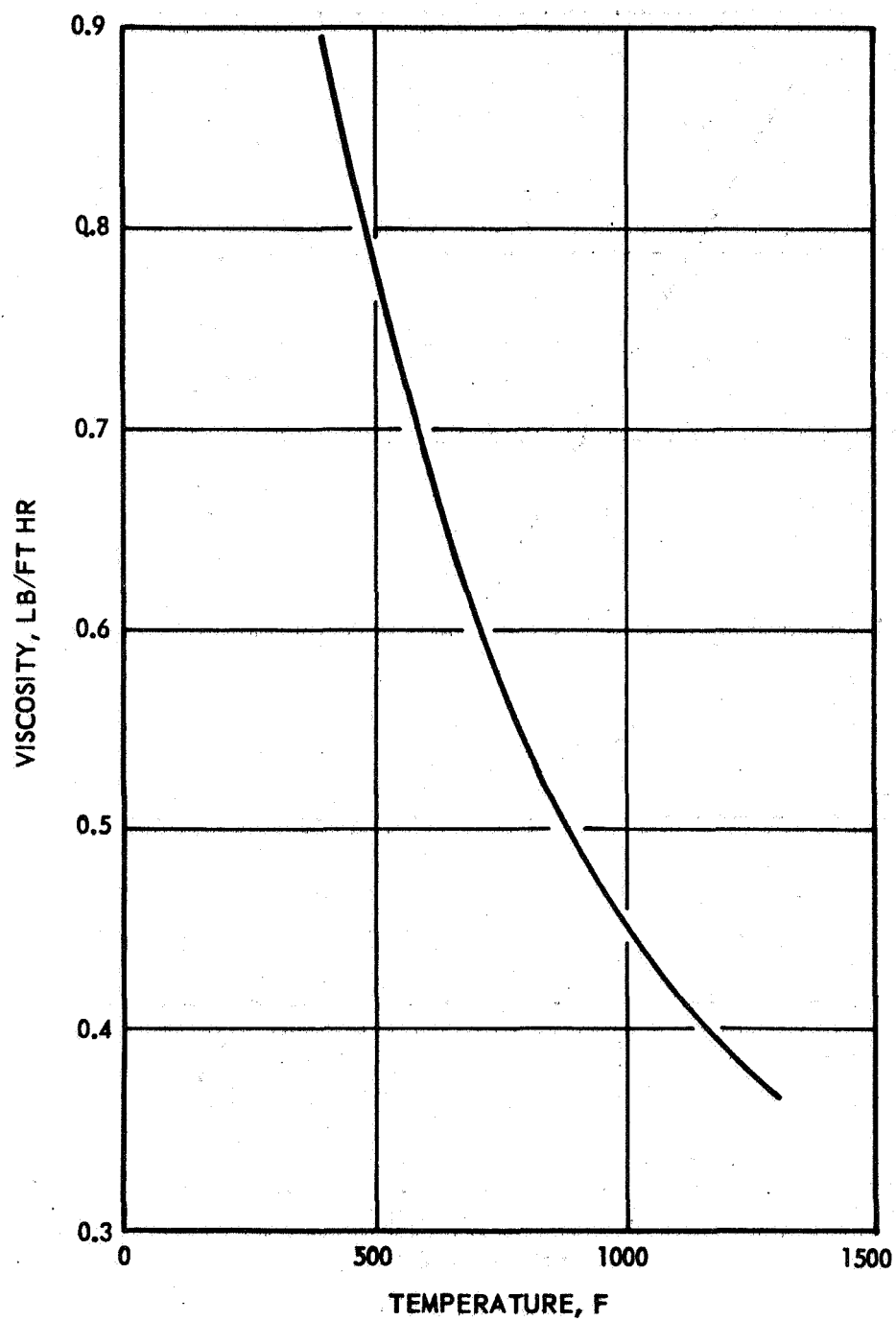
Figure 10. Viscosity vs Temperature, NaK-77
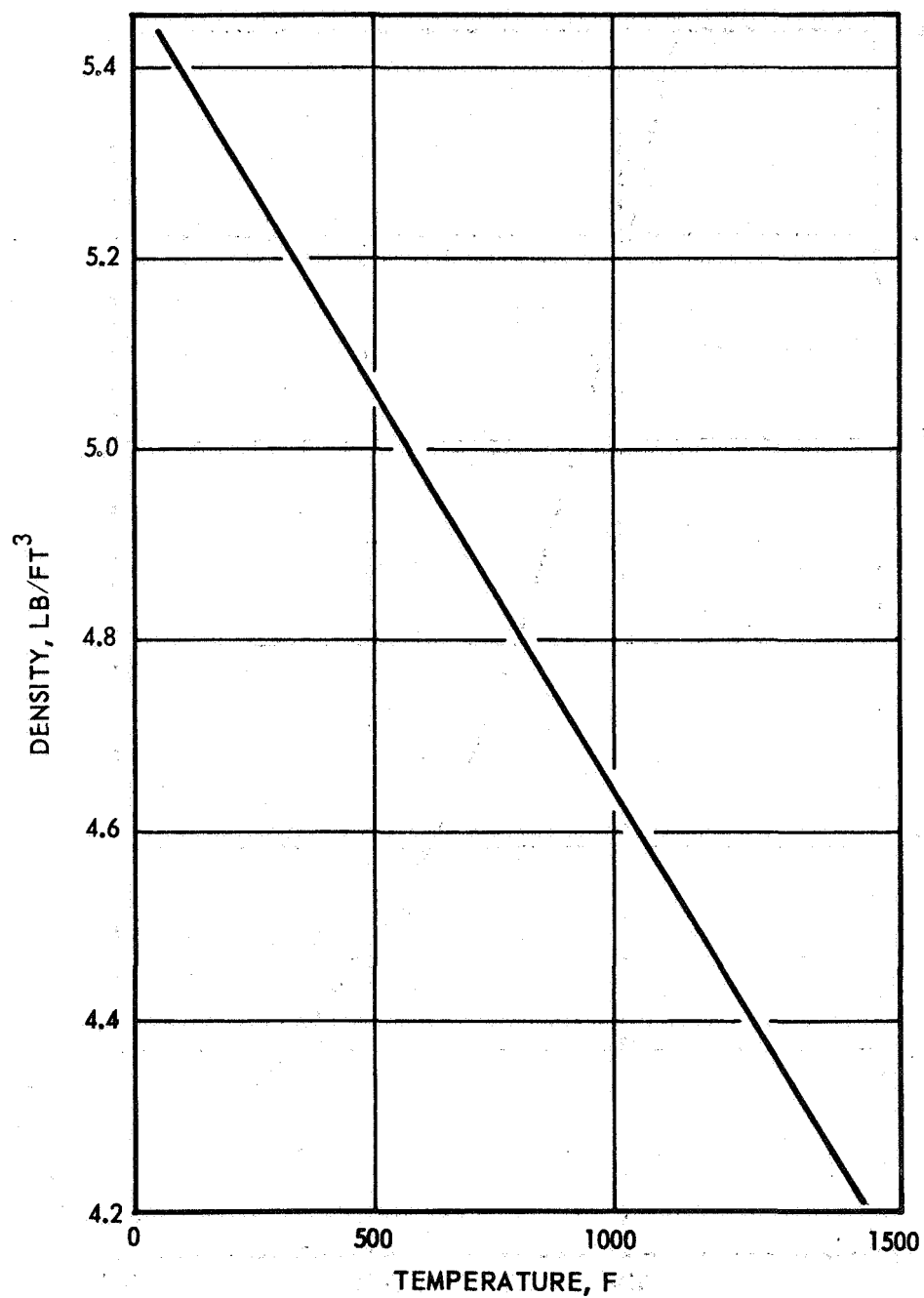
Figure 11. Density vs Temperature, NaK-77
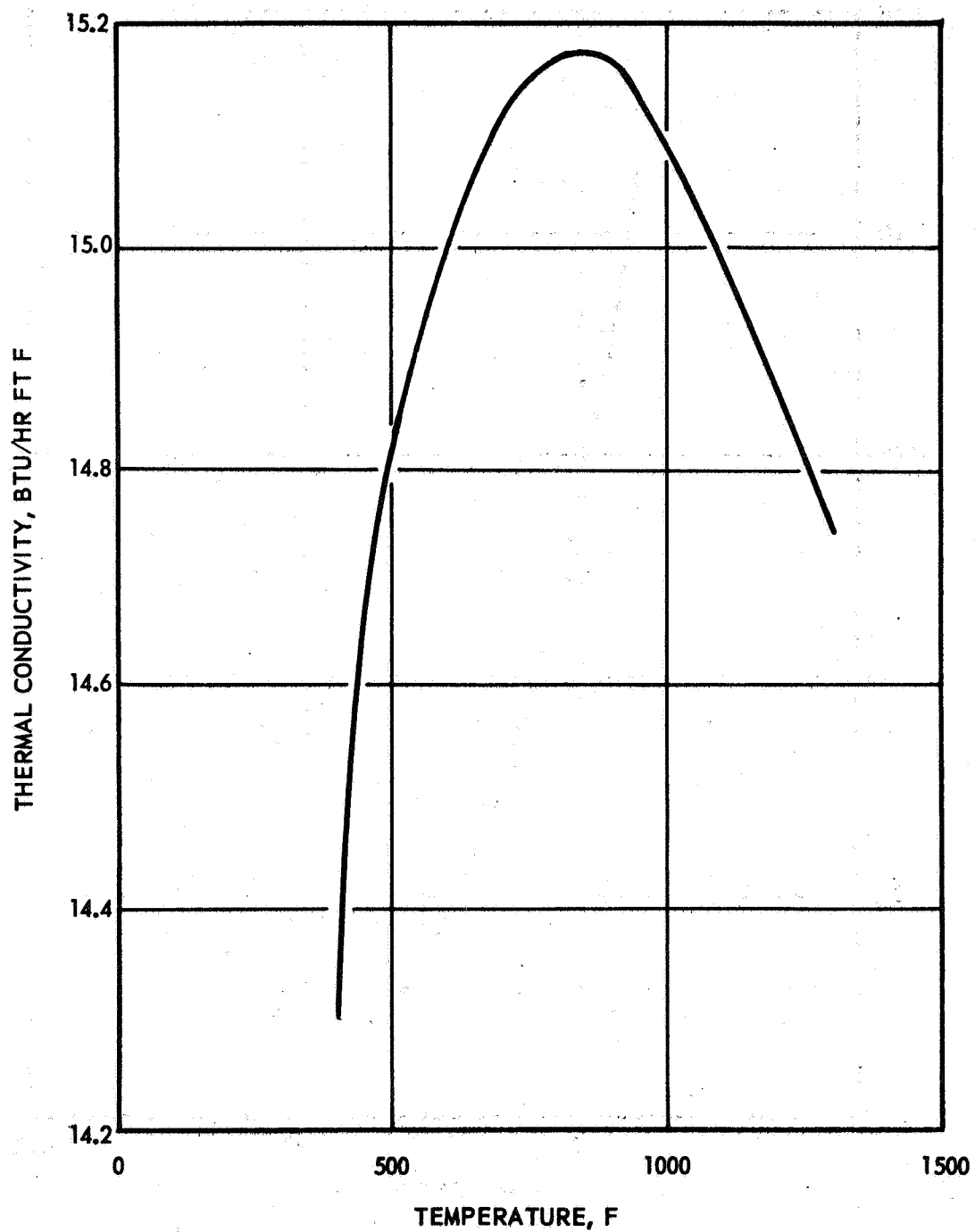
Figure 12. Thermal Conductivity vs Temperature, NaK-77
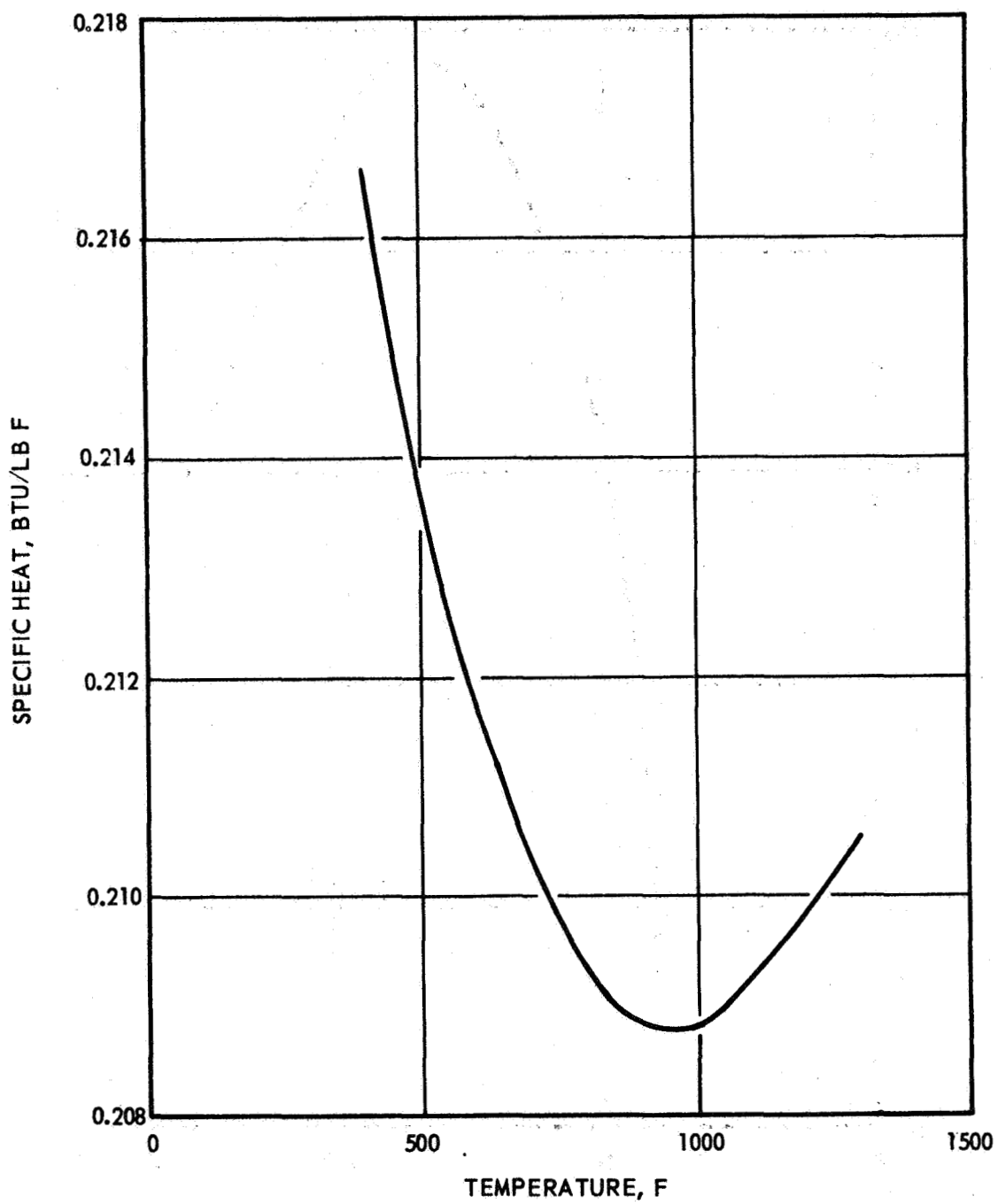
Figure 13. Specific Heat vs Temperature, NaK-77

5. Trichloroethylene froms highly unstable, dangerously explosive dichloroacetylene.

6. Natural hydrocarbons from refined petroleum oil are inert. Kerosene and white mineral oil are very useful in flushing the system and excluding air from the surface of NaK in open containers.

7. Carbon dioxide is considered dangerously reactive.

8. Fire extinguishing materials are dry calcium carbonate, dry sand, and dry sodium chloride.

Corrosive attack of NaK on Inconel 750 was considered to be a problem in high-temperature testing, one requiring investigation. There are several important modes of attack.

One is mass transfer, in which elements from one metal in one part of the system are dissolved and reprecipitated in another part of the system. Grain boundaries are also attacked through fingerlike dissolution along the boundaries, uneven surfaces, or as slivers of corrosion product in between grains. Dissolution of stringers of inclusions is a mode of attack of particular importance with welded bellows plates. Plate stock rolled in a "dirty" condition or else welded without proper cleaning will have soluible inclusions in the bellows plate as well as in the weld bead. NaK will dissolve these stringers and weaken the structural joint. Stress corrosion is also a potential failure mode with the welded bellows seal.

An Inconel 750 TIG welded bellows specimen, made under current state-of-the-art of seal vendor weld specifications, was submerged in NaK for 7 hours at 1000 F. The bellows specimen was compressed to induce tensile stresses in the bellows. Figures 14 and 15 show the test specimen after
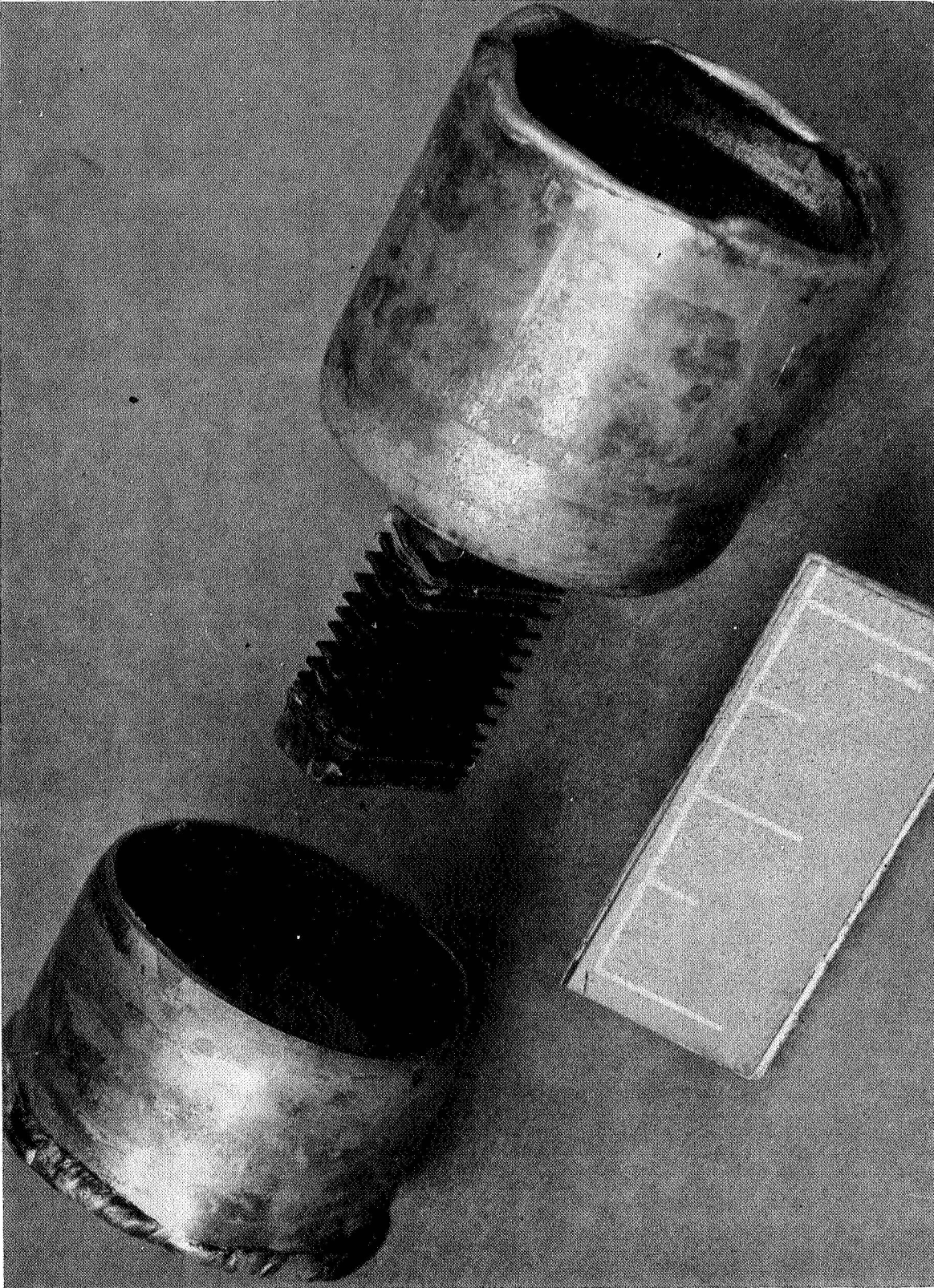
Figure 14. NaK Exposed Bellows (View A)
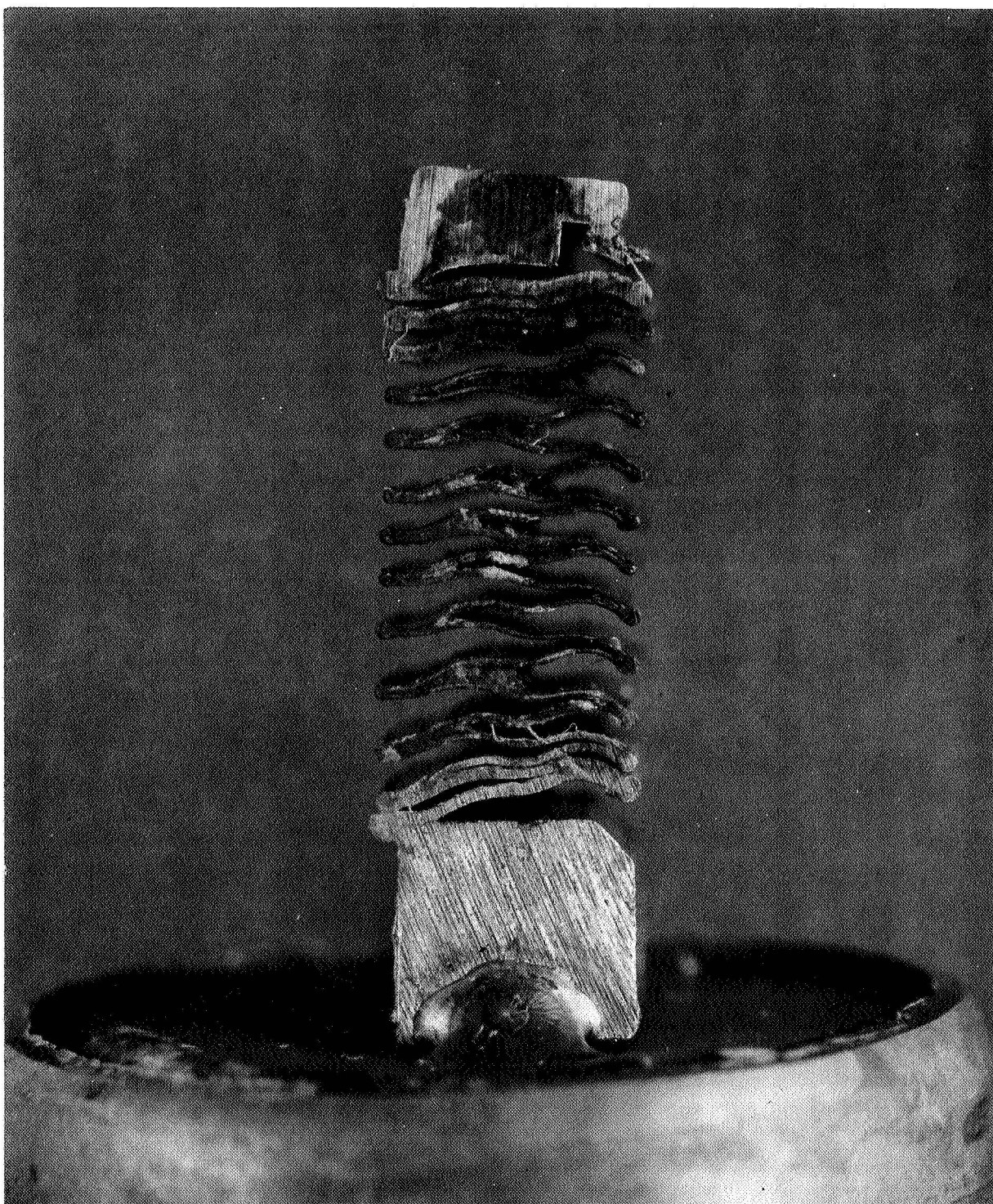
Figure 15. NaK Exposed Bellows (View B)

exposure. The bellows is Inconel 750, the end fittings are Inconel 600, and the can enclosure is Inconel 750. The can enclosure with the specimen and NaK was welded shut in an argon atmosphere. The residue between the bellows plates as shown in Fig. 15 is oxide scum formed when the specimen was cleaned with water after exposure.

Posttest inspection revealed the bellows to be satisfactory. Mass transfer and stress corrosion cracking were not observed; however, some dissolution did take place along the grain boundaries of the Inconel 600 end fitting. Oxide scale formed during welding in the bead root was dissolved. This attack was confined to the outer surface but does stress the importance of "clean" welds.

PARTICLE DAMPED SEAL

Initially, a feasibility study was conducted to determine the damping potential of metal powder. Molybolenum was selected on the basis of availability.

Various sizes of spherical powder was purchased and a simple test model was fabricated. The test model consists of two aluminum blocks with a series of drilled holes to contain the spherical particles. The blocks are clamped together on a spring beam and mounted to the vibration plate as shown in Fig. 16.
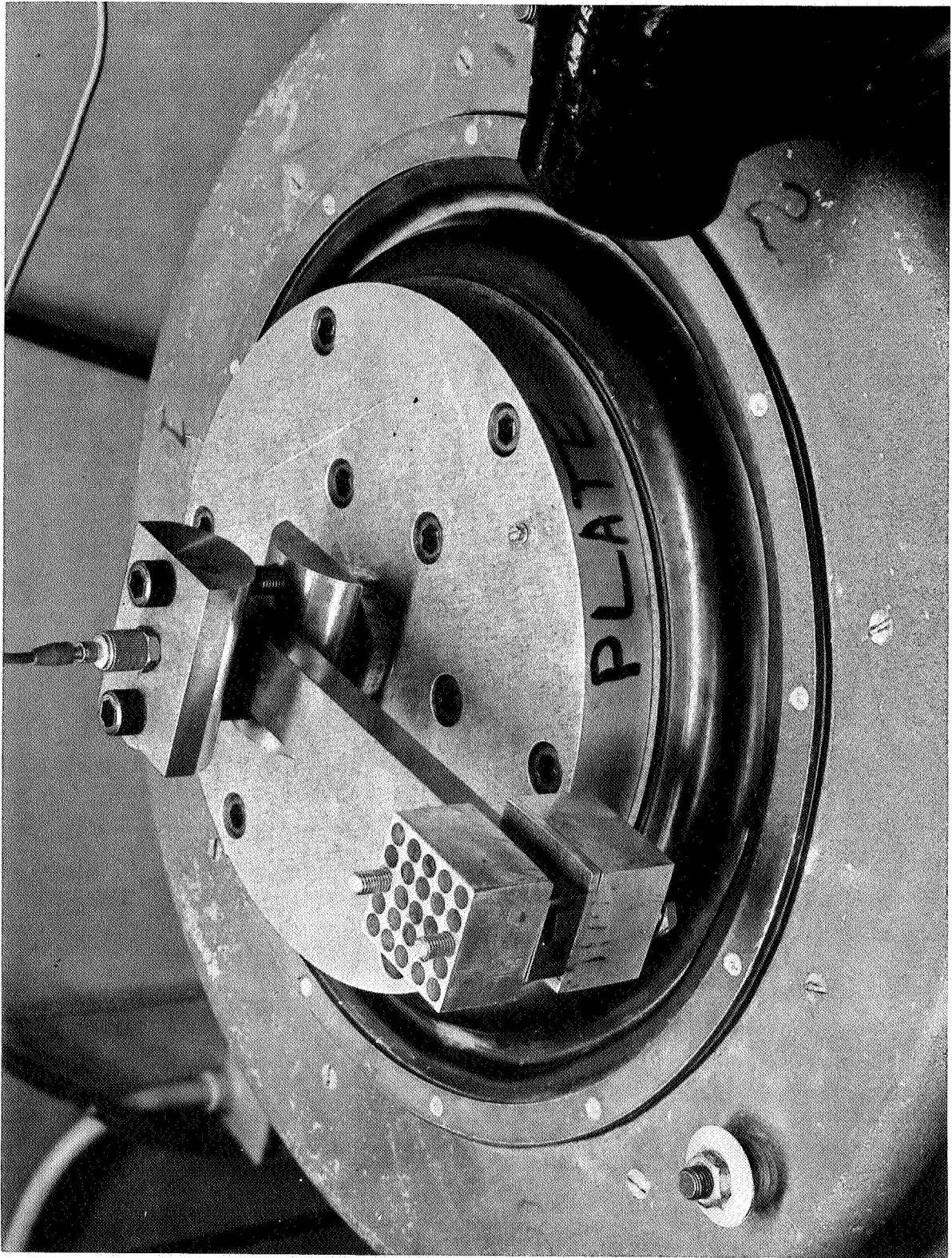
Figure 16. Particle Damping Test Setup

Table 3 gives the characteristics of the particles tested:

TABLE 3

SIZE, WEIGHT, AND DENSITY OF
SPHERICAL MOLY PARTICLES
(SIX SAMPLES CONSIDERED)

Sample No.	Diameter		Weight, Grams	Approximate Density, lb/in.^{3}
	Inches	Microns		
1	+0.0059	149	276.75	0.232
2	0.0059/0.0043	149/131	184.50	0.230
3	0.0043/0.0035	131/88	982.65	0.225
4	0.0035/0.0029	88/74	149.00	0.225
5	0.0029/0.0023	74/57.5	251.15	0.226
6	0.0023/0.0017	57.5/44	245.90	0.226

NOTE: The quantity of particles above represents the quantity
available for the test and not the amount actually
used.

Two methods of determining the amount of damping were employed: (1) forced
vibration, and (2) free vibration.

Forced Vibration

The exciting force is held constant (2 g-peak) and the exciting frequency
is varied. The damping is determined by measuring the bandwidth of resonance

peak at the half-power points in terms of normalized frequency. The formula
is as follows:

$$\Delta f \equiv \text{damping} \equiv 3.14 \left(\frac{f_2}{f_n} - \frac{f_1}{f_n} \right)$$

where

f_n = resonant frequency

f_1 = lower half-power frequency

f_2 = upper half-power frequency

Free Vibration

One end of the beam is fixed and the other end is deflected and then allowed
to freely return to its starting reference point. The damping is determined
from the rate of decay of oscillation. This method is defined as the logari-
thmic decrement, and it is the natural logarithm of the ratio of any two
successive amplitudes:

$$\Delta \equiv \text{damping} \equiv \ln \frac{X_2}{X_1}$$

where

ln = natural logarithm

X_1 = first cycle amplitude

X_2 = second cycle amplitude

The forced vibration method of testing was the most successful and reliable. Because of the loss of energy to the beam support, the data from the free vibration method was inconsistent.

In addition to damping, the frequency at resonance and the amplification at resonance were measured and recorded. The amplification is defined as the ratio of the acceleration into the beam to the acceleration out of the beam.

$$\text{Amplification} = \frac{G \text{ out}}{G \text{ in}} \quad \text{or} \quad \frac{Ao}{Ai}$$

Tests were run on all six particle sizes with the fixture half-full and on four particle sizes with the fixture full. There were not enough particles of the No. 2 and No. 4 sizes to fill the fixture. The results of the tests are as follows:

Particle	Half Full				Full			
	Fn	Ao/Ai	Δ f	Δ	Fn	Ao/Ai	Δ f	Δ
No. 1	165	10.80	0.368	0.288	155	4.51	0.735	0.523
No. 2	164	11.00	0.282	0.157				
No. 3	163	8.91	0.325	0.214	143	3.38	1.156	0.521
No. 4	162	7.36	0.416	0.273				
No. 5	162	6.49	0.543	0.300	149	3.61	1.081	0.826
No. 6	159	5.82	0.663	0.434	149	3.87	0.950	0.877
Empty	170	37.80	0.100	0.070				

Fn = resonant frequency Δ f = forced vibration damping

Ao/Ai = amplification Δ = free vibration damping

The results of the test clearly indicate that the best damping character-
istics are obtained with the No. 6 size particles. As the particle diameters
decreased, from size No. 1 to Size No. 6, the resonant frequency decreased,
the amplification decreased, and the damping from both the free and the
forced vibration increased.

A test was conducted to determine what portion of the damping was caused
by the mass of the particles and what portion was caused by the motion of
the particles.

Two steel masses (equal to the particle mass) were attached to the empty
particle holders and the test conducted in the same manner as the previous
tests. The test was repeated with one of the steel masses removed. The
results shown below indicate that the masses caused the resonant frequency
to decrease, the amplification to increase, and the damping to decrease.

Weight, grams	Fn, cps	Ao/Ai	Δ F	Δ
91.5	144	59.8	0.054	0.094
185.5	129	50.0	0.074	0.094

Comparing the test results further indicates that damping can be attributed
to relative movement of the particles in the container and that a solid
mass of particles would have no effective damping.

Damping was next measured with the No. 6 particle size varying the quantity
by weight from 50 to 200 grams. This was done to determine the effects
of different amounts of the same particle size on damping. Figures 17 and
18 show the results of the tests from forced vibration and free vibration.
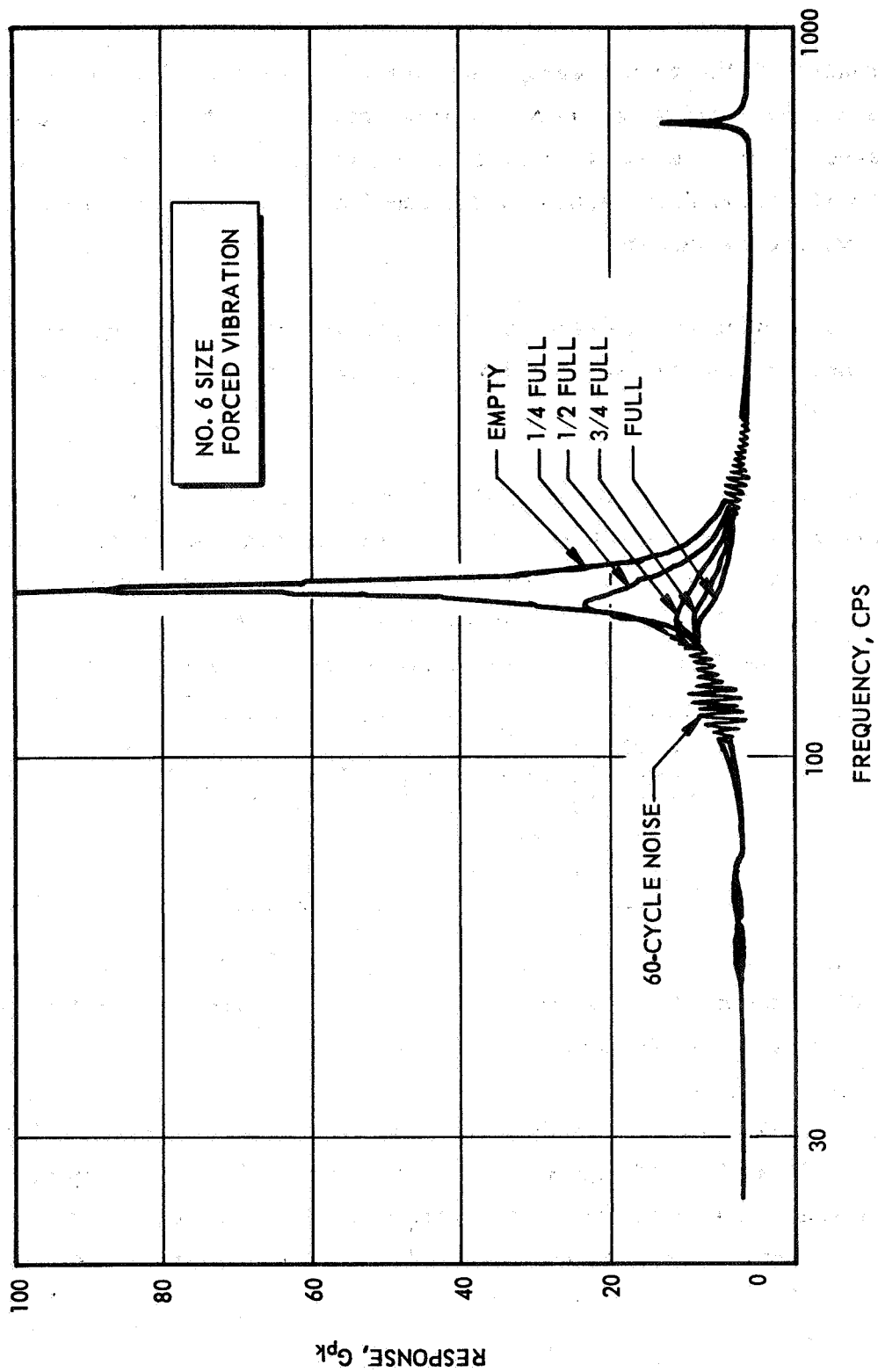
Figure 17. Particle Vibration Test
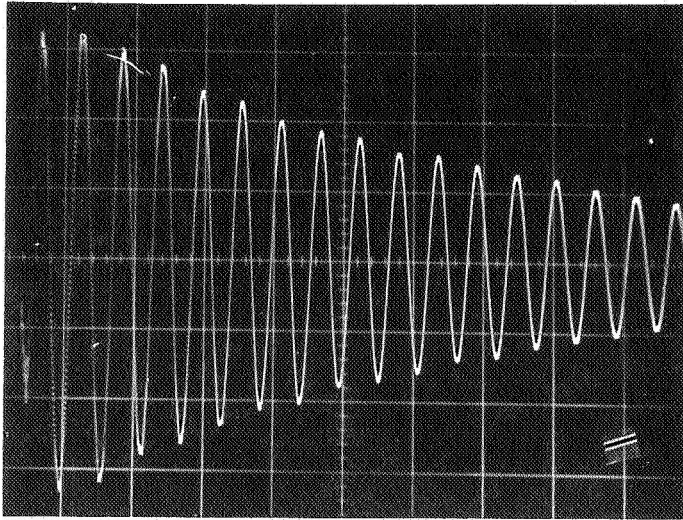
Test 3

No. 6 Size Particles

Empty
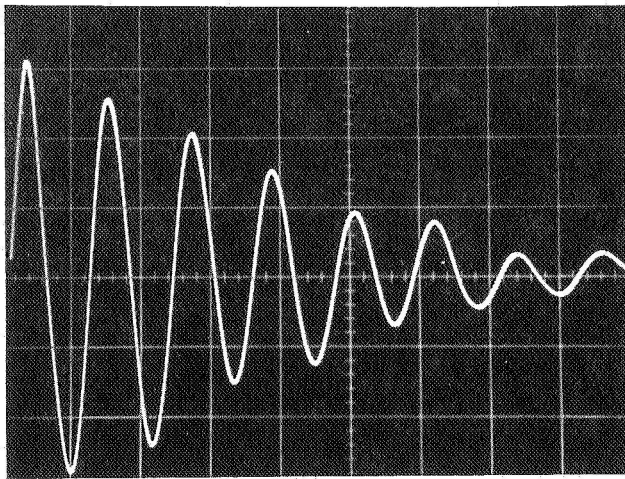
One-Fourth Full
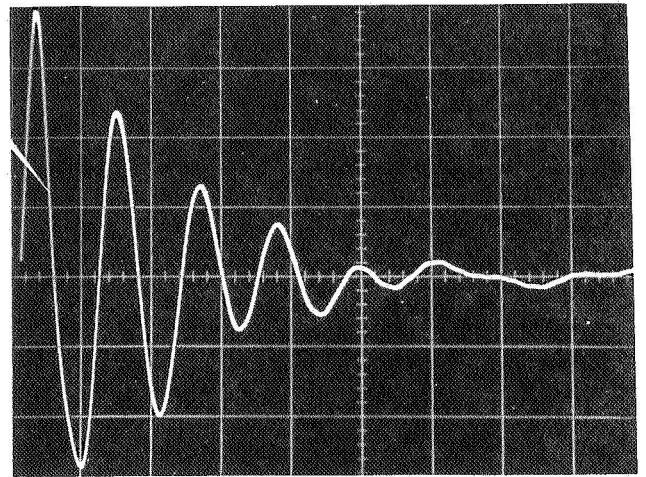
One-Half Full.
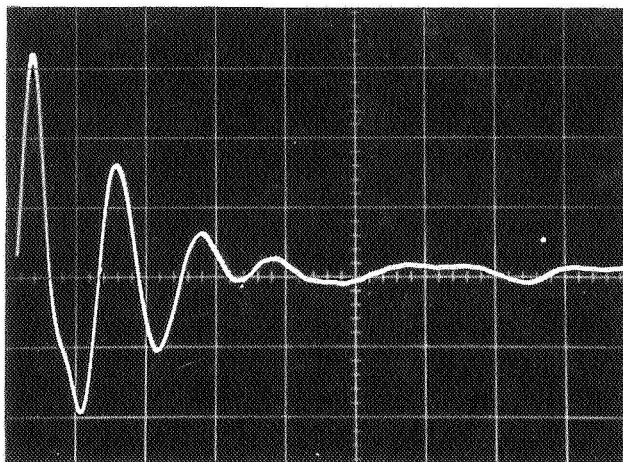
Three-Fourths Full
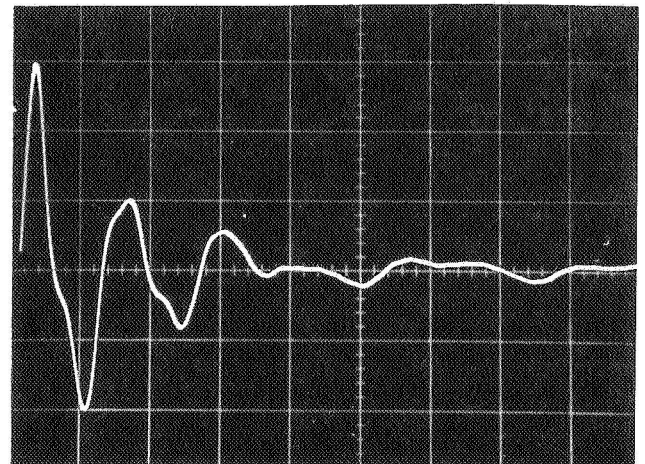
Full

Figure 18. Free Vibration Test Data

43

The tabulated results shown below indicate that as the number of particles increase, the resonant frequency decreased, the amplification decreased, and the damping increased. The results also show that only a small change in damping occurs from half-full to full.

	Weight, grams	Fn, cps	Ao/Ai	Δf	Δ
Empty	–	172	49.10	–	–
1/4 full	50	162	11.90	0.281	0.211
1/2 full	100	156	5.60	0.700	0.622
3/4 full	150	146	4.10	1.086	0.679
Full	200	144	3.99	1.003	1.076

A test was also conducted to note any change in effective damping when a given mass of particles is loaded in two different ways. One hundred grams of the No. 6 size particles were loaded in such a way that all of the holes were half-full. The forced vibration test was then run, and repeated with the same mass loaded, in which half the holes were empty and the other half were full. The results showed that no significant change in resonant frequency, amplification, or damping occurred.

The following general conclusions were drawn:

1. Particle damping is effective on the basis of the test model considered.

2. Damping increases with decreasing particle diameter.

3. Damping increases with increasing quantity of particles within the known limits of the test model considered.

4. Damping is unaffected by how a given mass of particles is loaded in the fixture.

44

Based on the results obtained from the vibration tests, several methods were conceived to encapsulate the particles and apply the effective damping to a bellows seal. The dimensional size of the seal was based on the mass ratio of the test model. The mass characteristics being as follows:

Mass of the spring system including the beam and particle holders is

$$M = 0.0034 \text{ lb sec}^2/\text{in.}$$

and mass of the particles contained in the holders is

$$M = 0.00116 \text{ lb sec}^2/\text{in.}$$

which gives a mass ratio of 3:1 (spring mass to particle mass).

After detailed evaluation, a design having a mass ratio of 1.5:1 was selected and is shown in Fig. 19. To reduce the cost of fabrication, tooling from the piston damped seal was used for construction of the bellows.
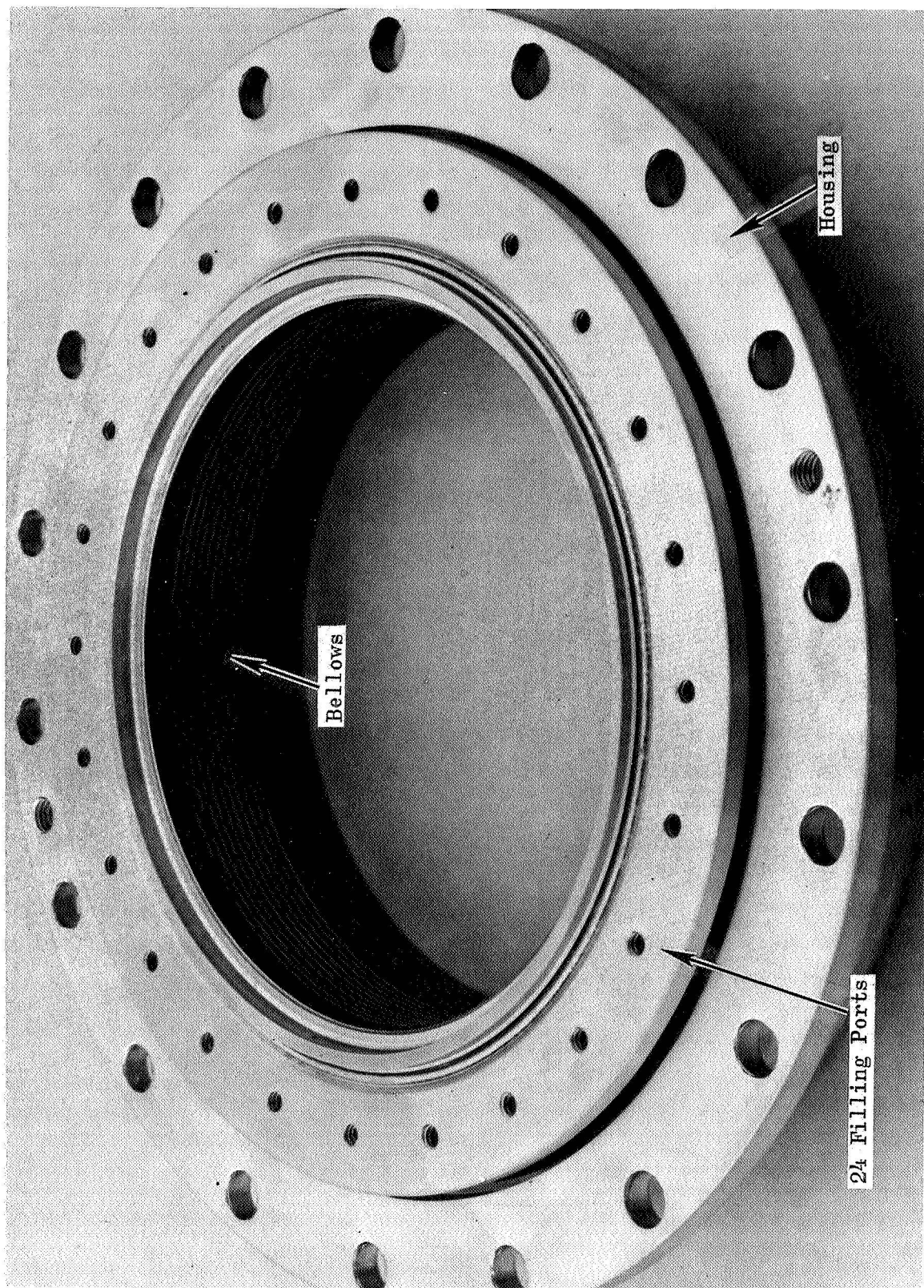
5AJ34-8/26/66-C1A

Figure 19. Particle Damped Seal

TEST PROGRAM AND HARDWARE DESCRIPTION

TEST PROGRAM

The seals in this program were not designed for a specific turbopump application or planned for rotational tests. However, requirements and operational criteria are based on conditions consistent with advanced turbomachinery. The following tests were specified.

Static Leakage and Proof Pressure

Static leakage and proof pressure tests are conducted at GN_2 pressures up to 375 psi to verify mechanical integrity and design requirements. Leakage across the seal face as well as a mass spectrometer check (where applicable) for porous weld beads is made.

Total Face Loading

Total load tests are conducted to measure the effective seal face unit loading as a result of combined bellows spring load and either pneumatic or hydraulic loading. This is conducted using an Instron machine having a rate of stroke range from 0.0003 ips to 0.83 ips which will allow a dynamic measure of seal face loads.

Pressure Cycling

Pressure cycling is a measure of the bellows integrity to withstand pressure pulses up to 200 ±50 psig in a liquid nitrogen environment. Seal leakage is measured throughout the test. Tests at 1000 F are not conducted because of difficulties in designing a pressure pulsing system at this temperature. Over 10^6 cycles were planned.

Mechanical Cycling

Mechanical cycling tests are conducted to monitor seal integrity when exposed to displacements of ±0.030 and ±0.015 inches at 16 to 100 cps in LN_2 and 1000 F GN_2. Seal leakage and displacement rate was recorded for a period of 10^6 cycles.

Recovery Rate

The recovery rate test involves displacement of the mating ring from the maximum design bellows compression of the seal to the minimum compression with the intent to show the ability of the seal face to follow the mating ring. Seal leakage is also observed.

Vibration

Vibration tests consist of the following:

1. Resonance Search. Record the frequency of all resonant points observed in a 2 g peak-to-peak sweep from 15 cps to 2000 cps in the axial axis of the seal.

2. <u>Sinusoidal Resonance Test</u>. Subject the seal to its major resonant frequency for 10 minutes in the axial axis at the following levels:

   15 to 50 cps, at 0.2-inch double amplitude

   50 to 500 cps, at 12 g peak

   500 to 1000 cps, at 0.0006-inch double amplitude

   1000 to 2000 cps, at 30 g peak

   NOTE: $g = 0.0511 \, f^2 d$ (gravity units)

   where

   f = frequency in cps

   d = double amplitude in inches

HARDWARE DESCRIPTION

Mechanical Cycle Tester

The mechanical cycle and recovery rate tester Fig. 20 has the capability of mechanically cycling the seals of this program at ±0.015 to ±0.030 inch amplitude at 16 to 100 cps. The test housing contains eight 525-watt cartridge heaters to maintain a 1000 F gas environment at the seal OD while pressurized up to 250 psig. The test housing also contains ports for filling and maintaining LN_2 in the cavity exposed to the seal. Thermal insulation surrounds the test housing to reduce heat losses.

The piston housing has two cavities separated by a piston; the end cavity can be pressure pulsed to move the shaft for recovery rate studies.
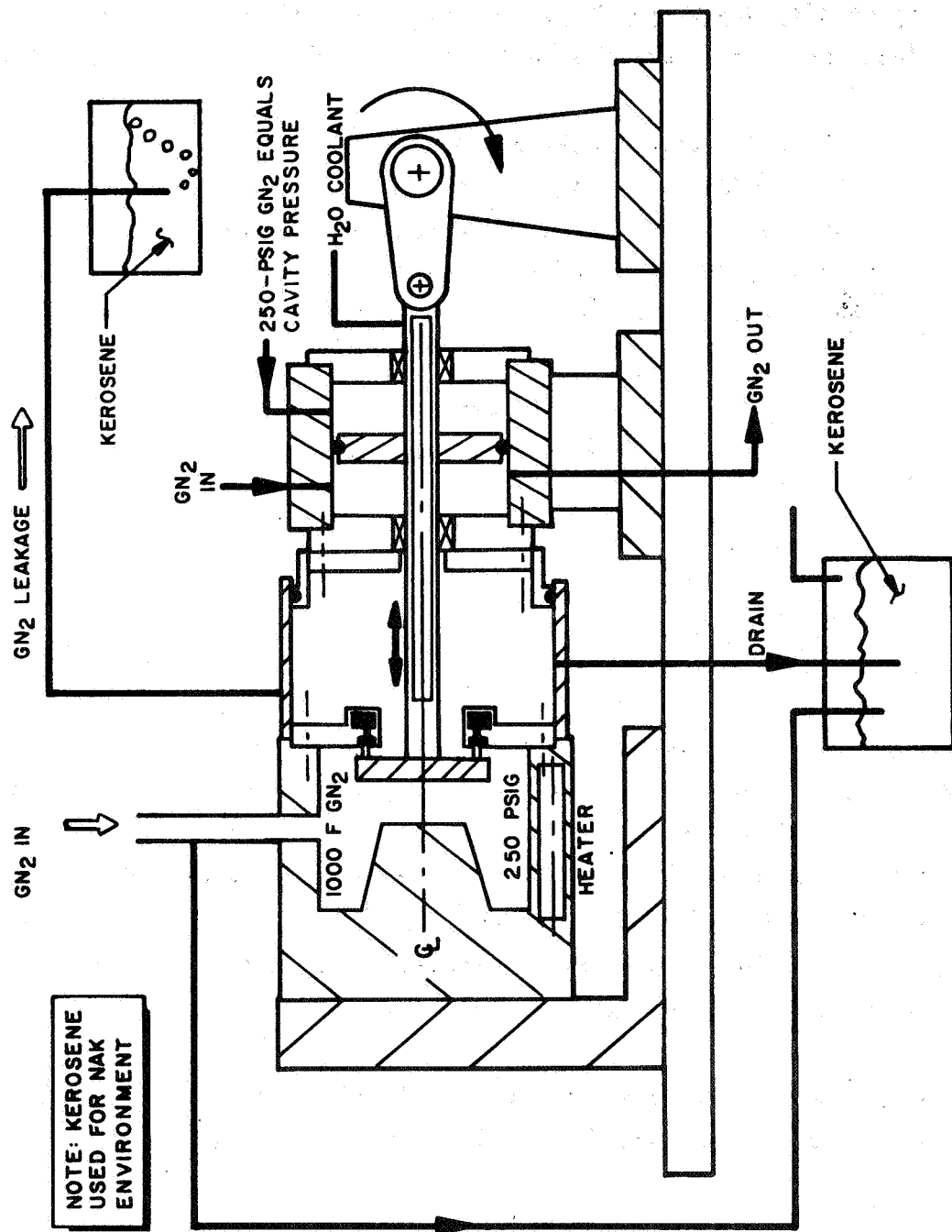
Figure 20. Mechanical Cycling Tester

Vibration Tester

The vibration fixture consists of a housing and mounting face for the seal. The test housing contains heaters and LN_2 ports to be used in the mechanical cycling test. The back side of the seal can be fitted with a cap to measure leakage or without the cap for visual observation of bellows vibration and seal response. Proof pressure and static leakage tests can also be made in this fixture.

Total Load Tester

The total load tester (shown in Fig. 34) consists of a mounting fixture and associated hardware for the seal to be mounted in an Instron test machine to measure the total seal face load within operating pressure and displacement specified.

Steady-state pressures are measured with standard gages; pressure pulses are measured with pressure transducers. The pressures are those primarily imposed on the seal during test. Thermocouples are used to monitor the temperature close to the seal face. Seal leakage, either LN_2 or 1000 F GN_2, is ported through a heat exchanger to a flowmeter. Accelerometers are used to measure displacement input and output in addition to linear transducers where applicable.

Table 4 specifies the instrumentation used for the tests.

TABLE 4

INSTRUMENTATION

Test	Measurement	Location	Operating Range	Measurement Device
Mechanical Cycling	Seal Displacement	Bellows ID	±0.015 and ±0.030 inch	Linear Displacement Transducer and Recorder
	Seal Temperature	Bellows OD Cavity	-32 F and + 1000 F	Thermocouple
	Cycling Rate	Seal Face and Tester Shaft	16 to 100 cps	Cycle Recorder
	Seal Pressure GN2 and LN2	Bellows OD Cavity	200 psig to 250 psig	Direct Reading Gauge
	Seal Leakage	Seal Cavity	0 to 1000 scims	Flow Meter
Recovery Rate	Shaft Motion	Shaft	0.090 to 0.150 inch seal height	Linear Displacement Transducer and Recorder
	Seal Temperature	Bellows OD Cuvity	-323 F and +1000 F	Thermocouple
	Seal Pressure	Bellows OD Cavity	200 to 250 psig	Direct Reading Gauge
Pressure Cycling	Seal Pressure LN2	Bellows OD Cavity	200 ±50 psig	Pressure Transducer and Recorder
	Seal Temperature	Bellows OD Cavity	-323 F	Thermocouple
	Cyclic Displacement	Seal Face OD	Recorded Amplitude	Cycle Counter and Amplitude Readout
	Seal Leakage	Seal Cavity	0 to 1000 scims	Flow Meter

52

TABLE 4

(Concluded)

Test	Measurement	Location	Operating Range	Measurement Device
Total Load	Total Load	Seal Face	0 to 500 pounds	Load Cell
	Seal Height	Seal Face	0.150 to 0.090 inch	Dial Indicator
	Seal Pressure GN_2 and LN_2	Bellows OD Cavity	0 to 250 psig	Direct Reading Gauge
	Rate of Seal Compression	Seal Face	0.050 to 0.830 ips	Instron Console
	Seal Leakage	Seal Cavity	0 to 1000 scims	Flowmeter
Vibration	Seal Pressure	Bellows OD Cavity	200 to 250 psig	Direct Reading Gauge
	Vibration Input	Test Housing	0 to 30 g	Accelerometer
	Seal Displacement	Seal Face	Recorded output	Accelerometer/Linear Transducer
	Seal Temperature	Bellows OD Cavity	-323 F to 1000 F	Thermocouple
	Seal Leakage	Seal Cavity	0 to 1000 scfim	Flowmeter

TEST PROCEDURE AND RESULTS

MECHANICAL CYCLING TESTS

Upon completion of dimensional verification, static leakage, and pressure
tests, the piston damped and orifice damped seals were mechanically cycled.
The particle damped seals were not exposed to this test because sufficient
data was obtained from the piston damped seal both having the same bellows
configuration.

Piston damped S/N 3 was installed in the tester with a damping piston to
maintain a radial clearance of 0.004 inch. The bellows was cycled for a
total of 10^6 cycles at 16 cps with ±0.025 inch peak-to-peak amplitude in
LN_2 at 250 psig.

The seal face satisfactorily followed the cycling shaft at 16 cps as evid-
enced from the low and constant LN_2 leakage rates and comparisons of dis-
placement transducer traces. Surges in the leakage rates indicate a lag
in the response of the seal face with respect to the shaft. The leakage
rates during the mechanical cycling test varied between 0.4 and 0.6 scfm.

Two linear displacement transducers were used: one to monitor the cyclic
input axial displacements to the tester shaft, and one to monitor the seal
face axial movements in response to the inputs. Outputs from the two trans-
ducers were recorded on a CEC Recording Oscillograph. A typical output
is shown in Fig. 21 which shows that the seal face carrier followed the
shaft displacements.

55
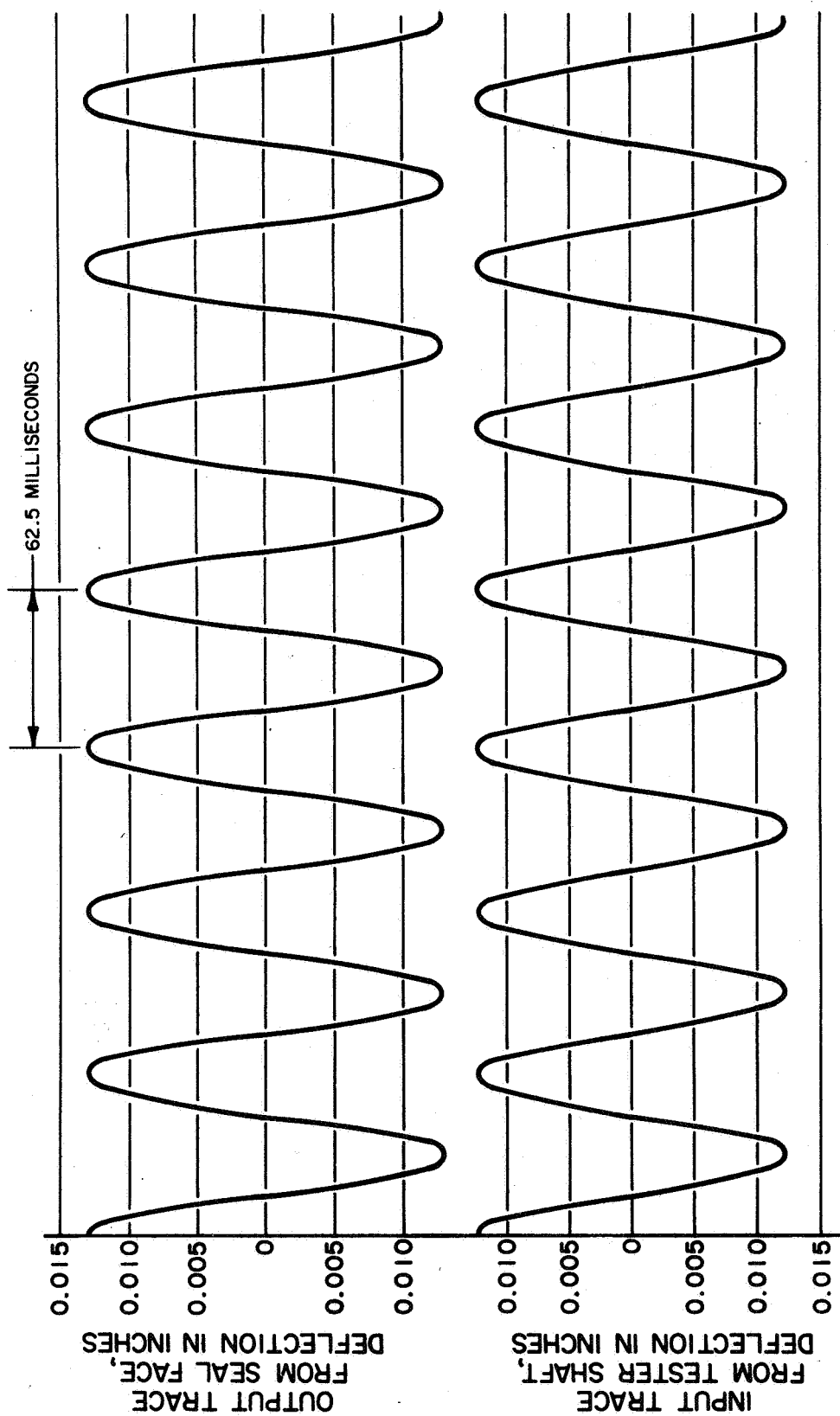
Figure 21. Typical Oscillograph Traces of Transducer Output

Posttest inspection of the seal revealed no failures in the welded bellows. However, welding of the displacement transducer probe tab to the seal face carrier ID had sufficiently distorted the carrier OD to allow rubbing contact between the carrier OD and the piston ring ID. A spring rate test indicated the drag to be only 1 pound.

The next piston damped seal, S/N 2, was mechanical cycled without a piston ring installed to obtain a comparison and to study seal performance without a piston installed.

The piston damped seal, S/N 2, was exposed to mechanical cycles at ±0.007 inch of amplitude at 100 cps in LN_2 at 250 psig. After 69,000 cycles, the seal leakage exceeded the range of the flowmeter and the seal was removed from the tester. Inspection revealed the seal to have a failed bellows in the ID weld at the heat affected zone of the third and eighth convolutions. The seal face apparently did not remain in contact with the mating ring at the 100-cps cycling rate, as evidenced by fretting between the seal face and mating ring and comparison of the displacement transducer traces. Normally, an increase in leakage would be indicative of seal face separation; however, because of the bellows failure, no increase in leakage could be observed.

The cycling displacement amplitude was found to be attenuated during the above 100-cps test to ±0.007 inch; the previous displacement amplitude at 16 cps was approximately ±0.013 inch. A spherical bearing was replaced in the linkage system in an attempt to reduce total system play. A checkout test further resulted in failure of the test hardware to the point of bending the tester support and displacement shaft. Because of the apparent limited capability of the tester, the frequency was reduced to 16 cps in all cases.

A metallographic analysis to determine the mode of failure was conducted;
the results showed the following:

1. The Inconel X-750 bellows failed as a result of fatigue along the
   base of the ID convolution welds.

2. The welds of the bellows were metallurgically sound and of
   acceptable geometry.

3. The parent metal microstructure of the bellows was metallurgically
   sound and did not contribute to the failure.

A transverse section of the bellows was removed and photographed to show
the relative location of the two failed areas shown in Fig. 22. Sections
through each of the two failed areas were prepared for metallographic
examination and measurement. A fractograph was taken (Fig. 24) which
establishes the failure to be caused by fatigue. Figures 23, 25, and 26
show the extent, nature, and location of the failures.

The bellows plate thickness was measured to be 0.006 inch, and micro-
hardness readings established that the bellows was in the heat-treated
condition. The parent metal Rockwell hardness was 35 Rc, and the welds
were approximately 37 Rc. All associated factors were favorable for
optimum service from the Inconel X-750 bellows.
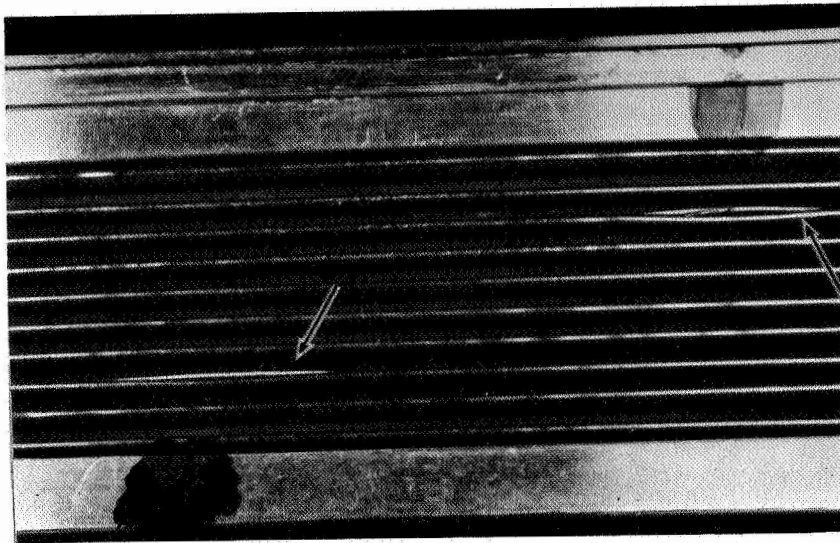
Mag: 3X

Figure 22. Section Removed From Inconel X-750 Bellows
Piston Seal Showing Ruptures (arrows) on
the ID Surface.
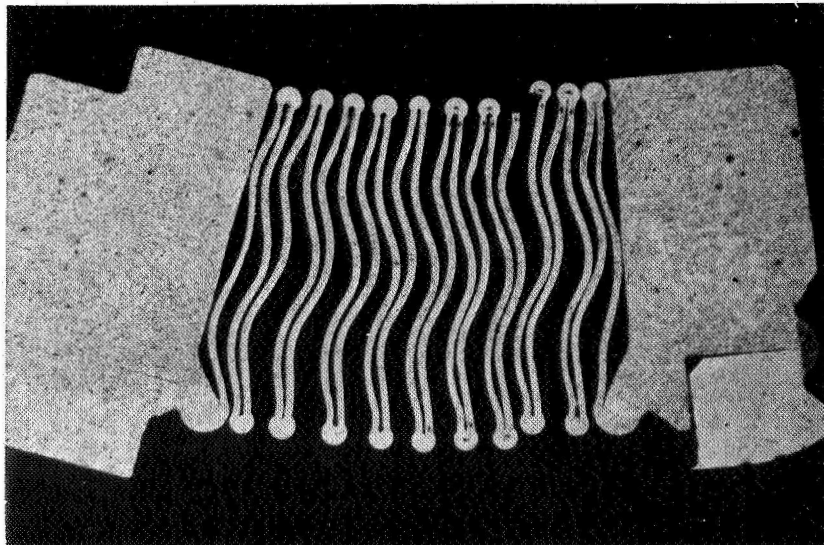
Mag: 8X   Etchant: Three Acids

Figure 23. Transverse Section Through Failed Area
(Third Convolution From Bottom, Fig. 1).
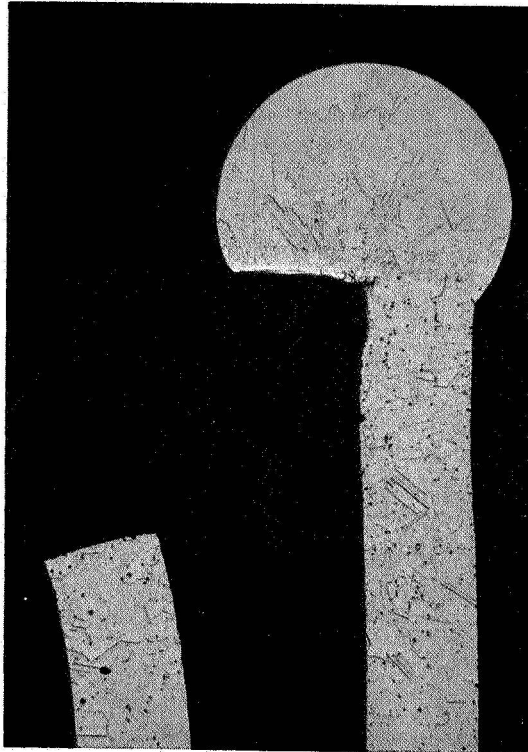
Mag: 100X   Etchant: Three Acids

Figure 24. Fracture Location Along
Base of Weld. (Note
Straightness of Fracture
Which is Typical of a
Transgranular Failure)

Mag: 250X   Etchant: 10-Percent Oxalic, Electrolytic

Figure 25.   Crack Initiation Sites at Natural Stress
             Risers. (Note clear evidence of trans-
             granular mode of failure)
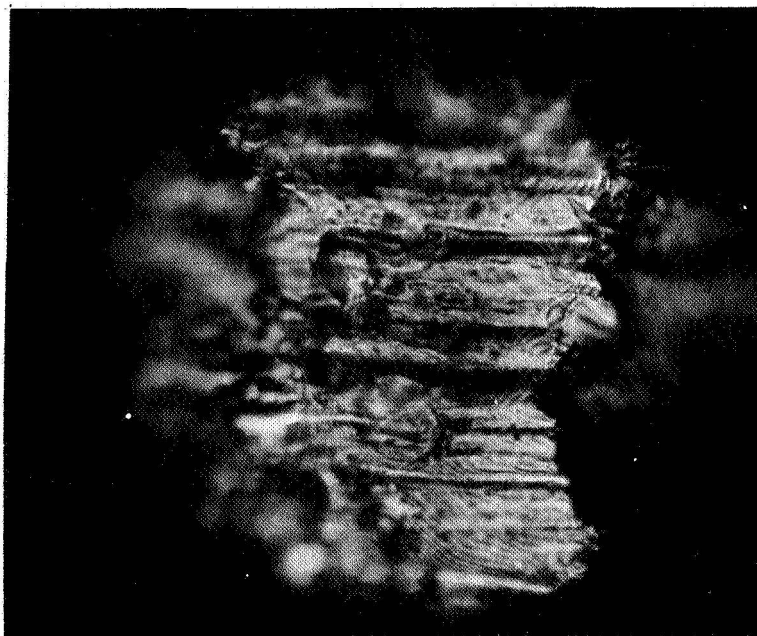
Mag: 1000X   Unetched

Figure 26.   Fracture Surface of Failed Inconel X-
             750 Bellows Showing Conchoidal Markings
             Which Denote the Progression of the
             Failure by Fatigue.

61

In accordance with the program plan, mechanical cycling of the piston damped seals was completed with the inclusion of S/N 4. A tabulated summary of the testing is shown in Table 5.

TABLE 5

TEST SUMMARY, PISTON DAMPED SEALS

S/N	Cycling Rate, cps	Displacement, inch	Piston Clearance, inch	Seal OD Environment	Cycles	Leakage, scfm
3	16	±0.013	0.0042	LN_2 at 250 psig	1,000,000	0.4 to 0.8
3	16	±0.030	0.0042	LN_2 at 250 psig	1,000,000	0.8
2	100	±0.015	no·piston	LN_2 at 250 psig	69,000	failure
4	30	±0.030	0.0072	LN_2 at 250 psig	1,000,000	1 to 5

The last test (S/N 4) completed on 22 April showed no change in bellows response when compared with data from previous tests. The higher leakage rate experienced on the last test is not necessarily a function of relative movement between the adjacent sealing surfaces because during all tests, a slight roughening of the contacting surfaces has been noted. Mechanical cycling of orifice damped seals S/N 4 and S/N 2 was completed in March 1966 with no problems at the test conditions shown in Table 6.

The failure of S/N 2 without a piston installed indicates the potential need of a piston, because no failure occurred with S/N 3 or 4. Although the cycling rate was greater for S/N 2, the displacement was only half of that imposed on S/N 3 and 4.

TABLE 6

TEST SUMMARY, ORIFICE DAMPED SEALS

S/N	Cycling Rate, cps	Displacement, inch	Seal OD Environment	Cycles	Leakage, scfm
4	30	±0.030	900 F GN_2 at 250 psig	1,000,000	0.3
2	16	±0.030	LN_2 at 250 psig	1,000,000	< 0.3

Posttest inspection showed the seals to be in excellent condition with only very minor scratches on the seal faces. A static leak check with GN_2 at 30 psig indicated a leakage of less than 10 scims. A typical test setup is shown in Fig. 27 , 28 , and 29.

On 12 May 1966, a mechanical cycling test was completed on seal S/N 6 with sodium potassium (NaK) in the bellows interior. The seal was filled with NaK under an argon blanket. When filled, the bellows were compressed from the free height (0.163 inch) to the design installation height displacing an excess volume of NaK. With the filling ports still open, the bellows were further compressed to displace an additional volume of 7 cc to account for a 11.5 percent volume increase of NaK when heated from 60 to 900 F. The ports were closed at this point leaving a volume of 52.5 cc remaining from an original volume of 69.5 cc.

The seal was installed in the tester at a compressed height of 0.120 inch. To verify the integrity of the closed system, the tester heater rods were energized and the seal heated to 900 F. The drive motor was started which
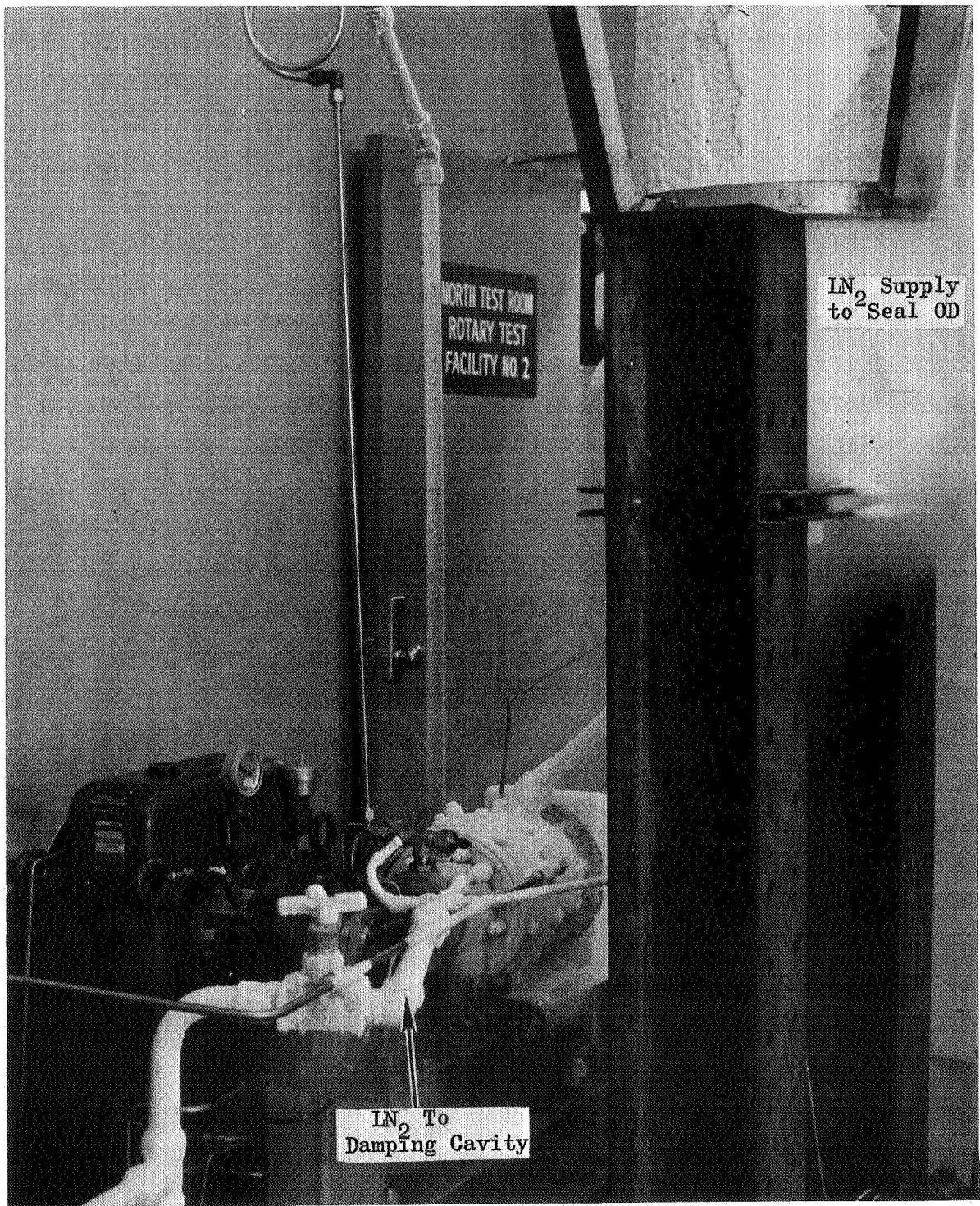
Figure 27. Test Setup, Orifice Damped Seal (View 1)

Time Reduction
Cool Down
Line

Damping Cavity
Inlet

Damping Cavity
Discharge
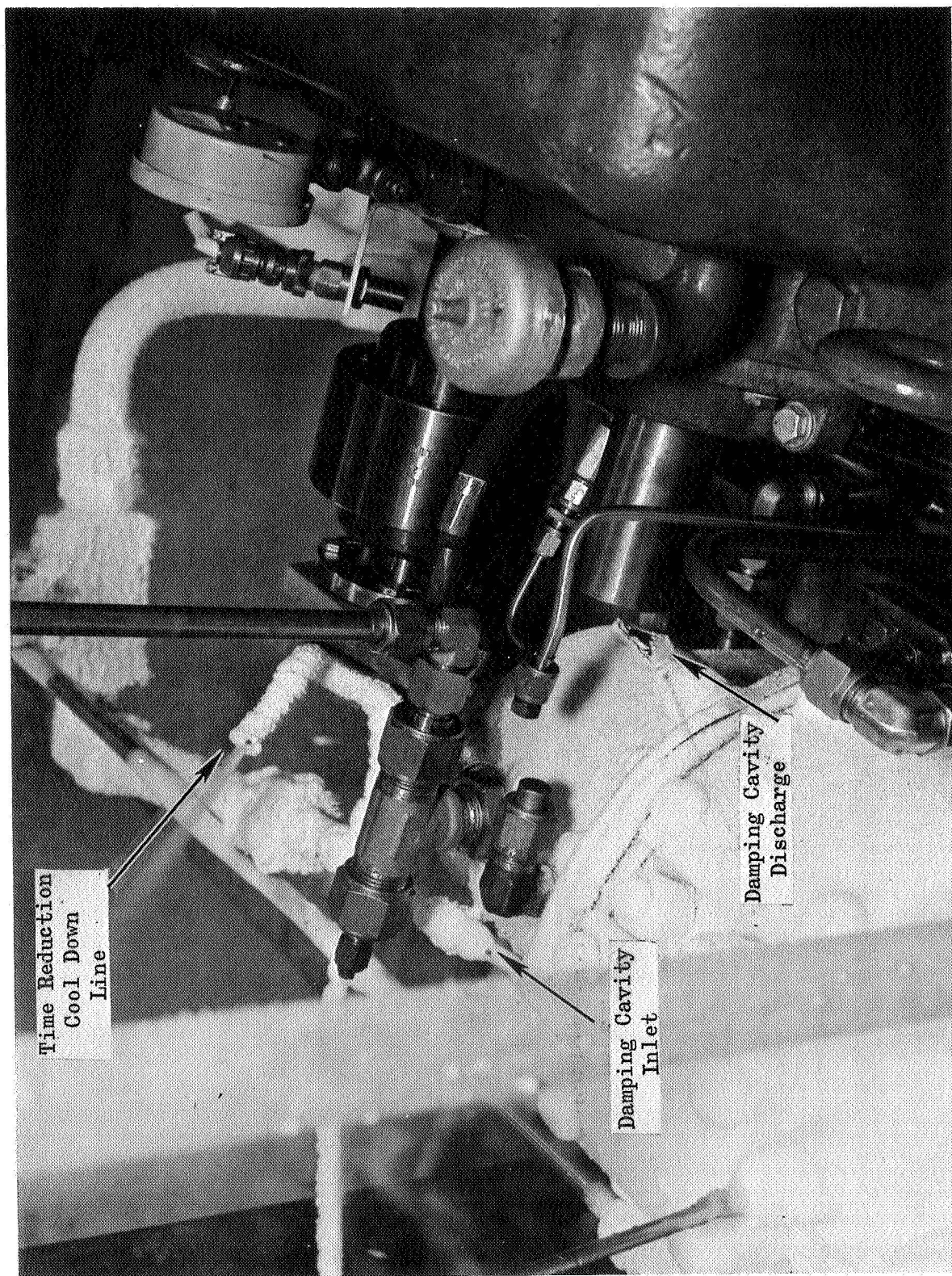
Figure 28. Test Setup, Orifice Damped Seal (View 2)

IN₂ Damping
Cavity Discharge
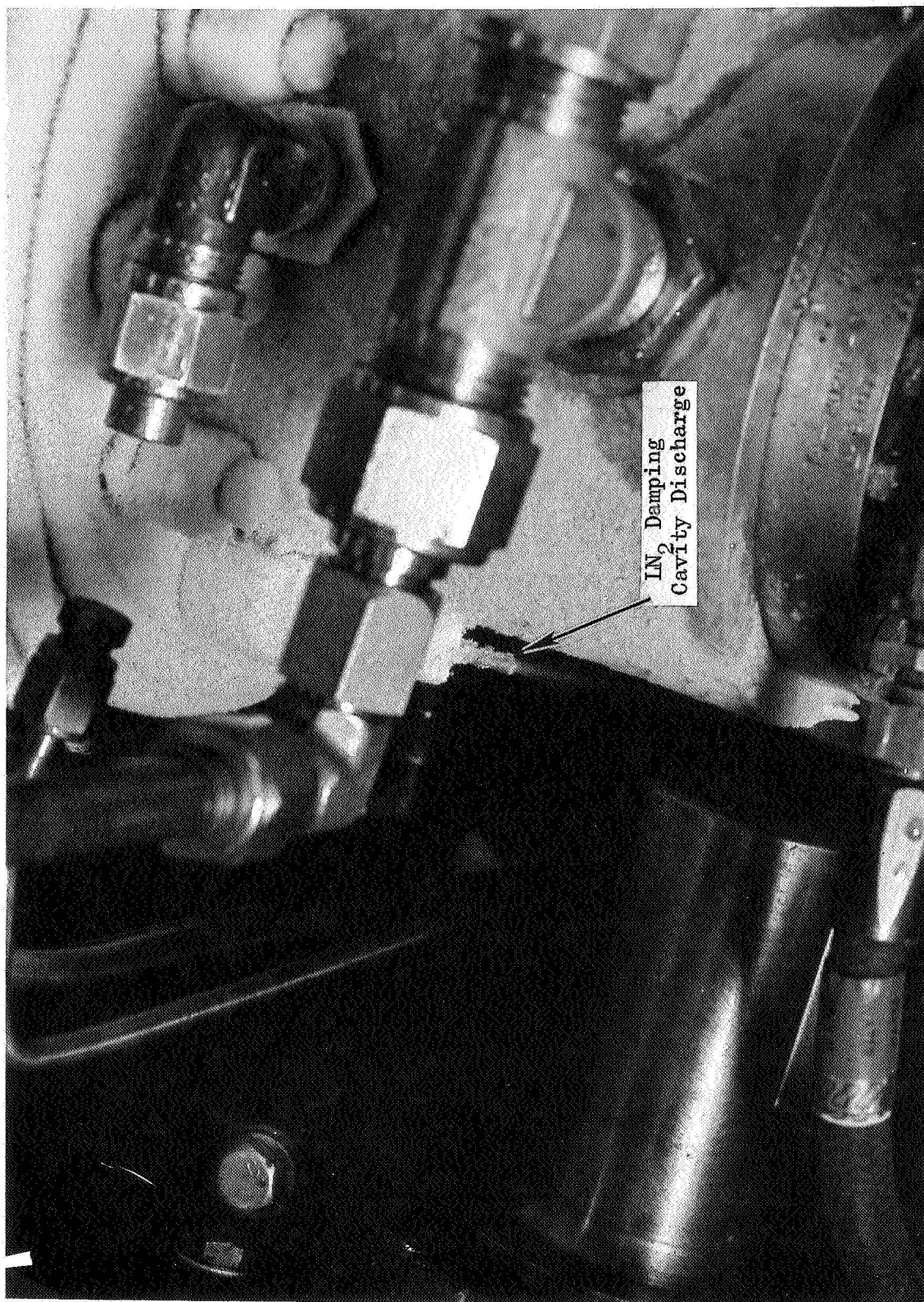
5AJ34-2/24/66-C1C

Figure 29. Test Setup, Orifice Damped Seal (View 3)

operated the eccentric crank to provide a shaft axial movement of 0.060 inch, thus compressing the bellows 0.030 inch and allowing the bellows to return 0.030 inch past the installed height. The motor speed was adjusted to maintain 30 cps for a period of 1,000,000 cycles. The test was completed with no mechanical difficulties.

Because of multiple leakage flow paths downstream of the bellows sealing face, a known leakage rate was not obtained. The housing does not accommodate a static seal capable of withstanding the 900 F environment. Asbestos cloth was used in place of the normally used rubber O-ring. Because of the porous nature of the cloth, it permitted the escape of GN_2 in the form of very small bubbles at a slow rate as indicated by the application of leak detection solution. The leakage can be described as very low and probably in a range of from 0.5 to 3.0 scfm as is normally the case. Posttest inspection of the seal was indicative of satisfactory performance. No residue was apparent on the seal to indicate a loss of NaK. The test results showed that the response of the bellows relative to shaft and mating ring displacement was not overdamped by the use of NaK. A mechanical cycling test would not normally show the effects of damping because the frequency is only 30 cps. Primarily, the mechanical cycling test is intended to demonstrate bellows integrity when the seal is exposed to a pressurized high-temperature system.

RECOVERY RATE TESTS

Following the mechanical cycling test of the orifice damped seal, a recovery rate test was conducted using the same seal containing the same volume of NaK. The test consisted of displacing the shaft and mating ring in a direction of decreasing bellows loading at a velocity greater than expected in advanced turbomachinery. Two linear transducers monitor displacement

outputs, one mounted on the bellows sealing face and the other mounted on the shaft. With the eccentric crank removed, the method of shaft displacement (depicted in the following diagram) was accomplished by actuation of a pressure solenoid to produce a force in cavity No. 2.
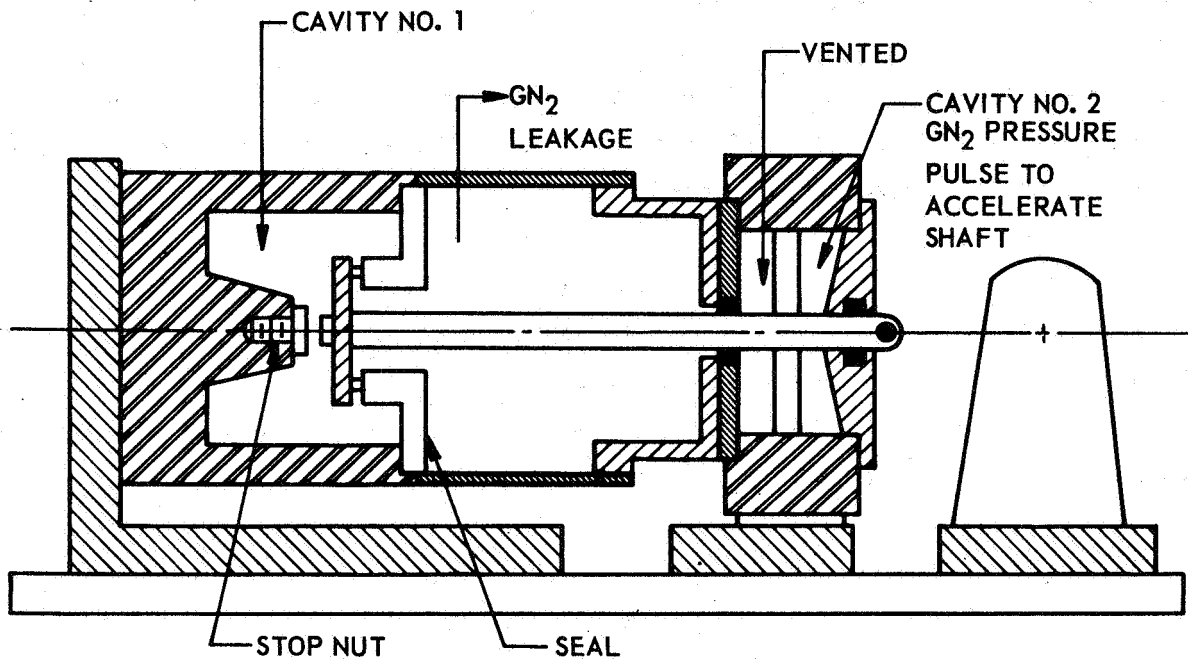
To reach the highest practical shaft velocity with the illustrated picture, the pressure in cavity No. 1 was reduced to 10 psig while the pressure in cavity No. 2 was 250 psig. The elapsed time to travel the distance of 0.060 inch to the stop was found to be 10 milliseconds. The following calculation is based on the model shown in Fig. 21 and indicates that the shaft would have to travel the distance in less than 4.5 milliseconds before separation could occur.
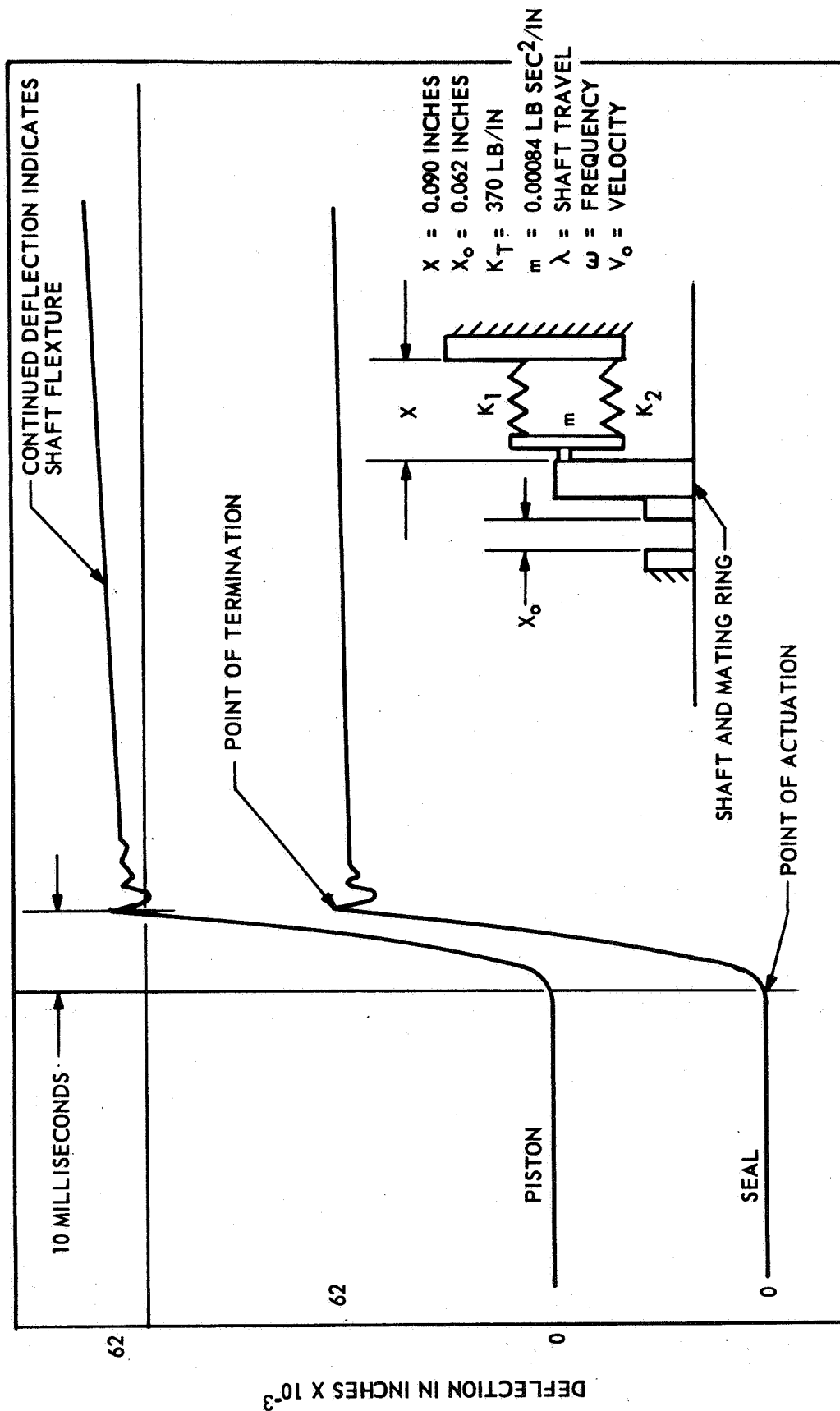
Figure 30. Recovery Rate Test Orifice Damped Seal (NaK Filled, S/N 6)

The spring mass system is represented by the equation

$$m \frac{d^2 x}{dt^2} + Kx = 0$$

Kx is positive because the bellows is in compression

where

$$w = \sqrt{\frac{K}{m}}$$

w = natural frequency

k = spring rate

m = spring mass

The general solution is given as

$$x = A \sin wt + B \cos wt$$

where

A and B are arbitrary constants

At the compressed height (x) of 0.90 inch, the following initial conditions exist:

at $t = 0$ (1) $X_0 = 0.062$ inch   when $t = 0$ the $\sin wt$ becomes 0

(2) $\frac{dx}{dt} = V_0 = 0$ $\therefore$ $A = 0$ and $B = X_0$

then the solution is $\lambda = X_0$ $\cos wt = \frac{\lambda}{X_0} = 1$

$$\therefore \ t = \cos^{-1} \frac{1}{w} = \cos^{-1} \sqrt{\frac{m}{K}} \quad \text{so,} \quad t = \sqrt{\frac{0.0074}{370}} = 4.5 \text{ milliseconds}$$

This time is based on a nondamped system. The test results show that the bellows are not overdamped at the conditions tested.

70

A recovery rate test was also conducted on piston damped seal S/N 3. The seal was installed at a compressed height of 0.090, and a mating ring displacement of 0.058 imposed which is 83 percent of the bellows free maximum travel height. With a ΔP of 240 psig, the mating ring and seal moved the 0.058 distance in less than 10 milliseconds without separation, and no increase in leakage was observed.

PRESSURE CYCLING TEST

An orifice damped seal was installed in the setup shown in Fig. 31 which was assembled from available hardware. The test consists of imposing oscillating LN_2 pressures on the primary seal bellows with the damping cavity filled with recirculating LN_2. The seal was installed at the mean design compression and remains at that compression unless influenced by the pulsating pressure as indicated by monitoring primary seal leakage.

The seal cavity and LN_2 accumulator bellows were pressurized to 200 psig, and the balance piston was pressurized to over 2000 psig to balance the force produced by the accumulator bellows assembly. The hydraulic actuator was energized by a servovalve to pulsate the LN_2 ± 50 psig. The response of the pressure transducer located in the seal cavity is shown in Fig. 32 for 3, 10, 20, and 30 cps. A pure sine wave was not apparent in the recorded data. The cause is due to a time lag in transducer sensing relative to the pressure actuation at the accumulator bellows. This condition is reflected at the transducer as a sine wave with a susperimposed harmonic stimulated by the accumulator bellows approaching a resonant condition. A further increase in frequency (from 10 to 30 cps) causes a greater change in amplitude. This increased amplitude was apparent during the test by a gross movement of the entire test apparatus.

71

Figure 31. Pressure Cycling Test
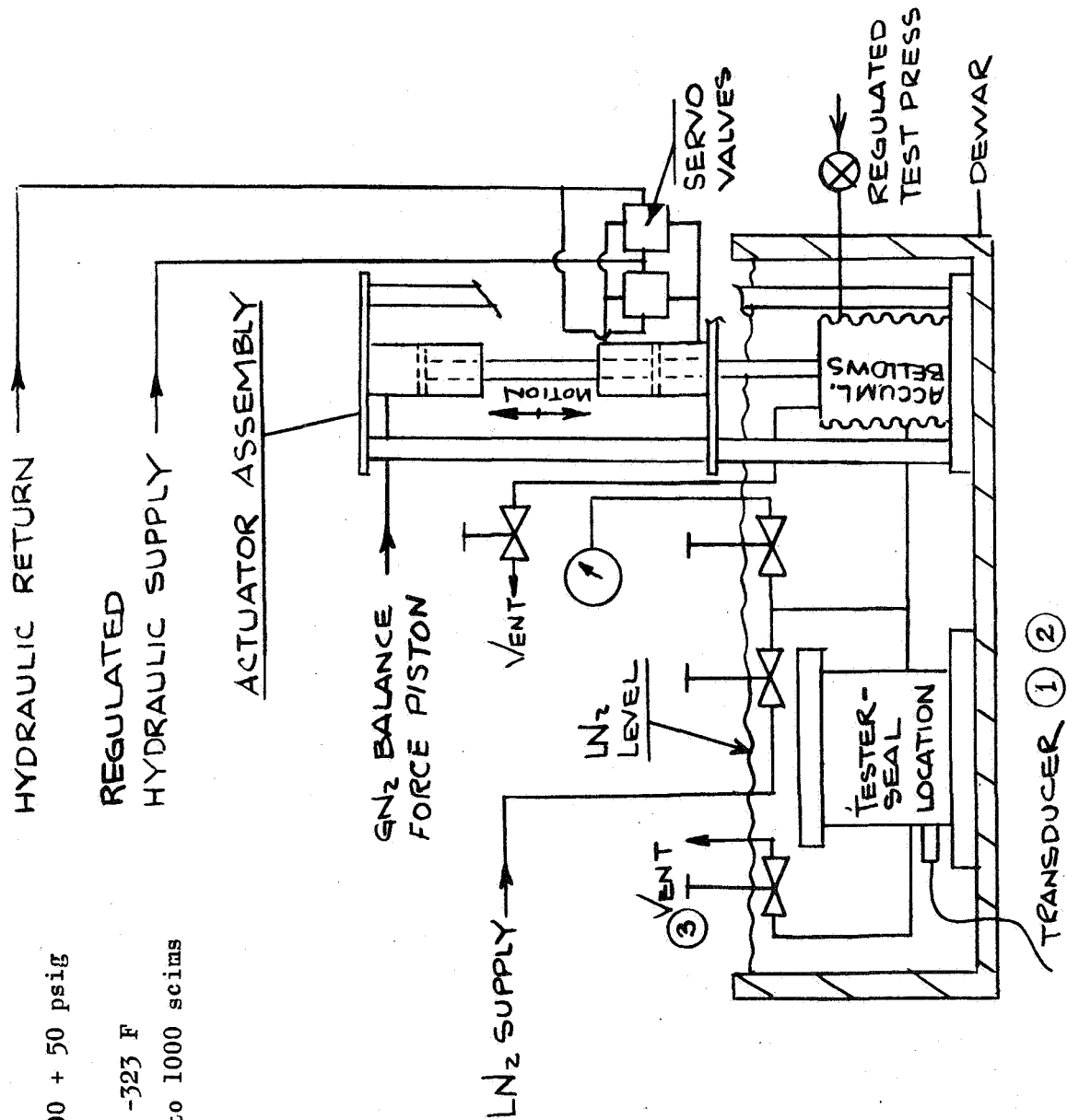
Seal Pressure: 200 ± 50 psig
at 100 cps

Seal Temperature: -323 F

Seal Leakage: 0 to 1000 scims

① ② ③
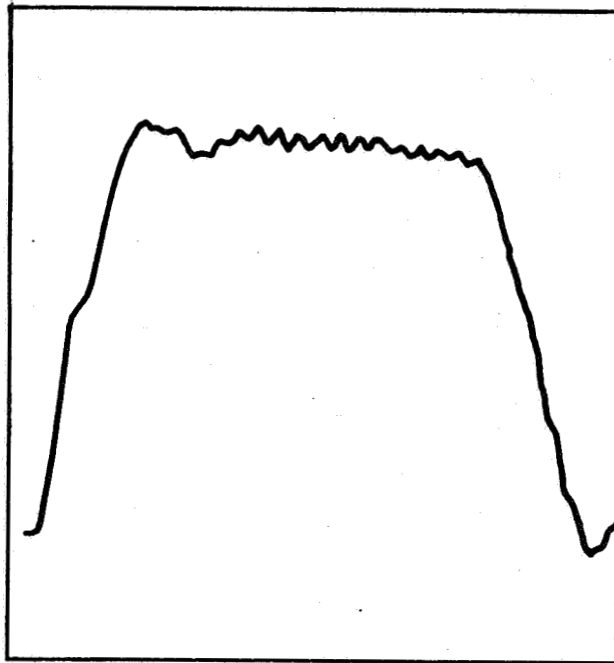
3 CPS

10 CPS
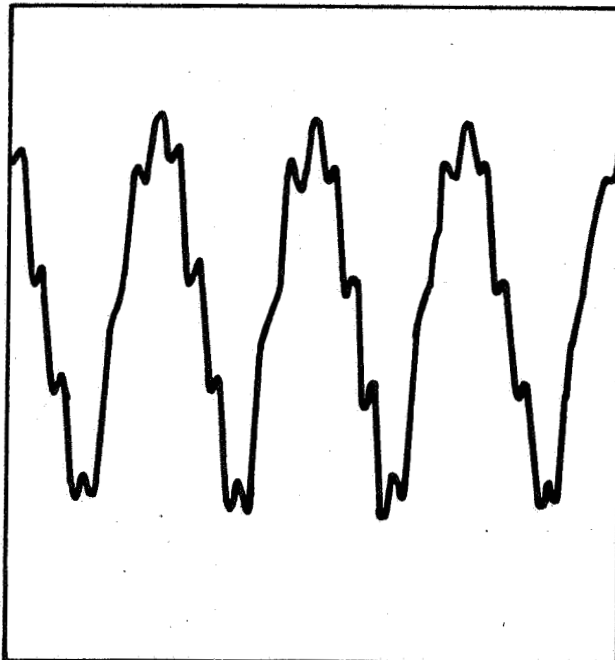
20 CPS
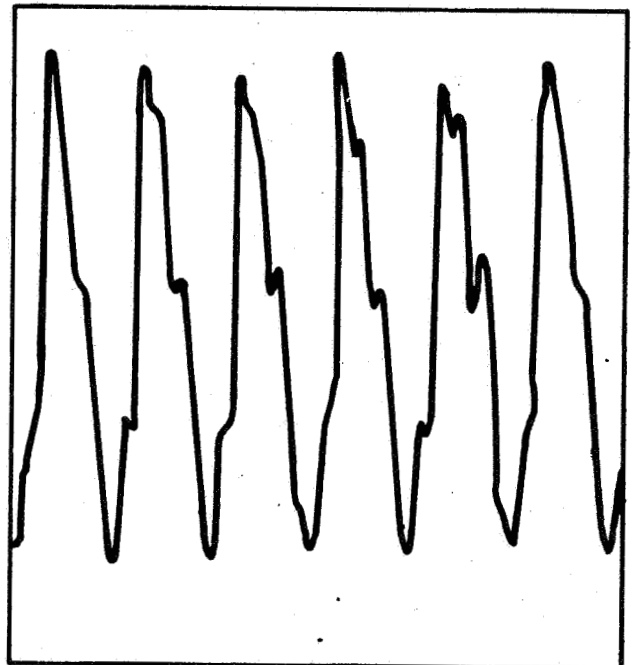
30 CPS

Figure 32. Pressure Cycling Test Data

73

Attempts to modify the system were considered; however, after 180,000 cycles (90 percent at 30 cps) excessive leakage was noted at the gas flow-rates and resulted in test shutdown. Disassembly of the tester and inspection of the bellows seal indicated a bellows rupture at the seond ID convolution approximately 1 inch long.

Mode of failure was ascertained to be fatigue of the convolution weld bead in the heat affected zone. The test duration of 180,000 cycles is the number of cycles produced by the actuator piston. The number of cycles imposed on the primary seal bellows is approximately 3 to 4 times 180,000 cycles, as can be noted in Fig. 32. The amplitude of the additional cycles is in the order of 10 psig.

The recirculating LN_2 used as the damping fluid was subject to a volume/density change which indicates it may be necessary to limit use of this design to fluids that can be contained and sealed in the damping cavity.

TOTAL FACE LOADING TEST

A series of total load tests were conducted on piston damped seal S/N 5 using the apparatus shown in Fig. 33 . The tester is used in conjunction with an Instron machine which controls the shaft movement and records the load exerted on the load cell. A remote system to supply and monitor the test pressure is also used. The Instron machine and tester are shown in Fig. 34. The recording equipment is located outside the test cell.

LOAD CELL

MYLAR DIAPHRAM

LOCATING PIN

PRESSURIZED
CAVITY

SEAL LEAKAGE

BELLOWS
SEAL

ADJUSTING
SCREW

BASE
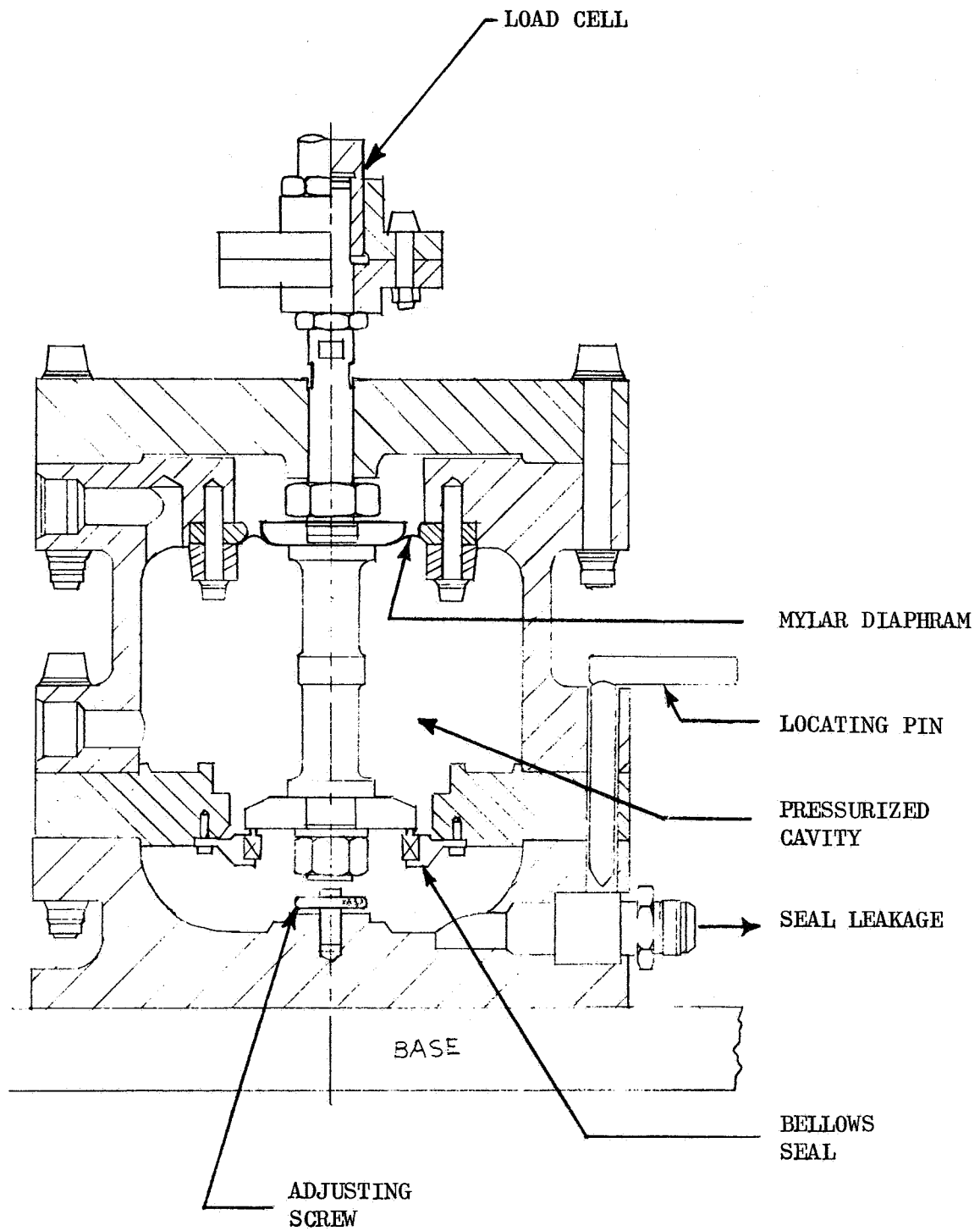
Figure 33. Total Face Load Tester
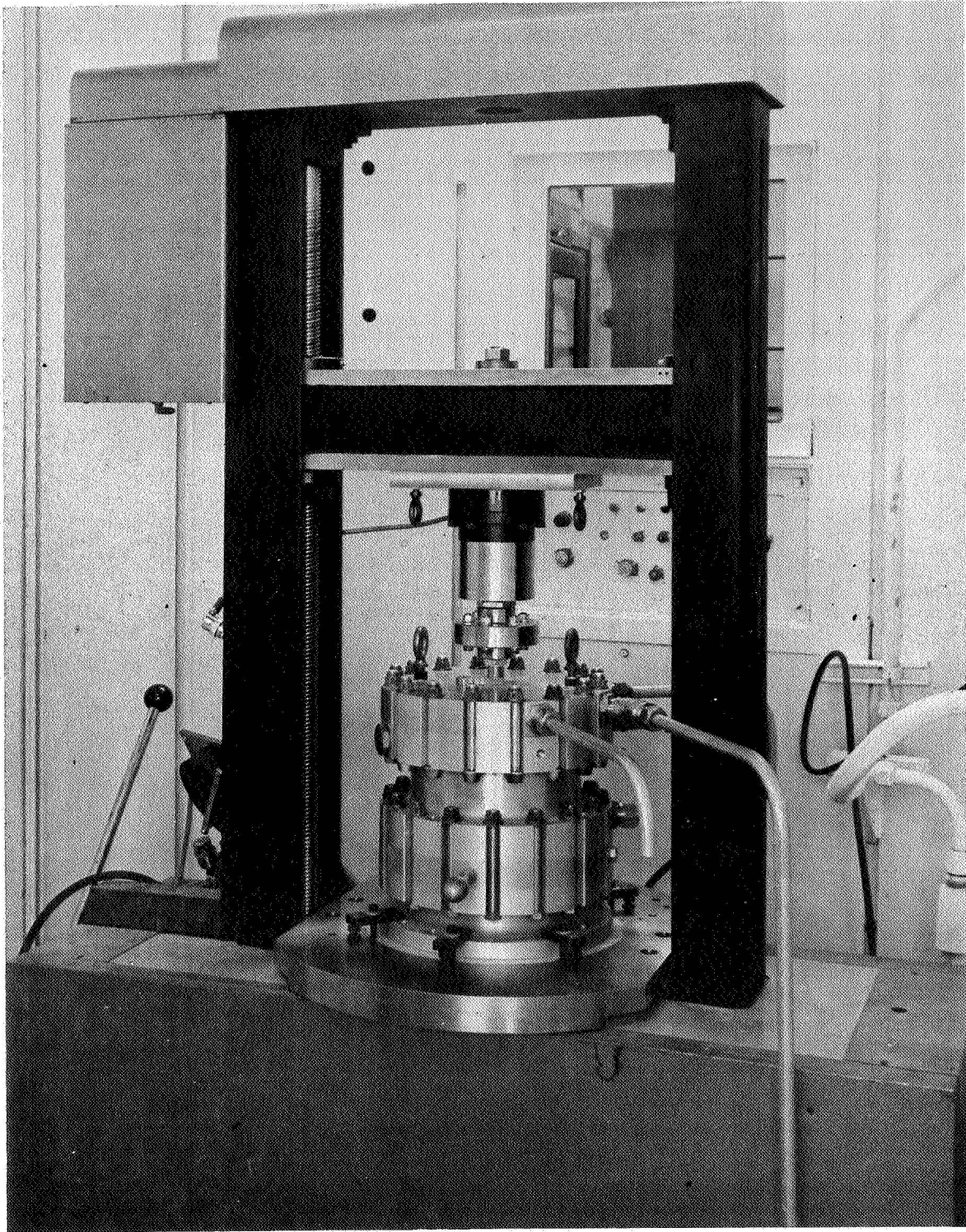
5AJ35-3/23/66-C1A

Figure 34. Total Load Test Setup

As discussed in the design section on the piston damped seal, the mechanical characteristics involved in face seal operation must be known to establish limits of design parameters. The primary factors concerned in bellows design which predict operational characteristics can be determined through total load tests are as follows:

1. Spring force of the bellows through the desired operating range

2. Effective hydraulic area

3. The change of the bellows effective diameter caused by deformation of the bellows plates when varying the operational pressure

4. The change of seal face unit loading with respect to a change in compressed length or a change in pressure

5. Seal leakage to test the adequacy of the pressure balance

The test conducted on the piston damped seal was accomplished with existing hardware with the exception of the Mylar diaphragm used in the tester to maintain a static pressure environment. Prior to installation of a seal, the diaphragm was calibrated through the planned operating range of the bellows to account for the effective area change of the diaphragm. Figure 35 represents the plotted total load data for S/N 5.

The plot of bellows effective diameter (Fig. 36) is calculated data based on the total load data of Fig. 35 . As can be noted some of the load values oscillate. These oscillations are assumed to be the result of bellows plate deformation under pressure causing plates to touch and share the load non-uniformly. Under normal operation, effective diameter change is only 0.005 inch at the design operating point of 200 psig.
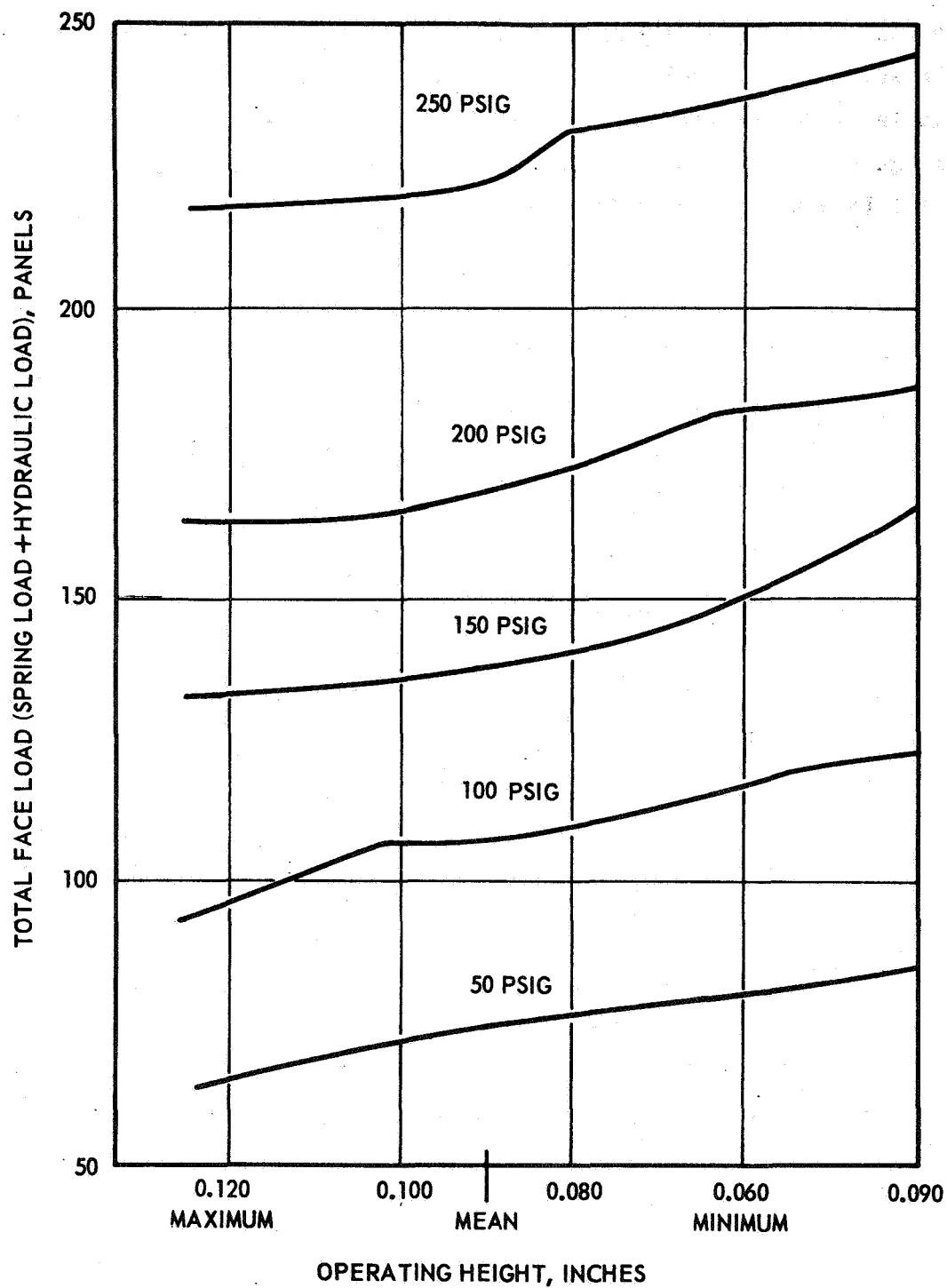
Figure 35. Piston Damped Seal S/N 5 (Data Compares Closely to Vendor Data)
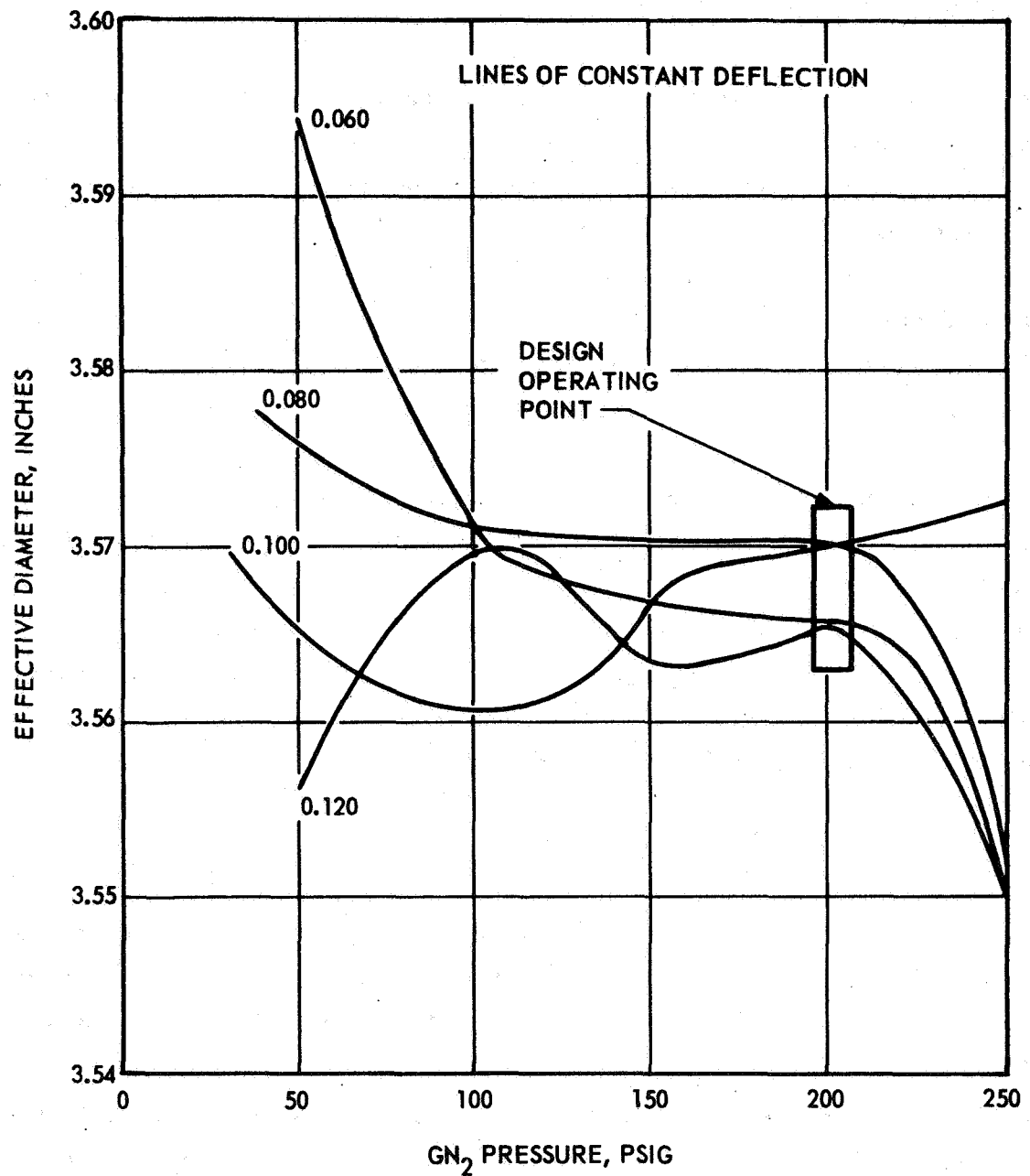
Figure 36. Effective Diameters Calculated Based on Total
Load Data Minus Spring Load

VIBRATION TESTS (PISTON SEAL)

A series of vibration tests was conducted on a piston damped seal with
and without a damping piston to observe seal face response at resonance.
The seal was installed without a piston at the mean operating height in
which the bellows is compressed 0.110 inch. A test housing encloses the
seal to provide a volume for a GN_2 or LN_2 environment at the bellows OD.
Displacement is monitored by two linear transducers, one attached to the
bellows carrier and one mounted on the test housing to monitor relative
movement.

With no piston installed, two tests were run at 2 g and 5 g. A frequency
sweep to 2000 cps showed three points of resonance (606, 1400, and 1800 cps).
Both transducers indicated a maximum amplitude of 250 microinches. With
a piston installed (0.002 clearance) the tests were repeated. The results
indicated no change in amplitude. The environment was gaseous nitrogen
heated to 900 F and pressurized to 200 psia. Results of tests support the
previous conclusion that damping will not occur with this system at
small displacement amplitudes.

To increase the possibility of seal face liftoff, the compression load of
the bellows was decreased beyond normal operation. With the bellows com-
pressed 0.010 inches, the seal was subjected to the same frequency sweep
but only the first indication of resonance was considered. The seal was
exposed only to normal room atmosphere; at approximately 600 cps, liftoff
occurred with a maximum amplitude of 0.002 inch. The test was repeated
using LN_2 to note any change in amplitude caused by a fluid condition
pressurized to 200 psig.

The resonant frequency and maximum amplitude decreased by a very small amount under LN_2 environmental conditions and indiated that little damping existed with the displacements involved and the type of fluid used. The quality or liquid/vapor fraction of LN_2 used may be questionable because considerable leakage occurred at the resonant frequencies. This amount of gas leakage from the liquid supply could cause a two-phase fluid condition.

VIBRATION TESTS (PARTICLE SEAL)

Initially, a series of tests were conducted to document the performance of the particle damped seal to compare the results with the beam testing described previously of the particle damped seal design and to establish the most effective level of fill of the particle containers. One piezo-electric accelerometer was bonded to the seal face with its exciting axis parallel to the seal's longitudinal axis. A control accelerometer was installed on the vibration table to monitor input excitation. The test setup used is shown in Fig. 37. No special environment was used nor was the bellows restrained. The motion of the seal was free axial movement responding to an input acceleration of 0.5 g. The molybdenum particles used to examine the damping effect were chosen based on previous beam tests which show that particles having a -325 sieve size rating give the best results. This sieve size includes particles of 44 microns and below. A random sample is shown in Fig. 38. Close examination shows the particles to be spherical in shape and having a relatively smooth surface.

The tests were conducted with an exciting force held constant (0.5 g peak) and the frequency varied from 20 cps to 1 kilocycle. Relative damping was determined by measuring the bandwidth of the resonant peak at the half-power
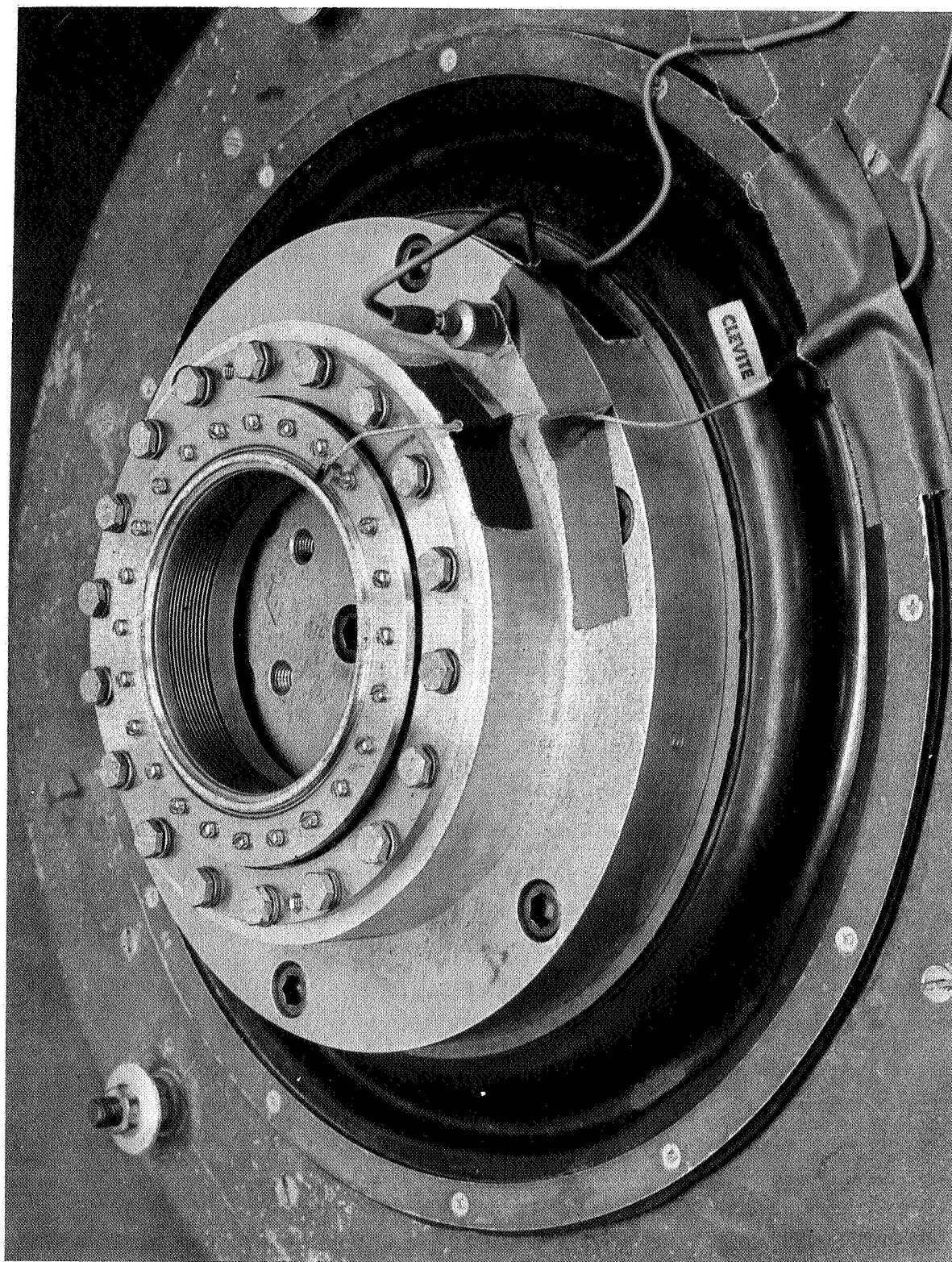
Figure 37. Vibration Test Setup, Particle Damping Seal

Texture of
Photo Paper

Blurred Edge is Due to
Magnification Resolution
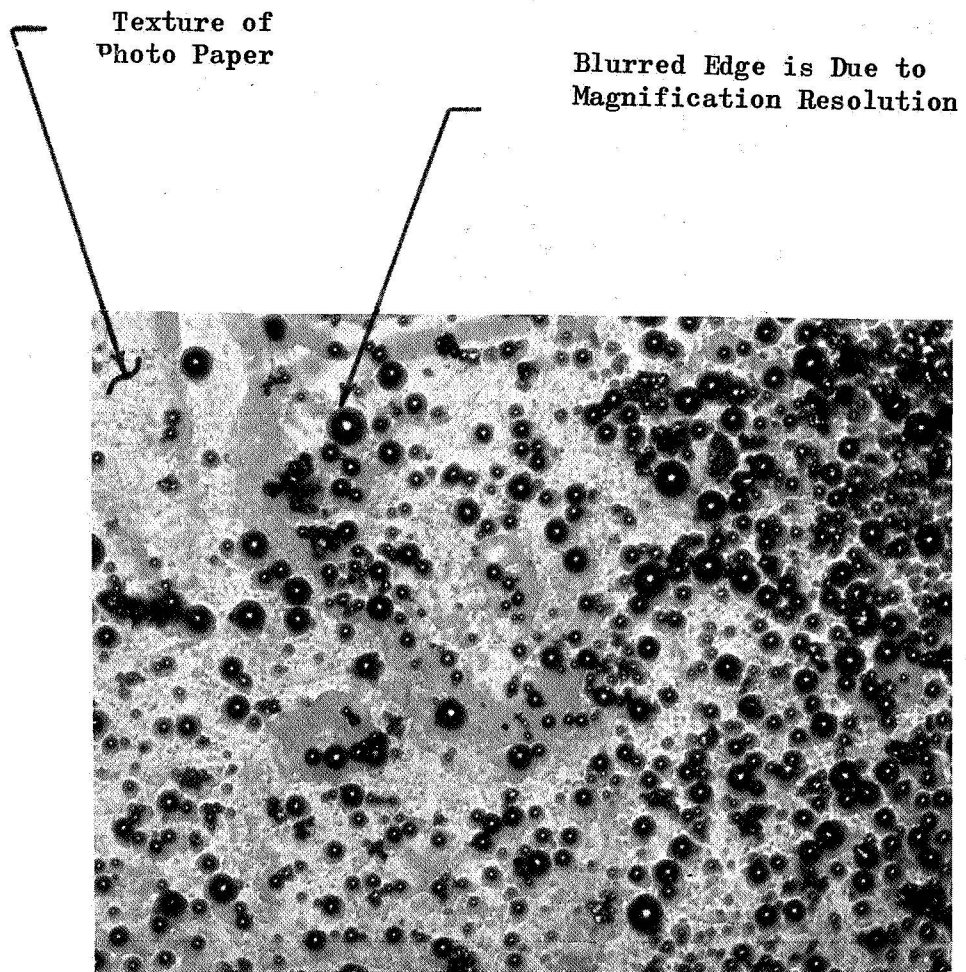
150 X

Largest Particle is
44 Microns in Size

Figure 38. Molybdenum Spherical Powder

points in terms of normalized frequency. The diagram below illustrates
the damping measurement.
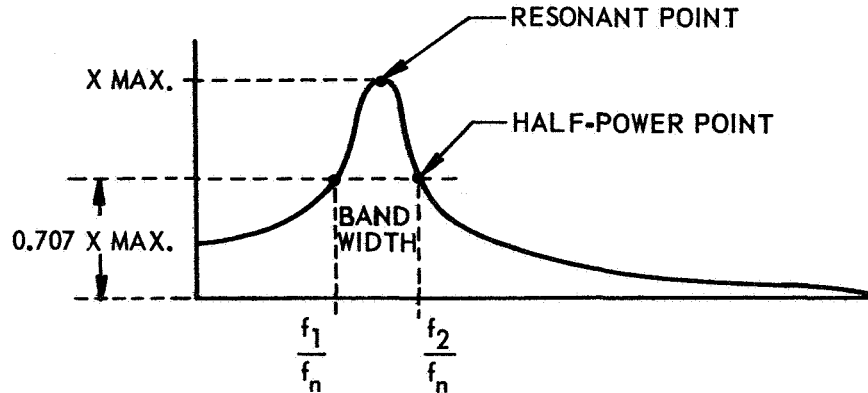
As the bandwidth increases, relative damping also increases. The formula
used to compute relative damping for this case is:

$$\Delta f = \text{Relative damping} \approx \pi \left(\frac{f_2}{f_n} - \frac{f_2}{f_n} \right)$$

where

f_n = resonant frequency

f_1 = lower half–power frequency

f_2 = upper half–power frequency

In addition to damping, the frequency at resonance and the amplification
at resonance were measured and recorded. The amplification is defined
as the ratio of acceleration into the mass to the acceleration out, and
is another term used to define effective damping.

$$\text{Amplification} = \frac{G \text{ out}}{G \text{ in}} \quad \text{or} \quad \frac{A_o}{A_i}$$

The following are the tabulated test results:

TABLE 7

TEST DATA, BELLOWS UNRESTRAINED

Test No.	Capsule Condition	f_1	f_n	f_2	Δf	A_o/A_i	G in	G out
1	Empty	75.5	75.9	76.3	0.033	108	0.5	54
2	1/4 Full	71.1	72.5	72.6	0.065	51	0.5	25.5
3	1/2 Full	66.5	67.7	68.3	0.0835	43	0.5	21.5
4	3/4 Full	62.4	63.5	64.5	0.1039	35.2	0.5	17.6
5	Full	60.0	60.6	60.7	0.0364	93	0.5	46.5

The test results for two cases, empty and the most effective, show that a reduction in amplification of 66 percent occurs from empty to 3/4 full.

A series of tests were conducted to establish the amount of damping available with the spring mass system restrained as in actual operation. The bellows was compressed 0.085 inch by a disc mounted as an integral part of the vibration table, therefore imposing a constant load on the bellows.

Tests were conducted in a frequency sweep range from 30 cps to 2 kilocycles at vibration input levels of 1, 5, 10, and 20 g rms with the particle holders both empty and 3/4 full. A short test was also run at 3/8 full to verify the particle holder optimum filling level.

The accelerometer data was recorded on log paper plotting the frequency
vs bellows response (g rms). As a result of loading the bellows, several
points of resonance occurred at different frequencies. Damping could not
be defined in terms of the fundamental frequency and the half-power points
as was the case in the unrestrained bellows tests; therefore, maximum out-
put response (g rms) was used and damping referred to as the ratio of the
two outputs, empty and 3/4 full. Table 8 presents the data for the tests
showing damping as:

$$\Delta = \text{damping} = \frac{\text{g rms undamped}}{\text{g rms damped}} \text{ with constant input}$$

TABLE 8

TEST DATA, BELLOWS RESTRAINED

Input G_I	Maximum Response G_o	Frequency at Maximum Response	Damping Δ	Particles
1	28	1173		0
1	3.8	906	7.4	3/4 full
5	72	1039		0
5	34.8	1065	2.08	3/4 full
10	118	1021		0
10	53	1066	2.2	3/4 full
20	(damping not defined for 20 g case caused by bellows failure)			

A typical response plot is represented in Fig. 39 and 40 for the 10 g
case.
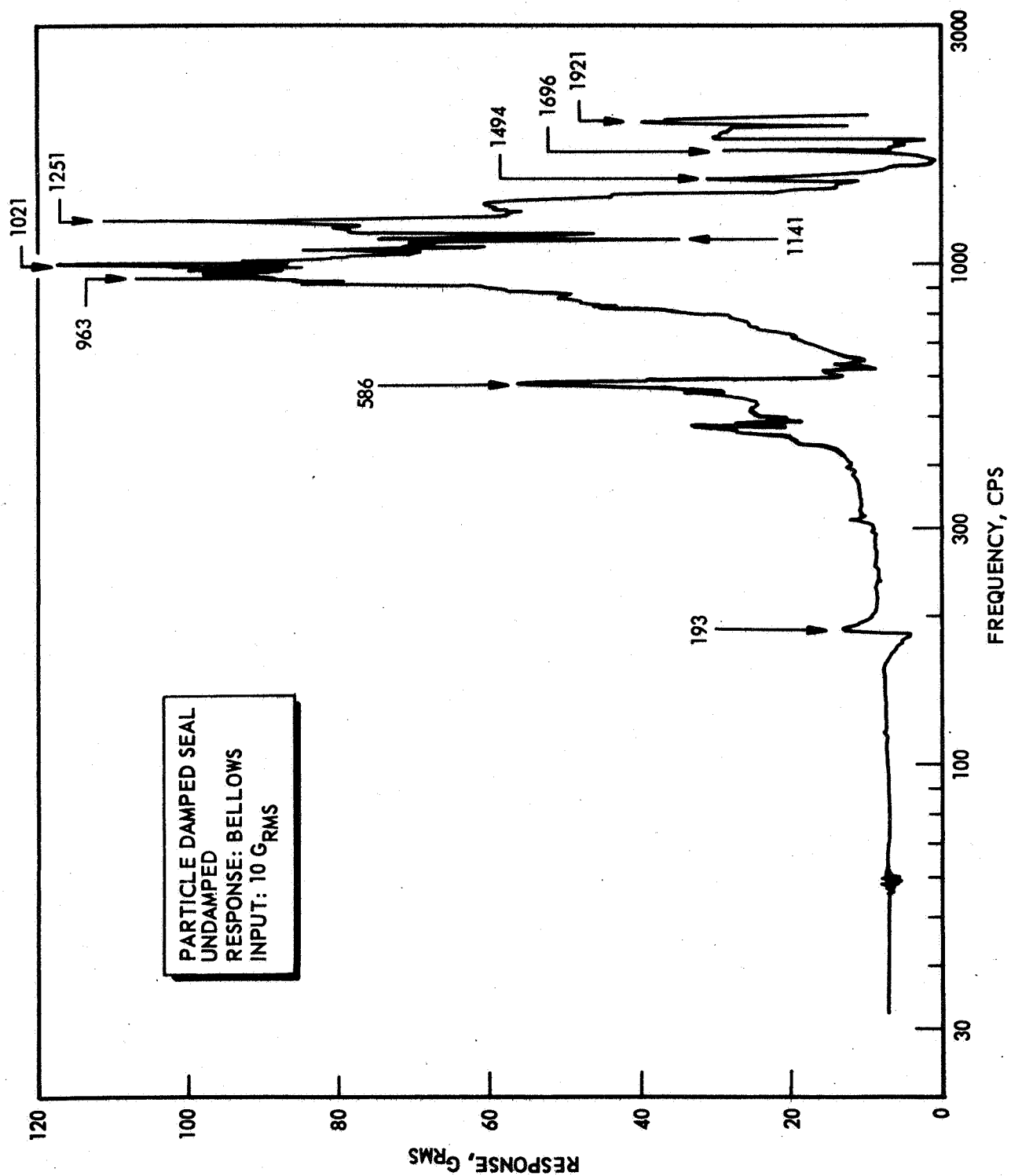
Figure 39. Bellows Response, 10 g, Particle Undamped

87
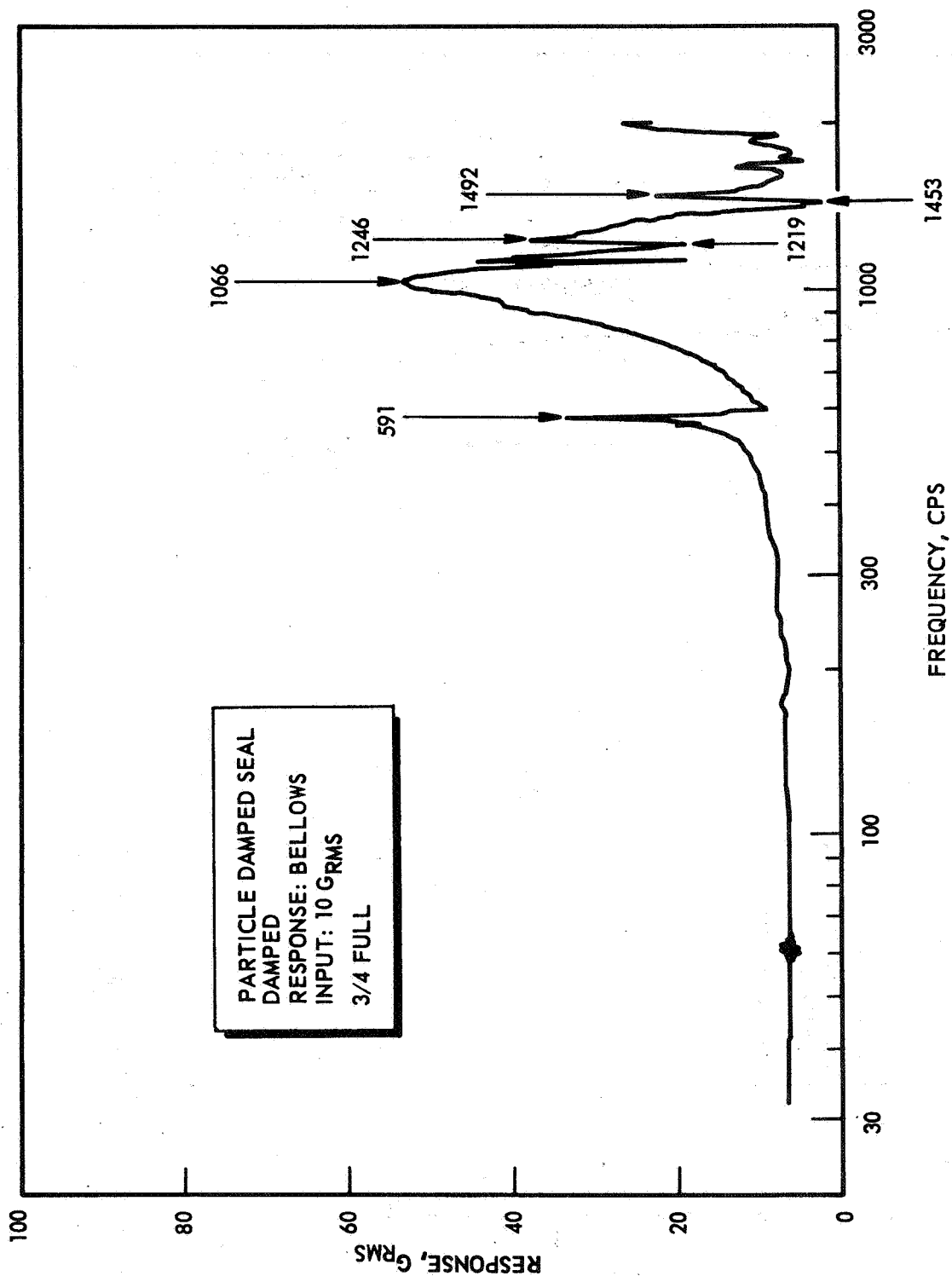
Figure 40.   Bellows Response, 10 g, Particle Damped

88

The 20 g data shown in Fig. 41 and 42 indicated an unreasonable response compared to the lower level inputs of 5 and 10 g. Disassembly of the test apparatus and inspection of the seal revealed a severe bellows rupture at the ID of the second convolution from the rear bellows carrier. The observed rupture is indicative of a fatigue failure. The occurrence of the failure shows that the bellows life for this case was in the range of 35- to 40-million cycles and represents the total of the testing presented in Table 8 , and includes an average frequency of 1000 cps of which 10 percent of that duration was at resonant conditions. As the vibration test continued, the data became more erratic indicating a pronounced failure. The extent of the rupture was observed to be 75 percent of the welded convolution.

To establish a comparison between conventional friction and particle damping, a test was conducted on an experimental frictional damped seal which has been used in the J-2 Mark 15 oxidizer turbopump. The turbopump test results indicated a very low carbon wear rate with low leakage. Wave springs loaded against both the carbon carrier and bellows convolutions supply the vibration damping medium.

The response of the bellows is shown in Fig. 43 at the 10 g level input, the output is 35 g at a maximum amplitude at 1900 cps.

Comparing this data with the 10 g input particle damped seal data, the following information is apparent:

1. With the same vibration input, the output of the particle seal is 50 g vs 35 g for the frictional damped seal.

2. While the damping characteristics appear to be better for the frictional seal, it should be noted that the spring mass of the particle seal is approximately 10 times as great as that of the conventional seal, and therefore the damping required is correspondingly greater.
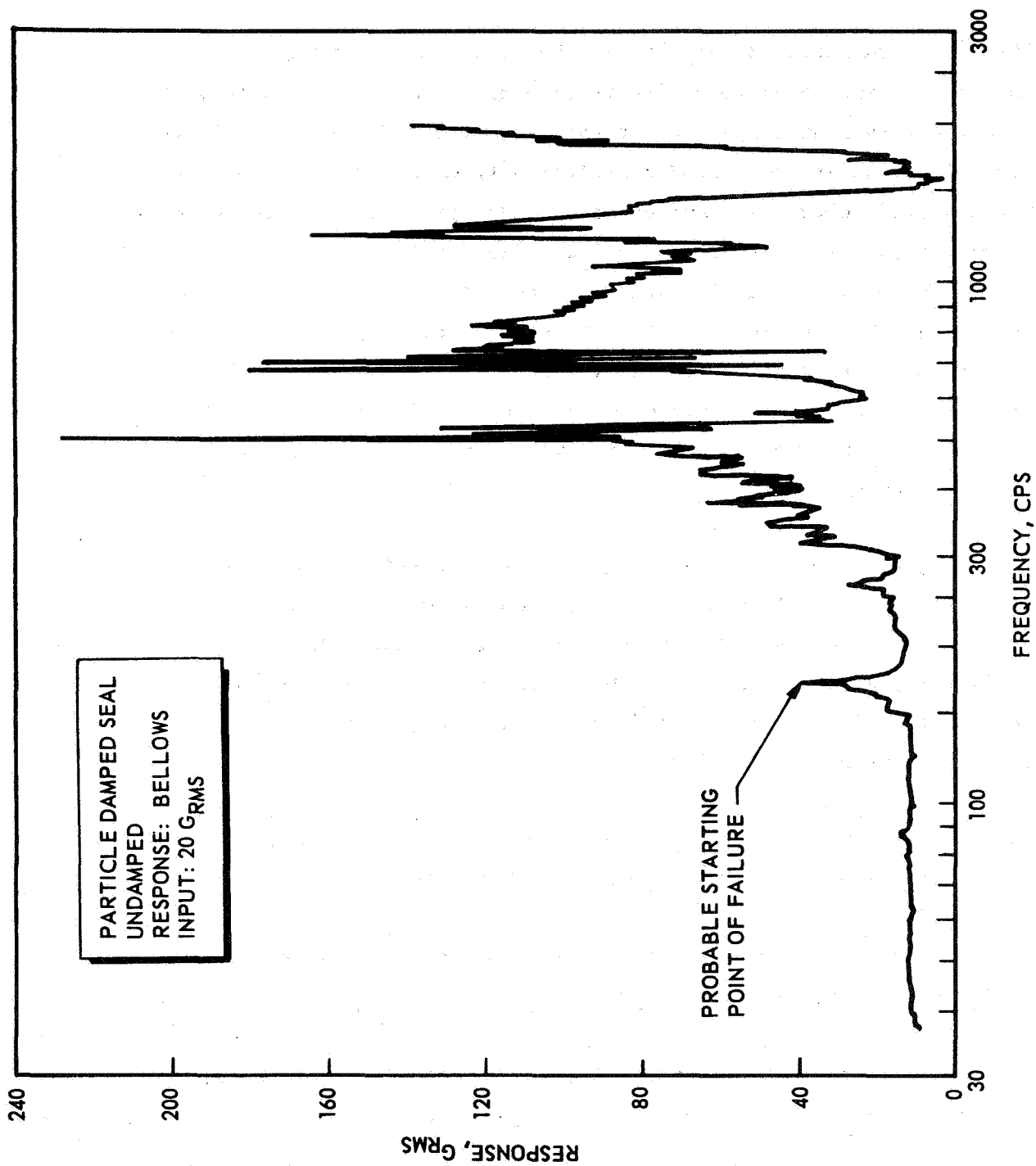
Figure 41. Bellows Response, 20 g, Particle Undamped
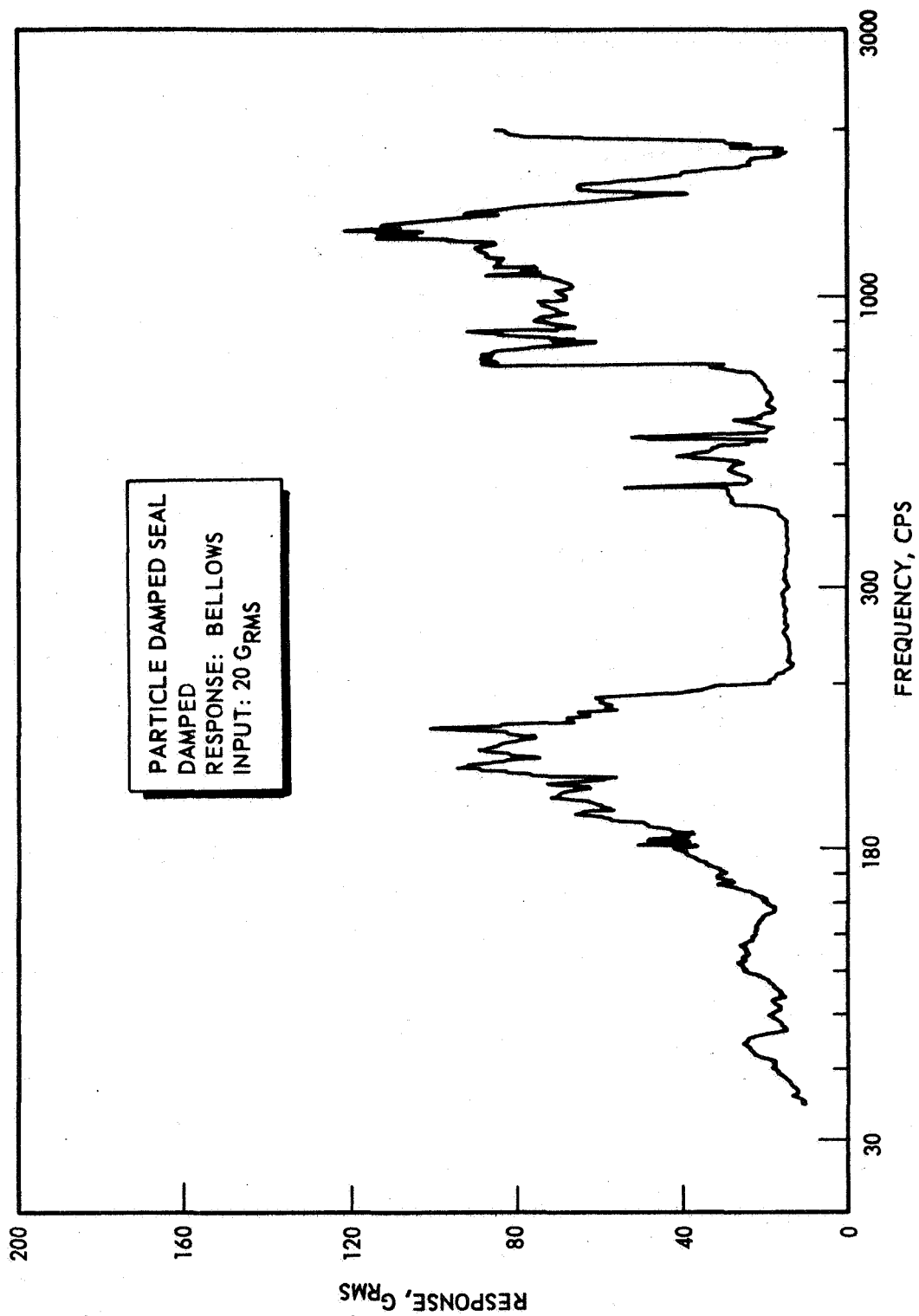
Figure 42. Bellows Response, 20 g, Particle Damped
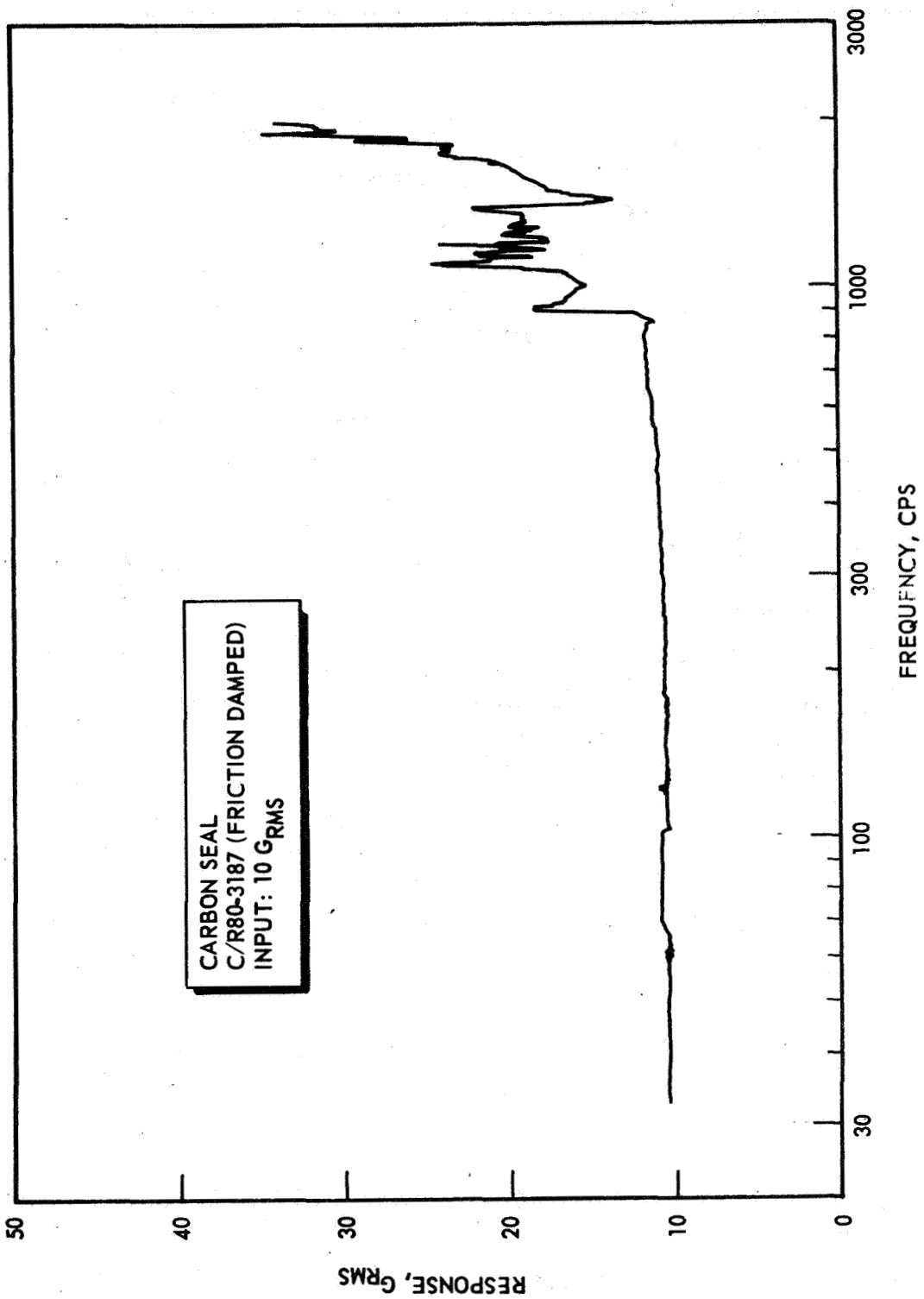
Figure 43. Bellows Response, 10 g, Friction Damped

CARBON SEAL
C/R80-3187 (FRICTION DAMPED)
INPUT: 10 G_{RMS}

RESPONSE, G_{RMS}

FREQUFNCY, CPS

PART II

PARTICLE DAMPED SEAL EVALUATION

Based on the results of vibration tests conducted in Part I of this report a program extension was granted for further investigation to demonstrate the dynamic use of particle damping when applied to a bellows shaft seal. The rotating environmental conditions were selected to represent seal operation in a liquid oxygen turbopump, and included contact velocities up to 320 ft/sec.

EVALUATION OBJECTIVES

1. Apply the particle damping concept within an envelope current with present turbopump design practice in regard to size and materials.

2. Construct a dynamic model to provide a method of determining seal performance and mechanical integrity with the application of particle damping.

3. Demonstrate the performance of and obtain data on the dynamic model when subjected to a simulated environment of a liquid oxygen turbopump at speeds up to 20,000 rpm.

SEAL DESIGN

The design of the dynamic test model was based on the configuration of the nonrotating model shown in Fig. 19 for which vibration data were obtained. The design of the dynamic model (Fig. 44) consists of the following:

1. Mass of spring system (no particles), 0.00272 $lb/sec^2/in.$

2. Mass of particles, 0.00103 $lb/sec^2/in.$

3. Mass ratio, 2.64

PARTICLE CONTAINERS
304 S.S.

HOUSING
304 S.S.

HIGH PRESSURE SIDE
LO$_2$

CARBON SEAL FACE
P692

WELDED BELLOWS
INCONEL 750

MATING SURFACE
INCONEL 718
CHROME PLATED

BELLOWS CARRIER
INCONEL 600

MOLYBDENUM SPHERICAL
POWDER-44 MICRONS
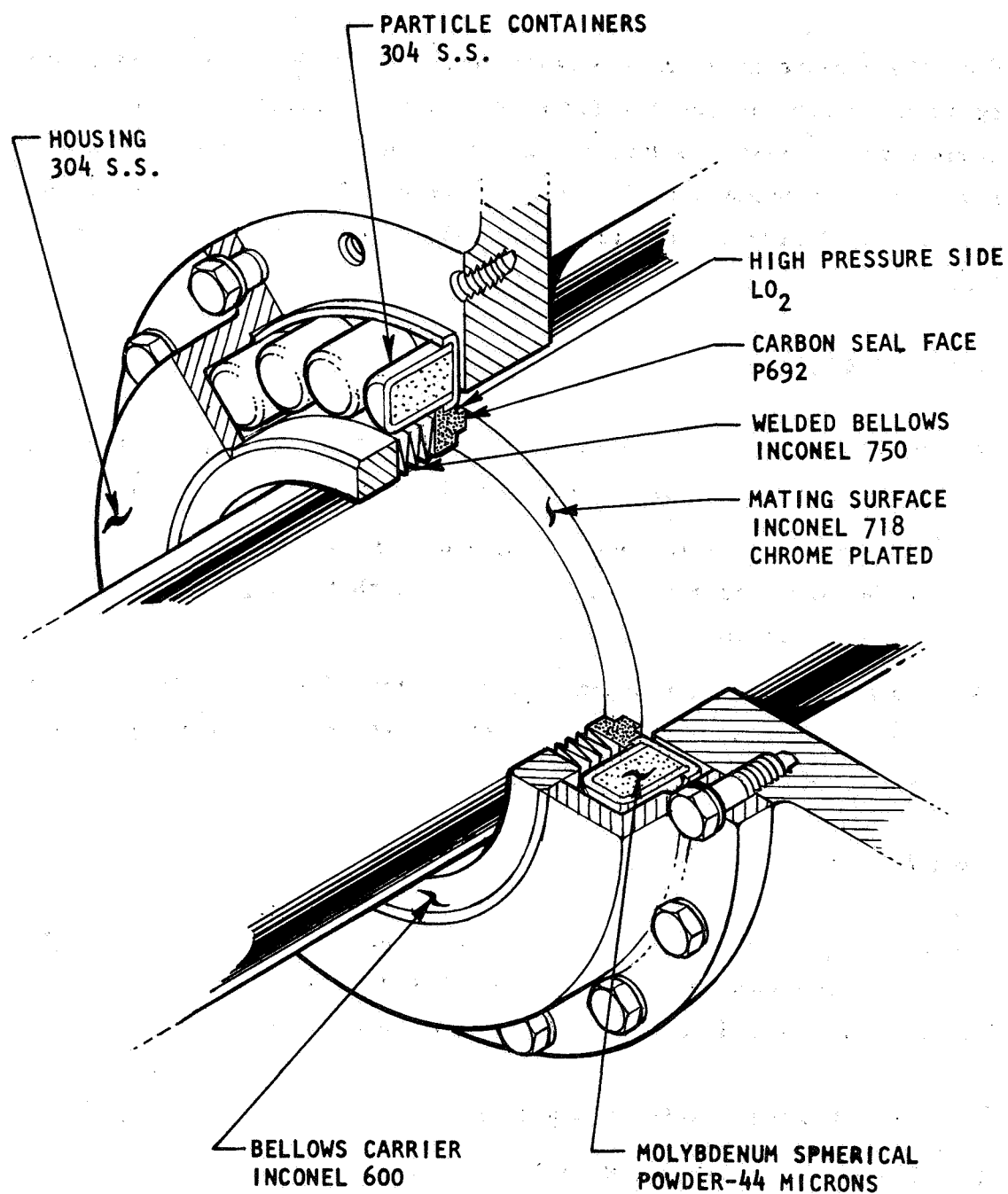
Figure 44. Particle Damped Seal

Based on hydraulic piston analogy, the forces produced on the bellows determining the load applied at the seal face are balanced to provide a desired condition. Balance characteristics are determined from the relationship of carbon nose OD, ID, and mean effective diameter (MED) of the bellows.

For the case of an OD pressurized bellows the releationship becomes:

$$\frac{OD^2 - MED^2}{OD^2 - ID^2} = \beta = \text{balance ratio}$$

The desired balance ratio for this seal was specified at 0.7, and was later reduced to 0.6 to further decrease the face loading. To determine the resultant load on the seal face, the following relationship, which is a summation of forces exerted on the carbon nose, can be expressed.

$$T_L = PA_N (\beta - \alpha) + S_F$$

where

T_L = Total load

A_N = Area of nose

β = Balance ratio

P = Environmental pressure

α = Pressure distribution across nose, 0.5 is assumed

S_F = Spring load of bellows at installed compression

The finalized seal has the following dimensional characteristics controlling the closing forces:

OD = 3.645 inches   MED (average), 3.550 inches

ID = 3.485 inches   Balance Ratio 0.6

Nose Area = 0.896 sq in.   Spring Force = 32 pounds (installed)

As a part of the finalized design considerations to improve particle
damping, a series of vibration beam tests was conducted. These were
similar to those conducted in Part I, with the addition of baffles in-
serted and positioned in the blocks. Two types of baffles were used,
as shown in Fig. 45 and 46. These are of a somewhat arbitrary arbitrary
design used for the purpose of dispersion of the particles in the event
that a packed condition that could affect damping efficiency occurs.

The test data indicate that packing or a dense cloud of particles does
not occur within the limits tested, and that the geometry of the baffles
used does not improve damping. The geometry of the baffles is such that
total freedom of the particles is prevented, resulting in a decrease in
damping as shown by the test results in Fig. 47.
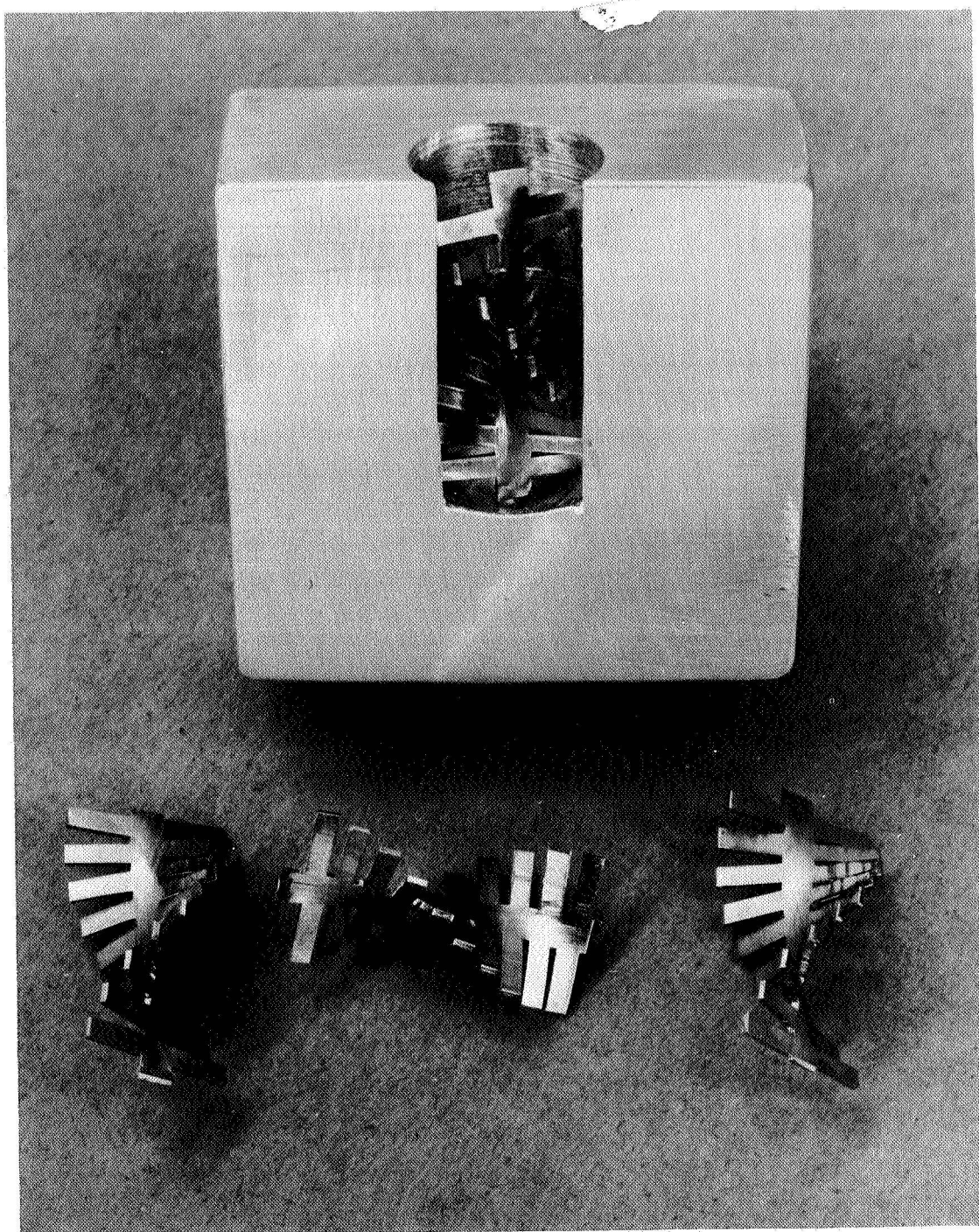
5AJ25-4/4/67-C1D

Figure 45. Spiral Baffle
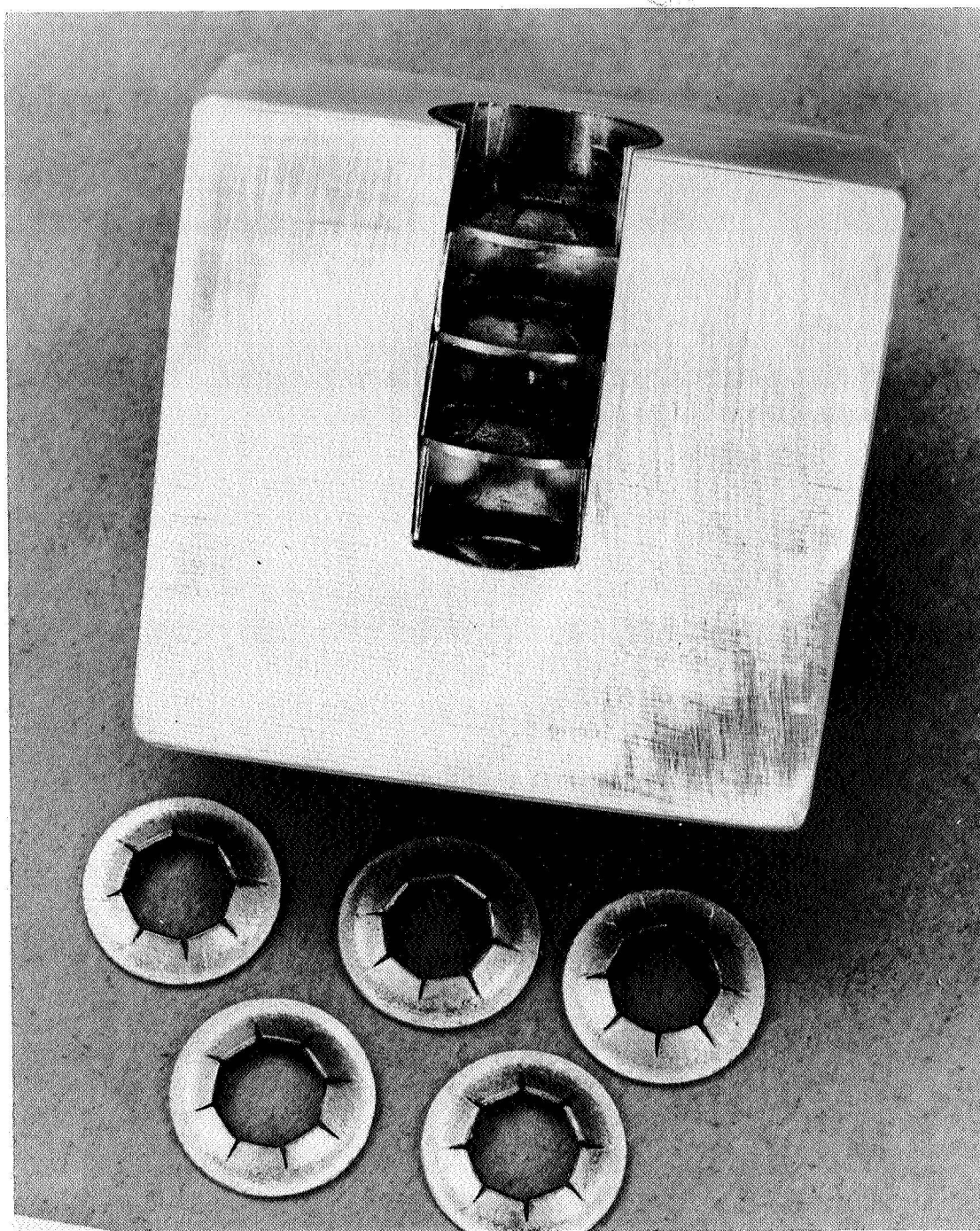
5AJ25–4/4/67–C1B

Figure 46. Disk Baffle
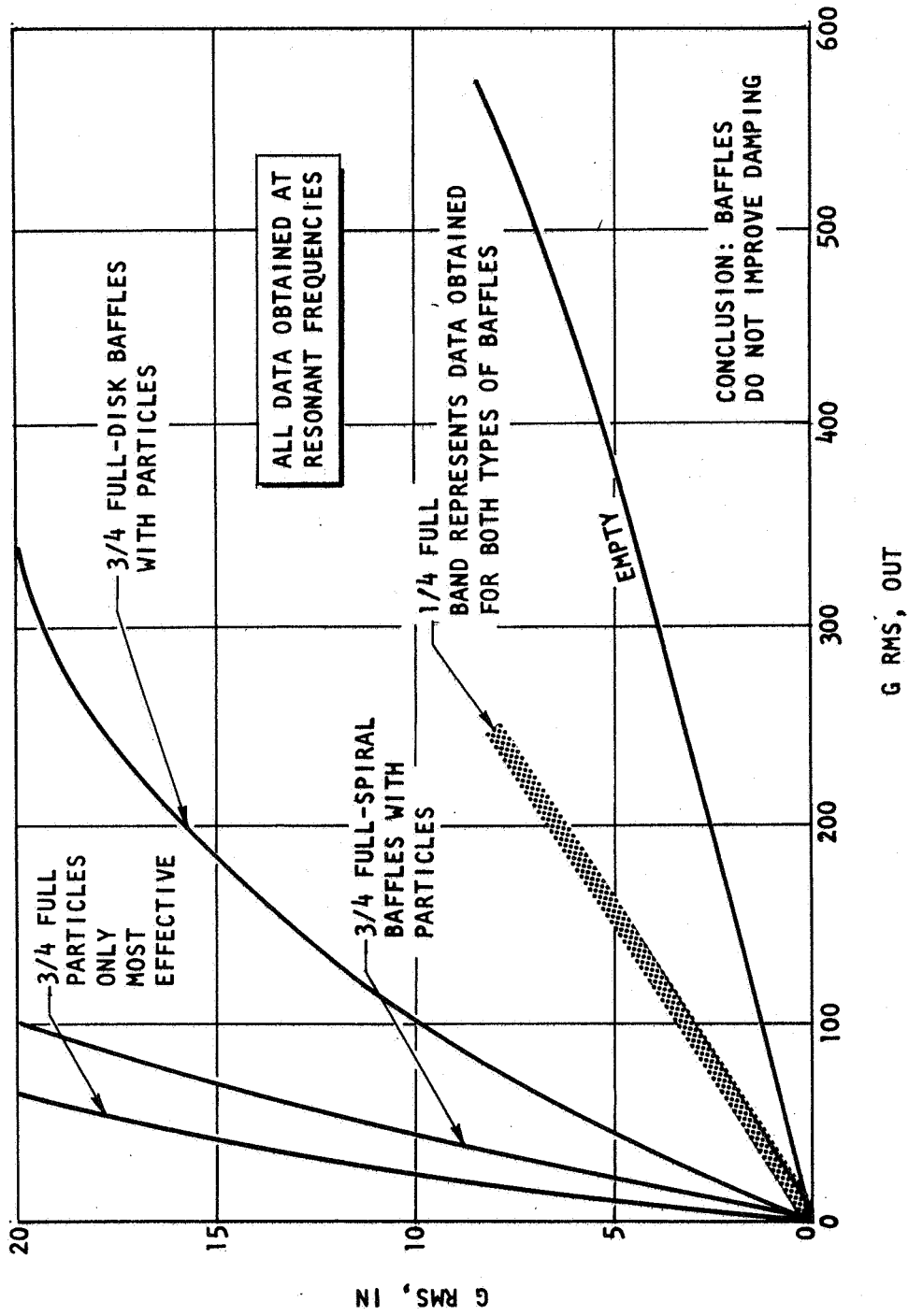
Figure 47. Test Results With Various Configurations

PARTICLE DAMPED SEAL TEST PROGRAM
AND HARDWARE DESCRIPTION

TEST PROGRAM

Five seals were designed and procured for static and dynamic operation to document the performance of the particle damped seal based on the requirements of the program. The dynamic operational criteria were based on conditions consistent with advanced turbomachinery. The same bellows configuration that was used in the construction of the nonrotating particle damped seal was used in the dynamic seal, therefore no tests to show the mechanical integrity of the bellows were necessary. The following tests were specified.

Liquid Oxygen Dynamic Tests

The objective of the dynamic tests was to obtain partial seal face behavior characteristics associated with carbon face wear and seal leakage, with and without the damping device employed. Three tests were planned, from which conclusions based on wear and leakage measurements were drawn. To aggravate the seal operating conditions, the seal was installed with a misalignment of 0.005 inch relative to the rotating mating ring. The mating ring was installed with an indicated axial runout of 0.002 inch, which tilted the ring and provided a wobbling effect.

The test environment was specified as pressurized liquid oxygen at pressures up to 250 psig, with a shaft speed of 20,000 rpm.

Initially the test plan shown in Table 9 was issued.

Dry Dynamic Tests

In addition to LOX environmental tests, two rotating tests using an available 150 hp d-c motor were planned. The tests were specified to be conducted dry at room temperature and pressure, with a shaft speed of 20,000 rpm. Seal face loading was set at a desired bellows preload. High-speed photography was used to monitor bellows movement for both tests.

TABLE 9

TEST PLAN

Test No.	Seal Serial No.	Objective	Operating Conditions
1	001	Duration 1800 seconds; determine static and dynamic leakage; measure carbon wear	Undamped Speed 20,000 rpm LOX pressure 225 psig LOX temperature -297 F Bearing coolant Flowrate 30 gpm Seal leakage Calibrated orifice $(\triangle P)$ for 0 to 10,000 scim
2	002	Duration 1800 seconds; determine static and dynamic leakage; measure carbon wear; compare with test No. 1	Damped Same operating conditions
3	003	Duration 7200 seconds; determine seal life characteristics	Damped Same operating conditions

Vibration Tests

A series of vibration tests was specified to establish bellows response with the seal spring mass restrained as in actual operation. In these tests, a seal is subjected to frequency sweep tests from 30 cps to 2 kc at input levels of 1, 5, 10, and 15 g rms, with the particle containers empty and with a selected effective fill level of 80 percent full. Damping for this system was defined as g rms undamped/g rms damped, with input excitation constant.

TEST HARDWARE

LOX Dynamic Tester

The tester used to accommodate the particle damped seal (Fig. 48) was coupled to a 350 hp electric motor for a drive source. The tester and
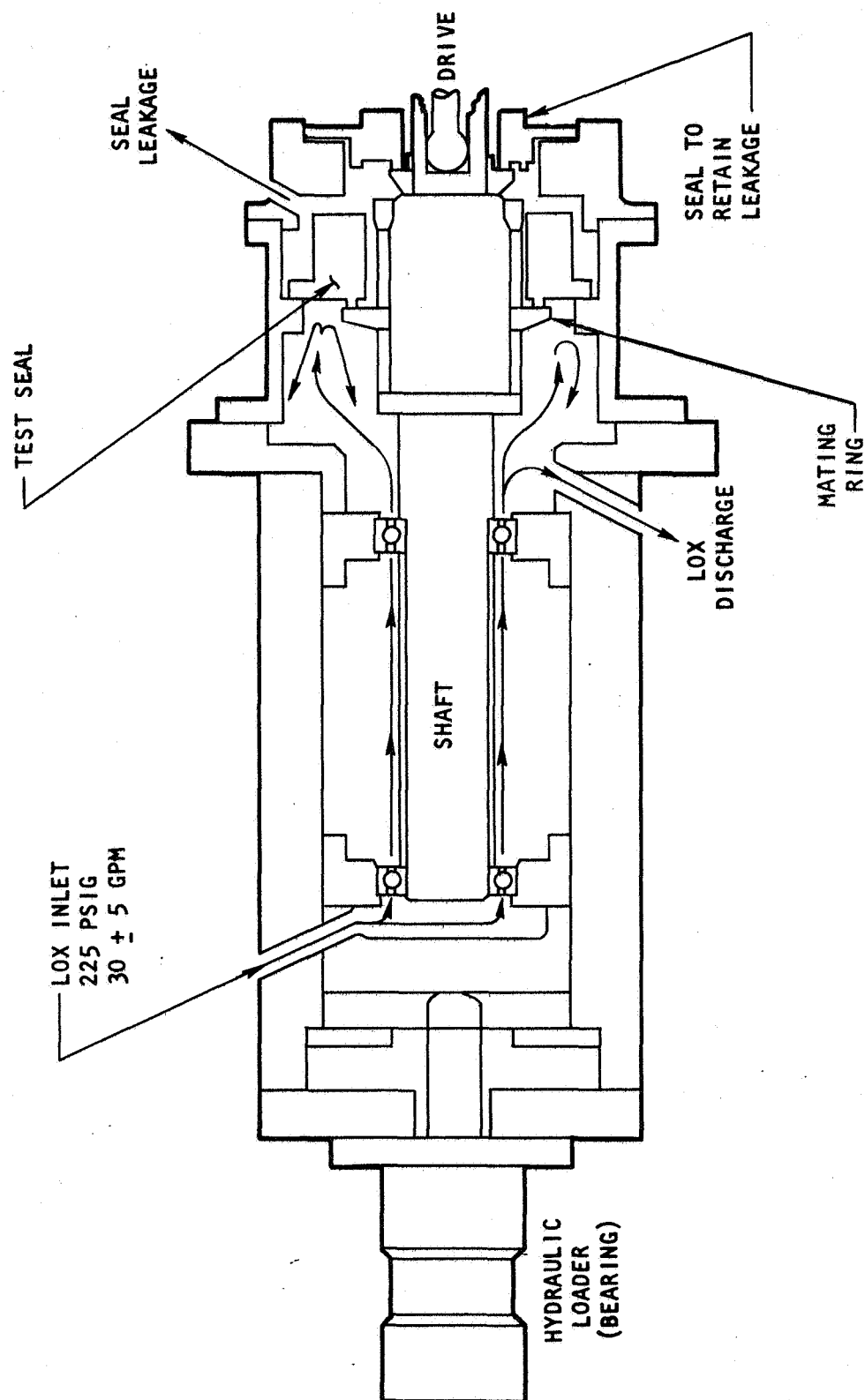
Figure 48. Bearing and Seal Tester

motor produce the torque and rotating speeds necessary to fulfill the needs of this program. Associated support equipment, including instrumentation to monitor all functions, is supplied at the Santa Suana test facility.

Vibration Tester

The vibration tests were conducted using an MB model C-10 shaker rated at 1200 pounds, with a frequency range of 0 to 3 kc. A typical test setup includes a plastic disk covering the carbon nose OD, with a threaded hole at the center, and a stud installed on the shaker. This provides adjustable bellows preload conditions between tests, and allows the observation with a strobe light to monitor decoupling at resonance. Accelerometers were used to monitor shaker output and seal response at the partical container support ring located between two filling ports. Response was measured only in the seal axial plane.

Dry Dynamic Tester

The output shaft of a 150-hp gear box arrangement was used to provide torque and required speed for the dry rotating tests. A simple fixture was fabricated (Fig. 49) to support and align the seal with the desired bellows compression to the mating ring. No special environment was used for the tests.

TEST RESULTS

LOX Dynamic Tests: First Series

Upon completion of the test setup without damping, the system was pressurized with LOX at 50 psig to cool the tester. At -275 F the pressure was raised to 225 psig. LOX flow was verified at 28 gpm. The drive motor was started. Upon approaching 15,000 rpm a 25-degree rise was noted at the tester LOX discharge port near the test seal after 60 seconds. The test was terminated for inspection of seal condition. The carbon face was
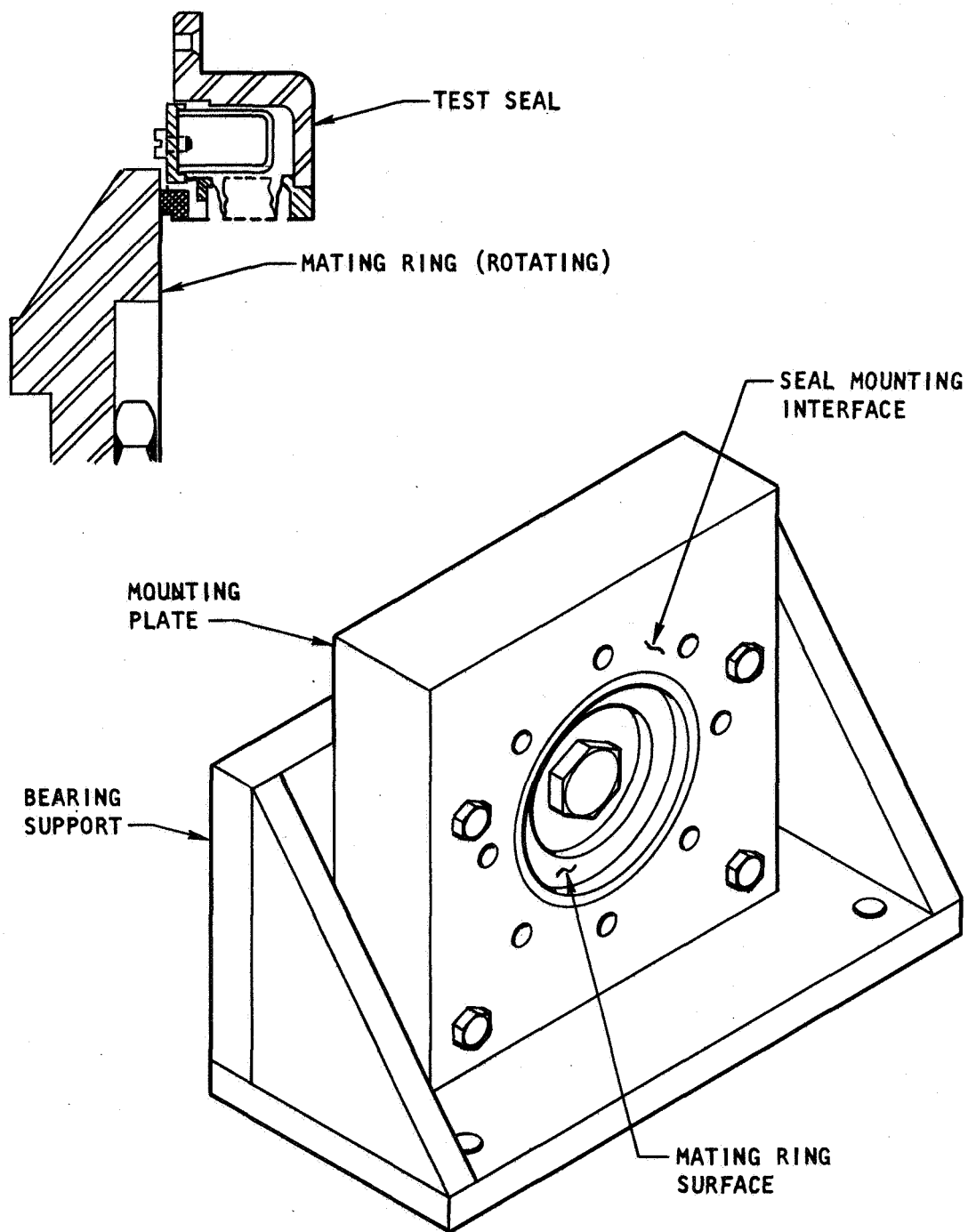
Figure 49.   Test Setup Dry Rotation Test

burned below the surface of the carbon retainer. The mating ring had a groove approximately 0.030 inch deep. An analysis was conducted to verify that the correct carbon and mating ring materials were used in the delivered seals, and, on the basis of examination of the carbon microstructure, the carbon was verified to be pure carbon grade P692. The mating ring was proved to be Inconel 750 chrome plated, 0.006 inch deep, and uniform throughout. Therefore, both materials were concluded to be as ordered.

During material analysis, the second seal was installed in the tester without particles. The test conditions were specified at lower operating values, reducing the tester pressure from 225 to 100 psig, which reduced the seal load (including hydraulic and spring load) to 50 pounds. The motor drive unit was started after pretest checkouts. After 56 seconds of operation, the same LOX temperature rise was noted at 15,000 rpm plus a high gaseous oxygen leakage. Testing was terminated. Inspection of the seal and mating ring showed the same general conditions, but to a smaller degree.

Analysis of the factors causing this type of failure within 60 seconds indicates the probable effect of the following:

1. Excessive interface load

2. Excessive speed in terms of linear velocity

3. Excessive vibration

4. A combination of the three variables

A condition causing the seal to bottom out could cause the damage observed. The tester was inspected for proper assembly and to verify shaft positioning to determine whether the seal could be compressed until no further bellows compression was available. Only minor discrepancies, which were not sufficient to cause any effect on operation, were noted.

The mechanical load conditions caused by hydraulic and spring forces were determined to be 50 pounds for the second test. This is not considered to

be extreme since many LOX seals in the industry operate successfully at higher values. A combination factor which generalizes seal operation was considered. This is called the PV factor, and uses the relationship of projected load relative to the linear velocity. For this case PV = 50/nose area (V_L) therefore PV = 50/0.911 (242) = 13,280 ft lb/sec in.^{2}, and is not considered to be higher than normal for LOX seal experience. Since the calculated total loads were not considered to be excessive during the previous tests, vibration was judged to be the most probable cause of seal failure. In an attempt to attenuate induced vibrations, the third and fourth tests were set up with the seal equipped with particles.

To verify seal performance and to ensure that no damage occurred at lower speeds, a 15-second test was conducted damped at 6000 rpm. Inspection of test hardware indicated satisfactory performance; the seal was reinstalled.

The fourth test was conducted to accomplish a planned speed of 20,000 rpm at a seal LOX pressure of 200 psig. After stabilization of pre-run parameters, the motor drive unit was started and speed increased incrementally to 15,250 rpm in 50 seconds. Speed was held constant for 67 seconds. The speed was further increased, and, upon reaching 16,800 rpm, the test was terminated by a fire which destroyed the seals after a total run duration of 118 seconds.

In consideration of the grooved condition of the mating rings during the first two tests and upon evaluation of the damaged hardware of Test No. 4, it was concluded that the damage was caused by excessive heat generation at the rotating seal interface; however, the mating ring surface involved in the fire (Fig. 50) displayed a short section of the wear path of which the surface was not destroyed but had experienced normal contact. This condition indicates that the fire did not necessarily arise from excessive energy input at the rubbing face, but from an undefined source. Since the steady-state load analysis did not indicate an excessive load for any of the test seals, it was further concluded that the damage observed after the first two tests probably resulted from vibration.
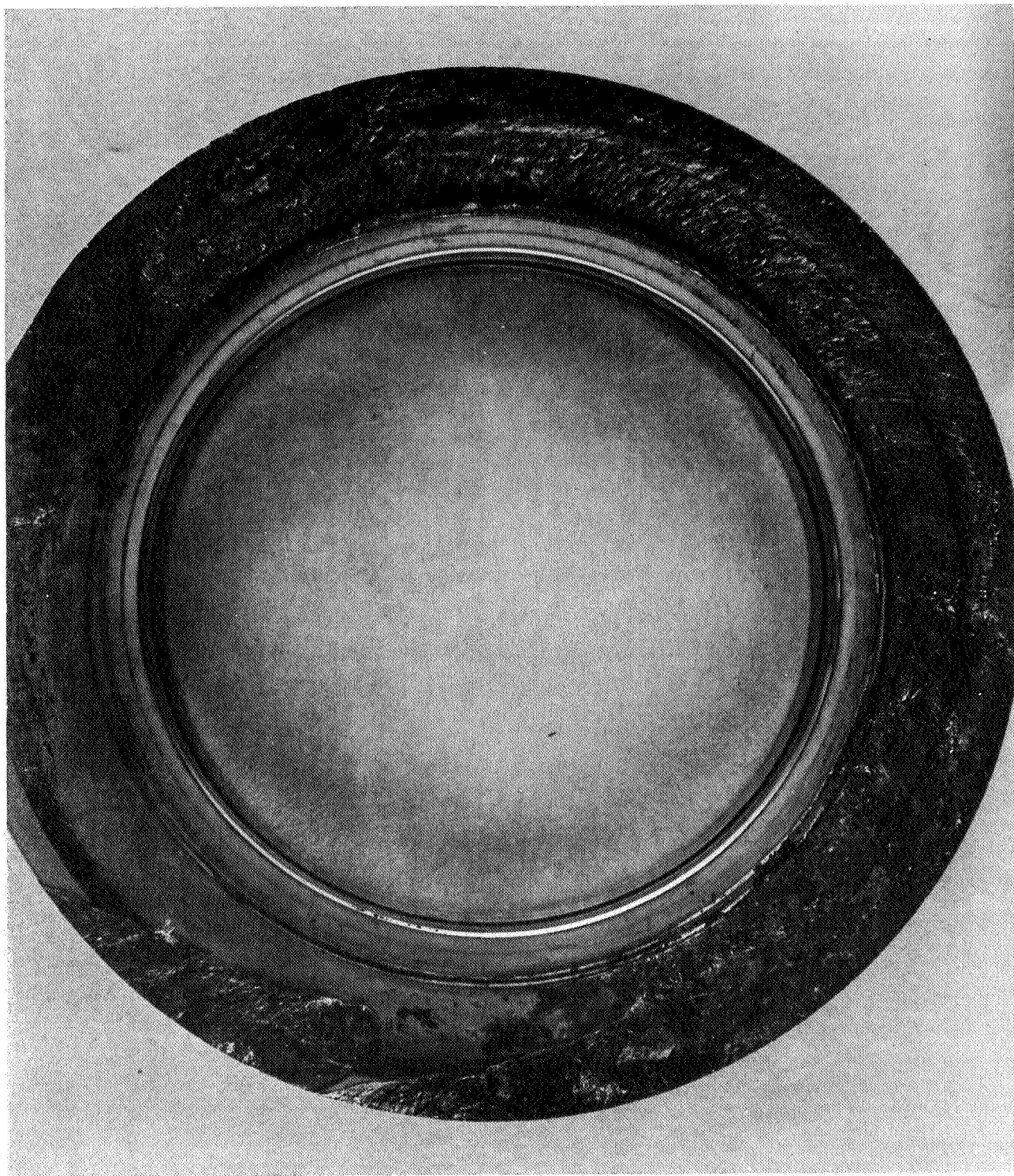
Figure 50. Seal Condition After Test No. 4

To investigate the potential mode of failure due to vibration, a fourth seal was set up for a vibration test series to document static performance when subjected to input loads up to 15 g rms and monitored over a bandwidth of 0 to 2 kc. A total of 22 tests was conducted with variable test conditions; only the more significant are discussed here. In all cases a frequency response curve is presented to depict the frequency response of the accelerometer attached at the particle damping support ring vs g rms response load to constant input loads.

Shown in Fig. 51 is the response plot of 1 g input. The resonant frequencies can be identified, the first of which occurs at 279 cps. This frequency compares to a shaft speed of 16,800 rpm, and is the speed at which the fire occurred. With the input of 1 g, the response was 13 g.

At a 5 g input (Fig. 52) the response was tuned at the same resonant point. The output of 80 g is only a relative value since the results can be varied by changing the bellows preload. The effect of damping is indicated by the result of Test No. 6, showing the undamped response to be 200 g as compared to 80 g damped in Test No. 2.

Since the resonant frequency of 279 cps is observed to be potentially responsible for the seal failure, steps were taken to modify the seal to increase the bellows spring rate driving the first resonant frequency up and/or damping the response to a negligible value.

To control the frequency response one-half of the bellows convolutions were bridged with a weld bead in four places beginning at the seal housing end of the bellows . This method also slightly reduces the spring mass. The results of the final test (Fig. 53) show no resonant point within the shaft speed range of 0 to 333 cps or equivalent to 0 to 20,000 rpm. Frequencies above 333 cps are of little concern for the projected test series.

To incorporate the increased bellows spring rate in the seal, a ring was fabricated and cut in four sections for assembly at the bellows ID. A
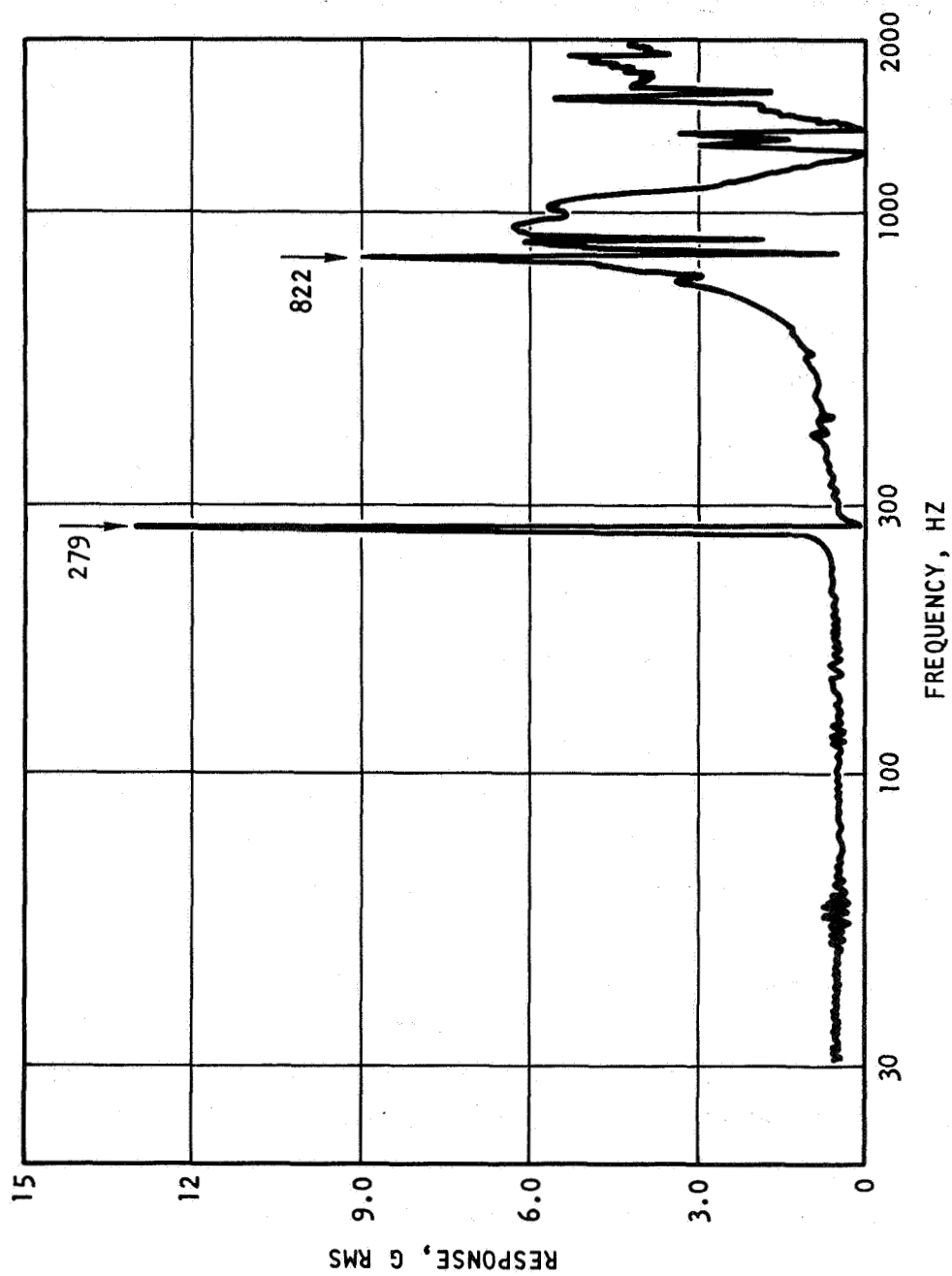
Figure 51. Particle Damped Seal, Damped Response, Bellows Input: 1 g rms, S/N 5

110
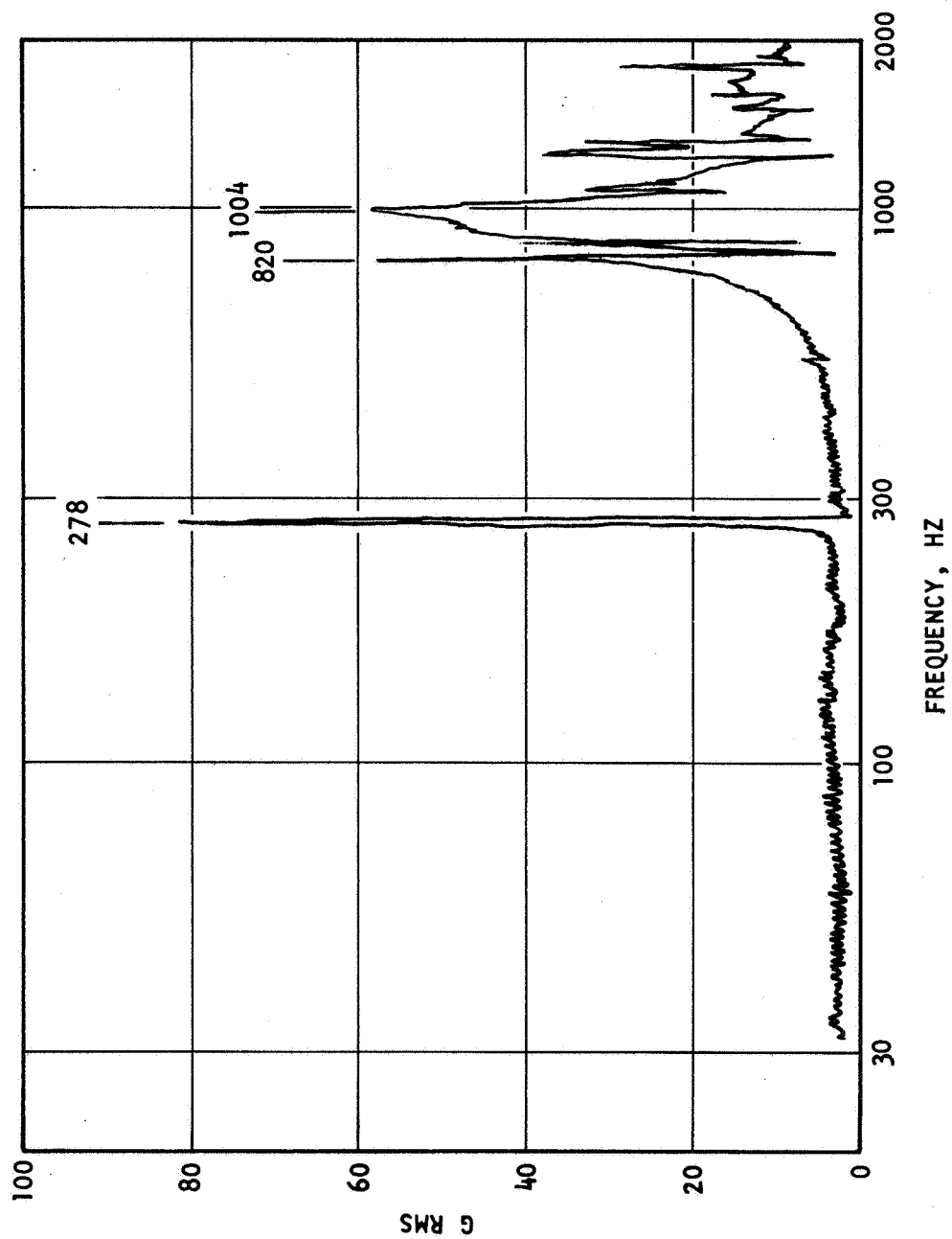
Figure 52. Particle Damped Seal, Damped Response Bellows
Input: 5 g rms S/N 5
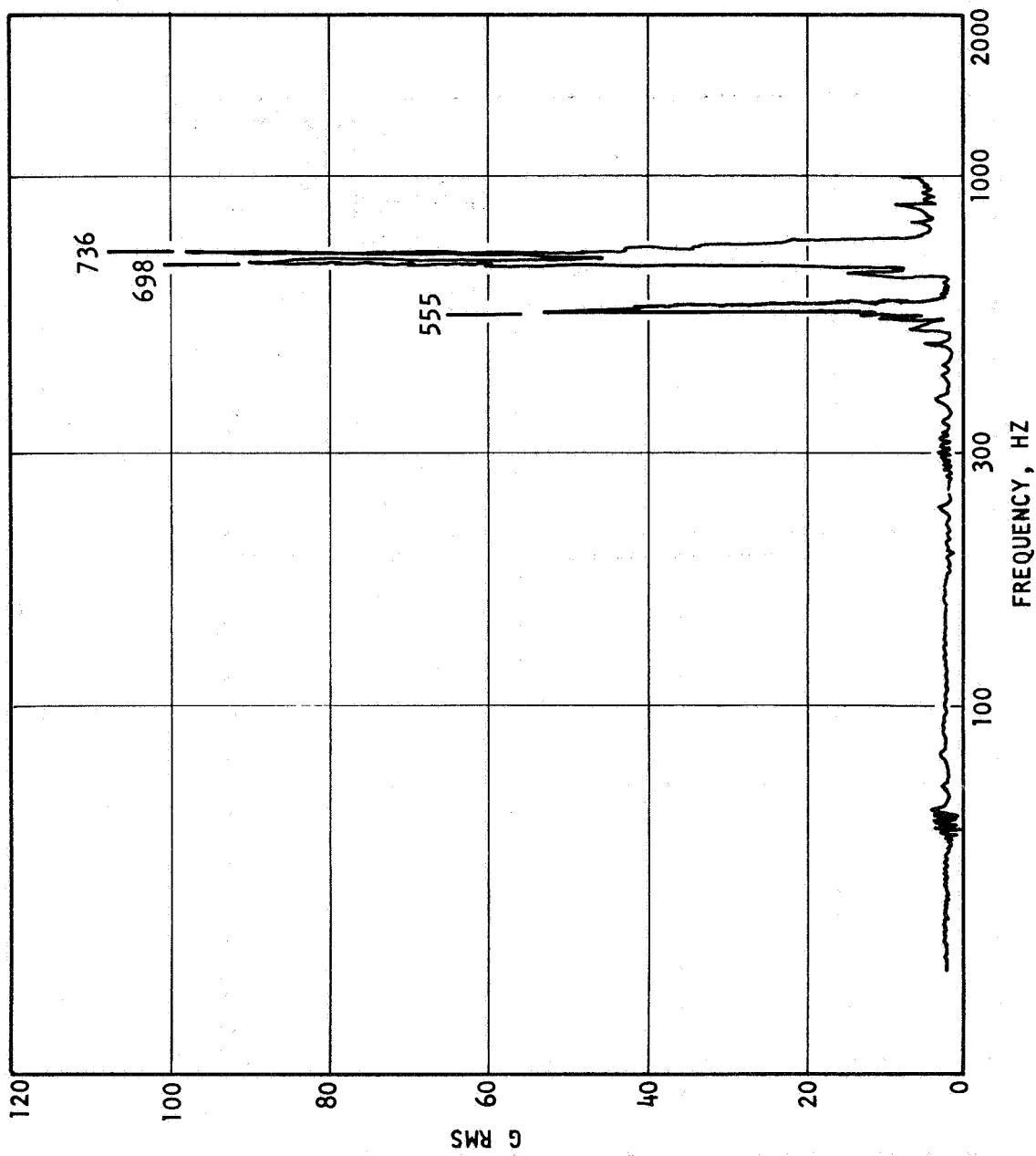
Figure 53. Particle Damped Seal, Undamped Response
Bellows Input: 5 g rms, S/N (Unwelded)

groove on the ring OD was cut at a location to encompass the center convolution weld bead. Then the sections were welded at the rear bellows carrier, thus inactivating half the available convolutions. This procedure approximately doubles the spring rate. The restraining feature was applied to the two reuseable seals. New carbon rings were installed and machined to diameters obtaining a balance ratio of 0.6. Upon completion of this task a short vibration test was conducted on each seal to verify that no resonant points occurred within the planned operating ranges.

LOX Dynamic Tests: Second Series

The second series of LOX dynamic tests on the particle damped seal represents the last phase of LOX testing accomplished within the scope of this program. The test procedure is essentially the same as that used for the first series. The plan initially was composed as shown in Table 10.

TABLE 10

PLANNED TESTING SEQUENCE

Test No.	Seal Serial Number	LOX Pressure, psig	LOX Flowrate, gpm	Shaft Speed, rpm	Duration, minutes	Remarks
1	C/R 1	200	30 ±5	5,000	3	Damped
2				10,000	3	
3				15,000	3	
4				20,000	10	
5	CR/3			15,000	3	Undamped
6	C/R 3			20,000	10	

The first three tests of the damped series were conducted in accordance with the test plan for durations of 3 minutes. At the end of each test the sealing surfaces were examined for carbon wear and mating ring appearance. The surface was in excellent condition, exhibiting a normal wear path on the mating ring.

The fourth test was conducted with the same seal using a new mating ring. The intended operating goal was 10 minutes at 20,000 rpm. Speed was first stabilized at 15,000 rpm for approximately 180 seconds and slowly increased to 18,200 rpm (294 ft/sec). At this point a redline condition of 50 psig in the seal drain line indicated high leakage and seal instability that required test termination. Based on previous instability problems during the first series tests, a new goal of 15,000 rpm was established with a test duration of 30 minutes. The reduction to 15,000 rpm remains sufficient to demonstrate face seal capability because the equivalent rubbing linear velocity is 242 ft/sec, and is 65 percent higher than any production turbo-pump at Rocketdyne for liquid oxygen application, at this time.

With a new mating ring installed, Test No. 5 was conducted. The first 400 seconds of the 30-minute test are shown in Fig. 54. A stable running condition after 200 seconds at 15,000 rpm is indicated. The oscillation that is apparent can be considered run-in time of the seal surfaces. Disassembly of the tester showed the hardware to be in excellent condition with only 0.010 inch total carbon nose wear. Figure 55 shows the posttest condition of the seal.

A series of two subsequent tests was conducted using seal S/N 2 without particle damping. The first test was run at 15,000 rpm for 3 minutes. Hardware condition was checked at test termination. Although seal leakage oscillation was apparent in the order of 8 to 12 psi, no visual damage had occurred. The second test was conducted using a new mating ring for a duration of 30 minutes. The first 400 seconds are shown in Fig. 56. Seal leakage pressure oscillations that are apparent occurred throughout the 30-minute duration. The pressure rise indicated at 150 seconds is the effect of speed, increasing from 10,000 to 15,000 rpm. Examination of the test hardware showed hot spots on the chrome plated mating ring plus carbon transfer as a result of stick slip. Carbon wear was measured at a total of 0.025 inch.
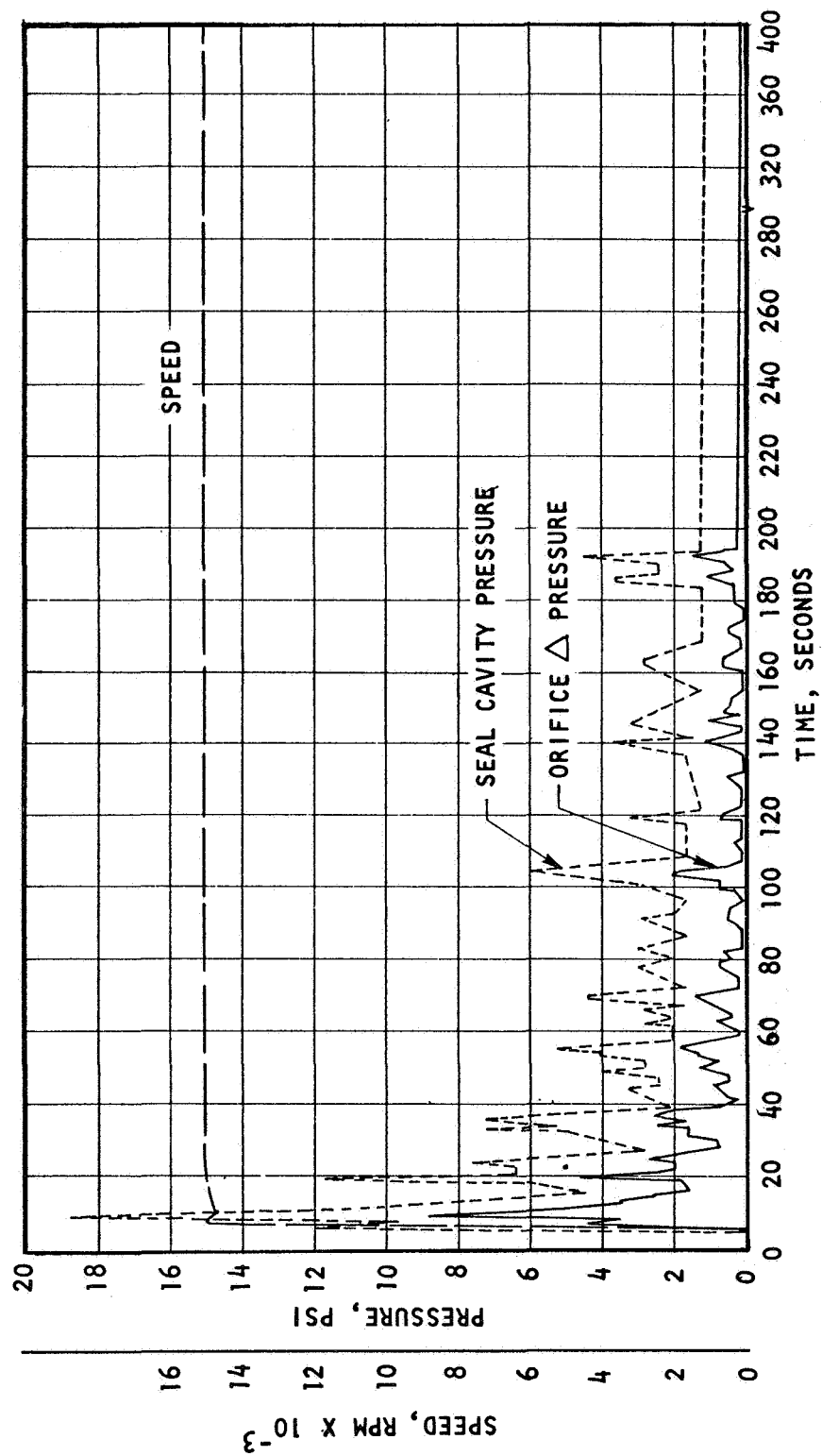
Figure 54. Particle Damped Seal S/N 3, Damped
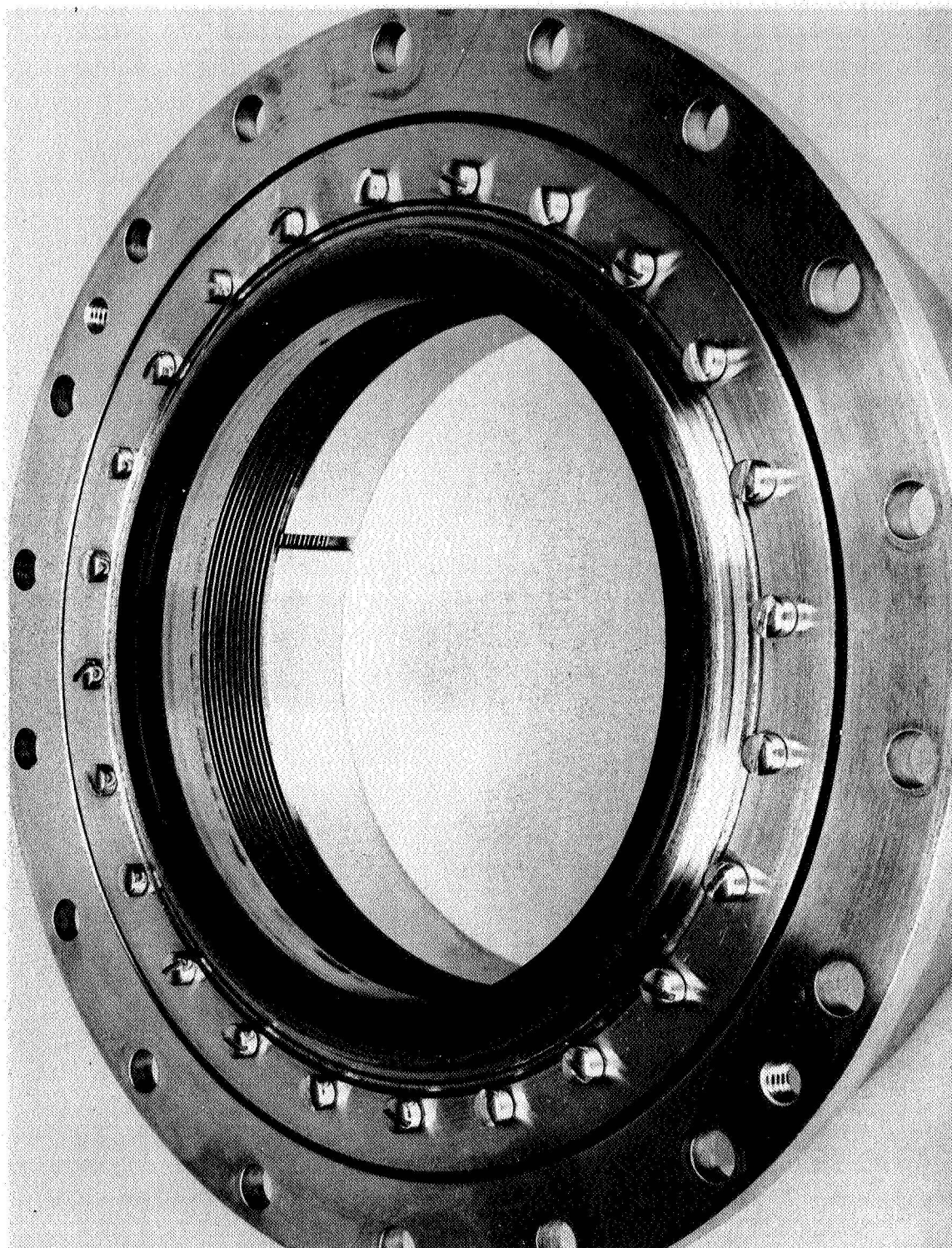
Figure 55. Seal Condition After Test No. 5
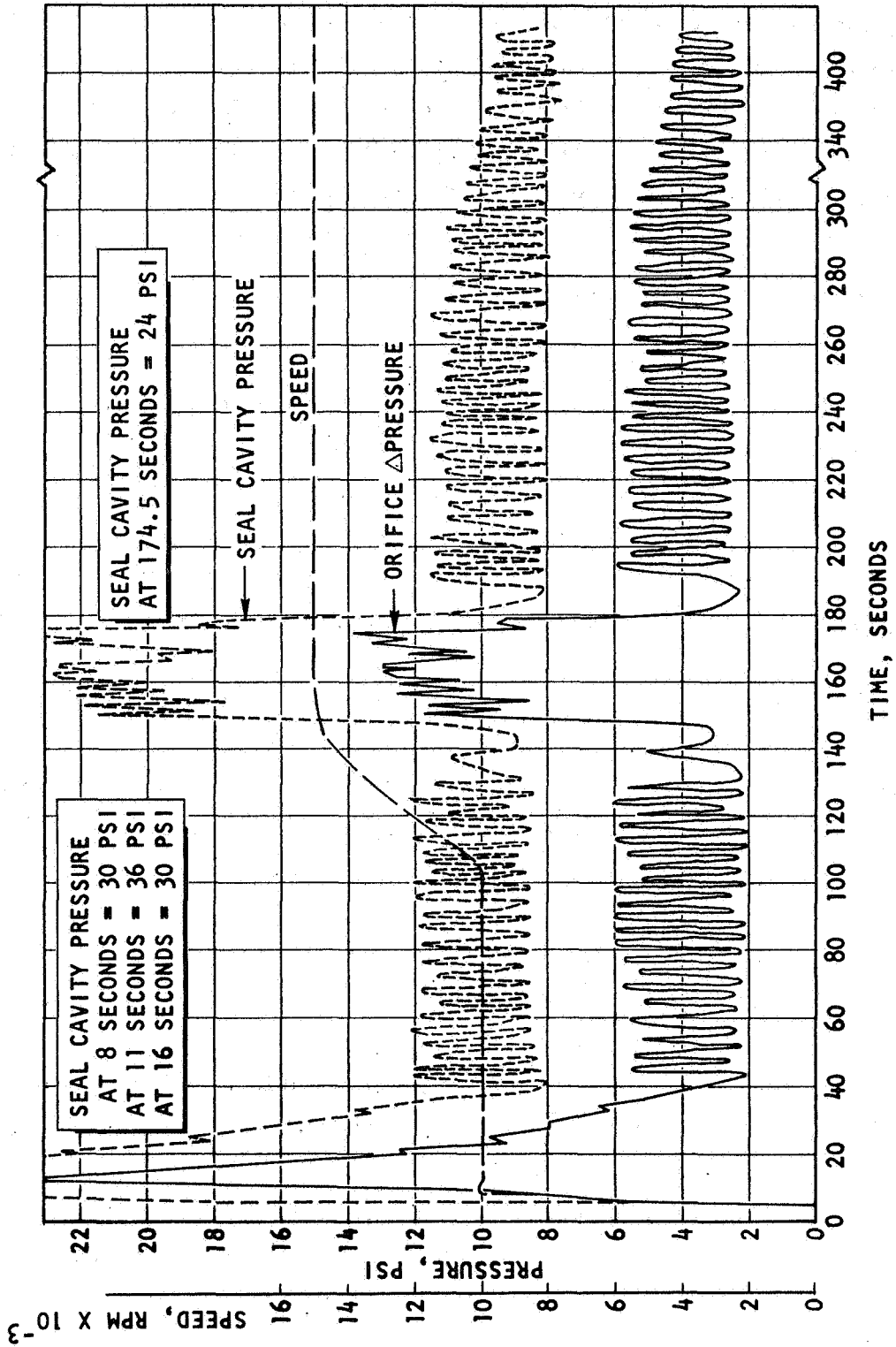
Figure 56. Particle Damped Seal S/N 2, Undamped

117

Figure 57 is a plot representing seal leakage discharge pressures shown in Fig. 54 and 56. The plot summarizes the results obtained when damped and undamped and notes the carbon wear and calculated leakage. Particle damping has been demonstrated to be an effective method to control bellows oscillatory movement without the potential danger of exposed rubbing surfaces in an explosive environment, and has the potential capability to function as an omni-directional damping system instead of a single plane. Further, evaluation in terms of efficiency could provide necessary information to reduce procurement costs and manufacturing difficulties.

Dry Dynamic Tests

A series of rotating tests was conducted to visually observe seal movement characteristics. The series was documented by high-speed photography at speeds up to 20,000 rpm. Both the undamped and damped cases were observed.

The tests consisted of installing the seal alternately at the same bellows compression of 0.095 inch, which provided a spring load of 20 pounds. Both seals were of the type used in the first series tests and were without later modifications to increase bellows spring rate. Initially, alignment of the undamped seal was set up with a mating ring axial runout of 0.004 inch to produce a wobbling effect. A pressurized environment was not used, reducing the carbon wear potential from hydraulic loading, and readily permitting high-speed camera access.

The first test, conducted without particles at 20,000 rpm, resulted in severe vibration and noise level; therefore, the induced wobbling effect was reduced by changing to a maximum axial runout of 0.001 inch. The second test indicated improvement, but substantial bellows and seal movement was apparent. At a film speed of 500 frames per second a nutating action of the seal face and bellows was recorded, which indicated the type response when undamped. Five hundred frames per second is equivalent to 12.5 ft/sec. Approximately 9 nutations were counted in 1 foot of film; therefore, 9 x 12.5 = 112.5 nutations/sec, or 112.5 cps.

118
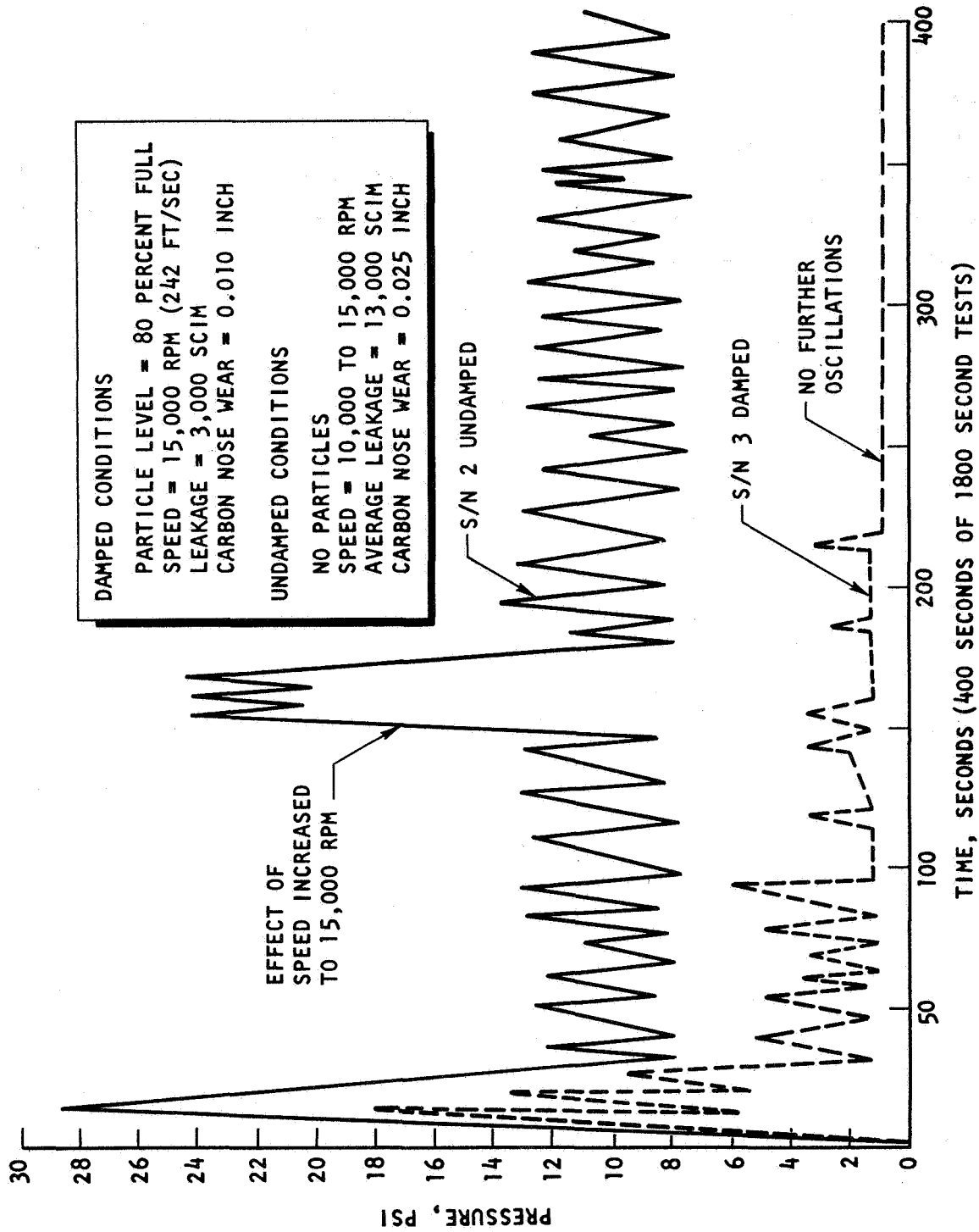
Figure 57. Leakage Seal Pressure

DAMPED CONDITIONS

PARTICLE LEVEL = 80 PERCENT FULL
SPEED = 15,000 RPM (242 FT/SEC)
LEAKAGE = 3,000 SCIM
CARBON NOSE WEAR = 0.010 INCH

UNDAMPED CONDITIONS

NO PARTICLES
SPEED = 10,000 TO 15,000 RPM
AVERAGE LEAKAGE = 13,000 SCIM
CARBON NOSE WEAR = 0.025 INCH

EFFECT OF
SPEED INCREASED
TO 15,000 RPM

S/N 2 UNDAMPED

S/N 3 DAMPED

NO FURTHER
OSCILLATIONS

TIME, SECONDS (400 SECONDS OF 1800 SECOND TESTS)

PRESSURE, PSI

119

At a shaft speed of 20,000 rpm (333 cps) the ratio of shaft speed to nutating frequency is 3:1.

Tests conducted with the same seal using particle damping showed no visible indication of nutating action at 20,000 rpm or less, and produced no discernible noise levels. Review of the film verified the results obtained from vibration tests and simulated turbopump tests, viz., the stable effect obtained with the use of particle damping.

APPENDIX A

DISTRIBUTION LIST

COPIES	RECIPIENT	DESIGNEE
	NASA Marshall Space Flight Center Marshall, Space Flight Center, Alabama 35812	
2	Office of Technical Information, MS-IP	(X)
1	Technical Library	(X)
1	Purchasing Office, PR-EC	(X)
1	Patent Office, M-PAT	(X)
1	Keith Chandler, R-P&VE-PA	(X)
1	Technology Utilization Office, MS-T	(X)
5	F. D. Pitsenberger (C.O.R.)	(X)
4	Chief, Liquid Exper. Engr'g., RPX	( )
4	Chief, Liquid Propulsion Technology, RPL Office of Advanced Research and Technology NASA Headquarters Washington, D.C. 20546	(X)
25	NASA Scientific and Technical Information Facility P.O. Box 33 College Park, Maryland 20740	(X)
1	Director, Launch Vehicles and Propulsion, SV Office of Space Science and Applications NASA Headquarters, Washington, D.C. 20546	(X)
1	Mr. Charles Donlan Director, Advanced Manned Missions, MT Office of Manned Space Flight NASA Headquarters, Washington, D.C. 20546	(X)
1	Mr. Leonard Roberts Mission Analysis Division NASA Ames Research Center Moffett Field, California 94035	(X)

NASA Field Centers

COPIES	RECIPIENT	DESIGNEE
2	Ames Research Center Moffett Field, California 94035	H. J. Allen
2	Goddard Space Flight Center Greenbelt, Maryland 20771	Merland L. Moseson Code 620
2	Jet Propulsion Laboratory California Institute of Technology 4800 Oak Grove Drive Pasadena, California 91103	Henry Burlage, Jr. Propulsion Div., 38
2	Langley Research Center Langley Station Hampton, Virginia 23365	Ed Cartwright Director
2	Lewis Research Center 21000 Brookpark Road Cleveland, Ohio 44135	Dr. Abe Silverstein Director
2	Marshall Space Flight Center Marshall Space Flight Center, Ala. 35812	Hans G. Paul Code R-P&VE-P
2	Manned Spacecraft Center Houston, Texas 77001	Dr. Robert R. Gilruth Director
2	John F. Kennedy Space Center, NASA Cocoa Beach, Florida 32931	Dr. Kurt H. Debus

GOVERNMENT INSTALLATIONS

1	Aeronautical Systems Division Air Force Systems Command Wright-Patterson Air Force Base Dayton, Ohio 45433	D. L. Schmidt Code ASRCNC-2
1	Commander, Office of Research Analysis (OAR) Holloman Air Force Base, New Mexico 88330	RRRD
1	Air Force Missile Test Center Patrick Air Force Base, Florida	L. J. Ullian
1	Space & Missile Systems Organization Los Angeles 45, California	Col. Clark Technical Data Center
1	Arnold Engineering Development Center Arnold Air Force Station Tullahoma, Tennessee	Dr. H. K. Doetsch
1	Bureau of Naval Weapons Department of the Navy Washington, D.C.	J. Kay RTMS-41
1	Defense Documentation Center Headquarters Cameron Station, Building 5 5010 Duke Street Alexandria, Virginia 22314 ATTN. TISIA	

COPIES	RECIPIENT	DESIGNEE
1	Headquarters, U.S. Air Force Washington 25, D.C.	Col. C. K. Stambaugh AFRST
1	Picatinny Arsenal Dover, New Jersey 07801	I. Forsten, Chief Liquid Propulsion Laboratory, SMUPA-DL
1	Air Force Rocket Propulsion Laboratory Research and Technology Division Air Force Systems Command Edwards, California 93523	RPRR/Mr. H. Main
1	U.S. Army Missile Command Redstone Arsenal Alabama 35809	Dr. Walter Wharton
1	U.S. Naval Ordnance Test Station China Lake California 93557	Code 4562 Chief, Missile Propulsion Div.

CPIA

1	Chemical Propulsion Information Agency Applied Physics Laboratory 8621 Georgia Avenue Silver Springs, Maryland 20910	Tom Reedy

INDUSTRY CONTRACTORS

1	Aerojet-General Corporation P.O. Box 296 Azusa, California 91703	L. F. Kohrs
1	Aerojet-General Corporation P.O. Box 1947 Technical Library, Bldg. 2015, Dept. 2410 Sacramento, California 95809	R. Stiff
1	Aeronutronic Philco Corporation Ford Road Newport Beach, California 92663	D. A. Carrison
1	Aerospace Corporation 2400 East El Segundo Boulevard P.O. Box 95085 Los Angeles, California 90045	John G. Wilder MS-2293 Propulsion Dept.
1	Arthur D. Little, Inc. 20 Acorn Park Cambridge, Massachusetts 02140	Library

COPIES	RECIPIENT	DESIGNEE
1	Astropower Laboratory Douglas Aircraft Company 2121 Paularion Newport Beach, California 92663	Dr. George Moc Director
1	Astrosystems International, Inc. 1275 Bloomfield Avenue Fairfiled, New Jersey 07007	A. Mendenhall
1	Atlantic Research Corporation Edsall Road and Shirley Highway Alexandria, Virginia 22314	Dr. Ray Friedman
1	Beech Aircraft Corporation Boulder Division Box 631 Boulder, Colorado	J. H. Rodgers
1	Bell Aerosystems Company P.O. Box 1 Buffalo, New York 14240	W. M. Smith
1	Bellcomm 1100 17th Street Washington, D.C.	Joseph Tuschurgi
1.	Bendix Systems Division Bendix Corporation 3300 Plymouth Road Ann Arbor, Michigan	John M. Brueger
1	Boeing Company P.O. Box 3707 Seattle, Washington 98124	Library
1	Boeing Company 1625 K Street N. W. Washington, D.C. 20006	Library
1	Boeing Company P.O. Box 1680 Huntsville, Alabama 35801	Ted Snow
1	Missile Division Chrysler Corporation P.O. Box 2628 Detroit, Michigan 48231	John Gates
1	Wright Aeronautical Division Curtiss-Wright Corporation Wood-Ridge, New Jersey 07075	G. Kelly

COPIES	RECIPIENT	DESIGNEE
1	Missile and Space Systems Division McDonnell Douglas Aircraft Corp. 3000 Ocean Park Boulevard Santa Monica, California 90406	R. W. Hallet Chief Engineer Advanced Space Tech.
1	Aircraft Missiles Division Fairchild Hiller Corporation Hagerstown, Maryland 10	J. S. Kerr
1	General Dynamics/Astronautics Library and Information Services (128-00) San Diego, California 92112	Frank Dore
1	Re-Entry Systems Department General Electric Company 3198 Chestnut Street Philadelphia, Pennsylvania 19101	F. E. Schultz
1	Advanced Engine and Technology Dept. General Electric Company Cincinnati, Ohio 45215	D. Suichu
1	Grumman Aircraft Engineering Corp. Bethpage, Long Island New York	Joseph Gavin
1	Ling-Temco-Vought Corporation Astronautics P.O. Box 5907 Dallas, Texas 75222	Warren C. Trent
1	Lockheed Propulsion Company P.O. Box 111 Redlands, California 92374	H. L. Thackwell
1	Lockheed Missiles and Space Co. ATTN: Technical Information Center P.O. Box 504 Sunnyvale, California 94088	Y. C. Lee
1	The Marquardt Corporation 16555 Saticoy Street Van Nuys, California 91409	Leo Bell
1	Denver Division Martin Marietta Corporation P.O. Box 179 Denver, Colorado 80201	Dr. Morganthaler
1	McDonnell Douglas Aircraft Corporation P.O. Box 516 Municipal Airport St. Louis, Missouri 63166	R. A. Herzmark

COPIES	RECIPIENT	DESIGNEE
1	Space Division North American Rockwell Corp. 12214 Lakewood Boulevard Downey, California 90241	Library
1	Rocketdyne (Library 586-306) 6633 Canoga Avenue Canoga Park, California 91304	Dr. R. I. Thompson
1	Northrop Space Laboratories 3401 West Broadway Hawthorne, California	Dr. William Howard
1	Astro-Electronics Division Radio Corporation of America Princeton, New Jersey 08540	S. Fairweather
1	Reaction Motors Division Thiokol Chemical Corporation Denville, New Jersey 07832	Dwight S. Smith
1	Space General Corporation 9200 East Flair Avenue El Monte, California 91734	C. E. Roth
1	Stanford Research Institute 333 Ravenswood Avenue Menlo Park, California 94025	Dr. Gerald Marksman
1	TRW Systems Group TRW Incorporated One Space Park Redondo Beach, California 90278	G. W. Elverum
1	TAPCO Division TRW Incorporated 23555 Euclid Avenue Cleveland, Ohio 44117	P. T. Angell
1	Thiokol Chemical Corporation Huntsville Division Huntsville, Alabama	John Goodloe
1	Research Laboratories United Aircraft Corporation 400 Main Street East Hartford, Connecticut 06108	Erle Martin
1	United Technology Center 587 Methilda Avenue P.O. Box 358 Sunnyvale, California 94088	Dr. David Altman

COPIES	RECIPIENT	DESIGNEE
1	Aerospace Operations Walter Kidde and Company, Inc. 567 Main Street Belleville, New Jersey 07109	R. J. Hanville Director of Research Engineering
1	Florida Research and Development Pratt and Whitney Aircraft United Aircraft Corporation P.O. Box 2691 West Palm Beach, Florida 33402	R. J. Coar
1	Rocket Research Corporation 520 South Portland Street Seattle, Washington 98108	Roy McCullough, Jr.

DOCUMENT CONTROL DATA - R & D

(Security classification of title, body of abstract and indexing annotation must be entered when the overall report is classified)

1. ORIGINATING ACTIVITY *(Corporate author)*	2a. REPORT SECURITY CLASSIFICATION
Rocketdyne, a Division of North American Rockwell Corporation, 6633 Canoga Avenue, Canoga Park, California 91304	Unclassified
	2b. GROUP

3. REPORT TITLE

Second Report Investigation of Positive-Type Shaft Seals

4. DESCRIPTIVE NOTES *(Type of report and inclusive dates)*

5. AUTHOR(S) *(First name, middle initial, last name)*

Rudy R. Hammond

6. REPORT DATE	7a. TOTAL NO. OF PAGES	7b. NO. OF REFS
25 September 1968	140	None

8a. CONTRACT OR GRANT NO.	9a. ORIGINATOR'S REPORT NUMBER(S)
NAS8-11325	R-6811-1
b. PROJECT NO.	
c.	9b. OTHER REPORT NO(S) *(Any other numbers that may be assigned this report)*
d.	

10. DISTRIBUTION STATEMENT

11. SUPPLEMENTARY NOTES	12. SPONSORING MILITARY ACTIVITY
	NASA, George C. Marshall Space Flight Center Propulsion and Vehicle Engineering Lab. Marshall Space Flight Center, Alabama

13. ABSTRACT

A series of new type seal concepts were generated, and three of the most promising were detailed for fabrication and testing to evaluate the designs for future turbopump applications. Descriptions of the various concepts, basis for the final selections of the seals for evaluation, and results of testing are included.

14. KEY WORDS	LINK A		LINK B		LINK C	
	ROLE	WT	ROLE	WT	ROLE	WT
Piston Damped Seal						
Orifice Damped Seal						
Particle Damped Seal						
Mechanical Cycling Tests						
Recovery Rate Tests						
Pressure Cycling Tests						
Total Face Loading Tests						
Vibration Tests						